Universidade de Aveiro Departamento de Engenharia Civil
2014

MANJIP SHAKYA

AVALIAÇÃO DA VULNERABILIDADE SÍSMICA DE ESTRUTURAS ESBELTAS DE ALVENARIA

SEISMIC VULNERABILITY ASSESSMENT OF SLENDER MASONRY STRUCTURES

Universidade de Aveiro Departamento de Engenharia Civil
2014

MANJIP SHAKYA

AVALIAÇÃO DA VULNERABILIDADE SÍSMICA DE ESTRUTURAS ESBELTAS DE ALVENARIA

Tese apresentada à Universidade de Aveiro para cumprimento dos requisitos necessários à obtenção do grau de Doutor em Engenharia Civil, realizada sob a orientação científica do Doutor Humberto Salazar Amorim Varum, Professor Associado com Agregação da Departamento de Engenharia Civil da Universidade de Aveiro e coorientação do Doutor Romeu da Silva Vicente, Professor Auxiliar da Departamento de Engenharia Civil da Universidade de Aveiro e do Doutor Aníbal Guimarães Costa, Professor Catedrático da Departamento de Engenharia Civil da Universidade de Aveiro.

Universidade de Aveiro Departamento de Engenharia Civil
2014

MANJIP SHAKYA

SEISMIC VULNERABILITY ASSESSMENT OF SLENDER MASONRY STRUCTURES

Thesis submitted to the University of Aveiro to fulfill the requirements to obtain the degree of Doctor of Philosophy in Civil Engineering, under the scientific supervision of Dr. Humberto Salazar Amorim Varum, Associate Professor with Habilitation, Department of Civil Engineering, University of Aveiro and co-guidance of Dr. Romeu da Silva Vicente, Assistant Professor, Department of Civil Engineering, University of Aveiro and Dr. Aníbal Guimarães Costa, Full Professor, Department of Civil Engineering, University of Aveiro.

o júri

presidente

Prof. Doutor Nelson Fernando Pacheco da Rocha
Professor Catedrático da Secções Autónomas de Ciências da Saúde da Universidade de Aveiro

Prof. Doutor Humberto Salazar Amorim Varum
Professor Associado com Agregação da Departamento de Engenharia Civil da Universidade de Aveiro

Prof. Doutor Fernando Farinha da Silva Pinho
Professor Auxiliar da Faculdade de Ciências e Tecnologia da Universidade Nova de Lisboa

Prof. Doutor Graça de Fátima Moreira de Vasconcelos
Professor Auxiliar da Escola de Engenharia da Universidade do Minho

Prof. Doutor Hugo Filipe Pinheiro Rodrigues
Professor Adjunto da Escola Superior de Tecnologia e Gestão do Instituto Politécnico de Leiria

Prof. Doutor Cristina Margarida Rodrigues Costa
Professor Adjunto da Departamento de Engenharia Civil do Instituto Politécnico de Tomar

the jury

president

Prof. Dr. Nelson Fernando Pacheco da Rocha
Full Professor, Autonomous Section of Health Science, University of Aveiro

Prof. Dr. Humberto Salazar Amorim Varum
Associate Professor with Habilitation, Department of Civil Engineering, University of Aveiro

Prof. Dr. Fernando Farinha da Silva Pinho
Assistant Professor, Faculty of Science and Technology, New University of Lisbon

Prof. Dr. Graça de Fátima Moreira de Vasconcelos
Assistant Professor, School of Engineering, University of Minho

Prof. Dr. Hugo Filipe Pinheiro Rodrigues
Assistant Professor, School of Technology and Management, Polytechnic Institute of Leiria

Prof. Dr. Cristina Margarida Rodrigues Costa
Assistant Professor, Department of Civil Engineering, Polytechnic Institute of Tomar

acknowledgements

The present work has been developed at the Department of Civil Engineering, University of Aveiro, Portugal. I wish to express my sincere gratitude to the following persons, which have contributed to make this work possible and helped me growing.

Firstly, I would like to express my gratitude to the scholarship under the Erasmus Mundus Action 2 Partnership, EU-NICE project, financially supporting to develop a PhD at Department of Civil Engineering, University of Aveiro, Portugal. I would also like to thank Dr. Giorgio Monti and Dr. Marco Faggella from EU-NICE project coordinating University, Sapienza Universiy of Rome, Italy for their help and support.

My gratitude goes to my supervisor, Dr. Humberto Salazar Amorim Varum, Associate Professor with Habilitation, and to my co-supervisors Dr. Romeu da Silva Vicente, Assistant Professor, and Dr. Aníbal Guimarães Costa, Full Professor, from the Department of Civil Engineering, University of Aveiro, who were my source of encouragement and motivation during the whole work. Their advice, suggestions and solution to bottleneck problems encountered during this work were just immensurable. Their technical excellence, unwavering faith and constant encouragement were very helpful and made this effort an enjoyable one. This research work was enabled and sustained by their vision and ideas.

I thank to all my colleagues from Department of Civil Engineering, University of Aveiro, for both academic and social interactions.

I would like to express my deepest gratitude, to my parents Ram Krishna Shakya and Surja Laxmi Shakya, to my wife Sushma Bajracharya and to all my family members for their love and invaluable support in everything. This thesis is dedicated to them.

palavras-chave

Estruturas esbeltas de alvenaria; torres; minaretes; chaminés; Pagode; Nepal; fragilidade estrutural; avaliação da vulnerabilidade; índice de vulnerabilidade; estratégias de melhoria do comportamento

resumo

Existem estruturas esbeltas de alvenaria por todo o mundo, e estas constituem uma parte relevante do património da humanidade, arquitetónico e cultural. A sua proteção face à ação sísmica é um tema de grande preocupação entre a comunidade científica. Esta preocupação surge, principalmente, do dano severo ou até mesmo perda total sofrida por este tipo de estruturas em eventos catastróficos, e da necessidade e interesse em preservá-las. Apesar dos grandes avanços na tecnologia, e do conhecimento em sismologia e engenharia sísmica, a preservação destas estruturas frágeis e massivas ainda representa um grande desafio. Com base na investigação desenvolvida neste trabalho é proposta uma metodologia que visa a avaliação do risco sísmico de estruturas esbeltas de alvenaria. A metodologia proposta foi aplicada na avaliação da vulnerabilidade sísmica de templos Pagode, no Nepal, que possuem procedimentos de construção simples e detalhes construtivos pobres relativamente às exigências de resistência sísmica.

O trabalho está estruturado em três partes principais. Em primeiro lugar, são discutidas as fragilidades estruturais específicas, bem como as características construtivas, de um importante património classificado da UNESCO que são os templos Pagode do Nepal, que afetam o seu desempenho sísmico e as propriedades dinâmicas. Na segunda parte deste trabalho apresenta-se o método simplificado proposto para a avaliação da vulnerabilidade sísmica de estruturas esbeltas de alvenaria. Finalmente, a metodologia proposta neste trabalho é aplicada no estudo dos templos Pagode do Nepal, e na avaliação da eficiência de soluções de melhoria do desempenho sísmico compatíveis com o valor cultural e tecnológico original.

keywords

Slender masonry structures; towers; minarets; chimneys; Pagoda; Nepal; structural fragility; vulnerability assessment; vulnerability index; retrofitting strategies

abstract

Slender masonry structures are distributed all over the world and constitute a relevant part of the architectural and cultural heritage of humanity. Their protection against earthquakes is a topic of great concern among the scientific community. This concern mainly arises from the strong damage or complete loss suffered by this group of structures due to catastrophic events and the need and interest to preserve them. Although the great progress in technology, and in the knowledge of seismology and earthquake engineering, the preservation of these brittle and massive structures still represents a major challenge. Based on the research developed in this work it is proposed a methodology for the seismic risk assessment of slender masonry structures. The proposed methodology was applied for the vulnerability assessment of Nepalese Pagoda temples which follow very simple construction procedure and construction detailing in relation to seismic resistance requirements.
The work is divided in three main parts. Firstly, particular structural fragilities and building characteristics of the important UNESCO classified Nepalese Pagoda temples which affect their seismic performance and dynamic properties are discussed. In the second part the simplified method proposed for seismic vulnerability assessment of slender masonry structures is presented. Finally, the methodology proposed in this work is applied to study Nepalese Pagoda temples, as well as in the efficiency assessment of seismic performance improvement solution compatible with original cultural and technological value.

CONTENTS

LIST OF FIGURES

LIST OF TABLES

LIST OF SYMBOLS

T_1	Natural period
f_1	Fundamental frequency
L	Plan dimension of the building in the direction of oscillation
E	Young's modulus
$\overline{m}$	Mass per unit of length
γ	Specific weight
ν	Poisson's ratio
f_c	Compressive strength
G_c	Compressive fracture energy
f_t	Tensile strength
G_f	Tensile fracture energy
$\emptyset$	Friction angle
τ	Characteristic shear strength
α_h	Horizontal seismic coefficient
λ	Slenderness ratio
δ_{max}	Maximum top displacement
H	Total height
B	Breadth at base
k	Radius of gyration
A	Cross-sectional area
I_{min}	Minimum moment of inertia
W_o	Lateral load intensity
β	Coefficient depending upon the soil foundation
F_o	Seismic zone factor for average acceleration spectra
$\frac{S_a}{g}$	Average acceleration coefficient

p	Foundation land slope
e_R	Relative eccentricity
Tt	Thickness of top wall
Tn	Thickness of non–supported top wall
Tb	Thickness of wall at base
Ht	Height of top wall
OA	Size of opening above base
OB	Size of opening at base
RC	Reinforced concrete
K_i	Numerical value of vulnerability classes
W_i	Weight
I_v	Vulnerability index
$I_{v,mean}$	Mean vulnerability index
μ_D	Mean damage grade
I	Macroseismic intensity,
V	Vulnerability index used in the Macroseismic Method
Q	Ductility factor
D_k	Damage grade
Γ	Gamma function
$P(D_k)$	Probability occurrence a certain damage grade D_k
$W_{uPt,k}$	Weights indicating the percentage of buildings with a certain damage level D_k
$P[R\|I]$	Repair cost probabilities for a certain intensity I
$P[R\|D_k]$	Probability of the repair cost for each damage level
$P[D_k\|I_v, I]$	Probability of the damage for each level of building vulnerability and intensity
$P_{collapse}$	Probability of collapse
$P_{unusable}$	Probability of unusable

CHAPTER 1

INTRODUCTION

Summary *This introductory chapter presents the background and motivation that underlines the development of this research proposal. The general and specific objectives of this research are listed. Finally, this first chapter is closed with the presentation of a detailed outline and organization of the present thesis.*

Chapter outline

1.1 Background

Historical slender masonry structures with different characteristics and functions are distributed all over the world and constitute a relevant part of the architectural and cultural heritage of humanity. The cultural importance of these structures poses the problem for their safety and preservation. Unfortunately, several historical constructions suffered partial or total collapse in the course of time due to earthquakes, fatigue, deterioration, soil movements, etc. The occurrence of these unexpected and unavoidable events has demonstrated that historical slender masonry structures are one of the most vulnerable structural types to suffer strong damage or collapse [1]. These losses are simply not quantifiable in economic terms, as nether lives nor can cultural heritage be reinstated by post–earthquake reconstruction plans.

Their protection is a topic of great concern among the scientific community. This concern mainly arises from the observed damages after every considerable earthquake and the need and interest to preserve them. Although the recent progress in technology, seismology and earthquake engineering, the preservation of these brittle and massive monuments still represents a major challenge [2]. The study of these historical

constructions must be undertaken from an approach based on the use of modern technologies and science. It is the responsibility of the experts to select and adequately manage the possible technical means needed to attain the required understanding of the morphology and the structural behaviour of the construction and to characterize its repair needs, the principles lay general criteria, research and diagnosis, and remedial measures and health monitoring. A multi–disciplinary approach is required and the peculiarity of heritage structures, with their complex history, requires the organization of studies and analysis in steps: condition survey, identification of the causes of damage and decay, choice of the remedial measures and control of the efficiency of the interventions. Understanding of the structural behaviour and material characteristics is essential for intervention over architectural heritage. Diagnosis is based on historical information and qualitative and quantitative approaches. The qualitative approach is based on direct observation of the structural damage and material degradation as well as historical and archaeological research, while the quantitative approach requires material structural testing, monitoring and structural analysis.

In the context of the seismic risk management of the built environment there are two main aspects. These aspects refer to the seismic risk assessment and seismic risk reduction. The seismic risk of a certain structure located in a seismic zone is determined by two factors, i.e. the seismic hazard and its structural vulnerability. Since the seismic hazard is unavoidable and is not in our hands to reduce or modify it, the seismic risk reduction may be attained by reducing their structural vulnerability. Therefore, the vulnerability assessment of this type of structure is necessary to establish the strengthening strategy in order to enhance their behaviour when subjected to major earthquakes. Modern requirements for an intervention include reversibility, minimal intensive repair and compatibility to the original construction, as well the obvious functional and structural requirements. Seismic vulnerability assessment of ancient masonry structures is an issue of most importance at present time.

The present research work is a step to preserve the cultural heritage for future generation. Seismic vulnerability assessment and seismic risk reduction are the two key issues for the preservation of slender masonry built heritage, such as Pagoda temples, towers, minarets and chimneys. The first issue, the hypothesis, corresponds to the possibility of assessing their seismic vulnerability by developing a simplified vulnerability

assessment method. The second issue (i.e. achieving the seismic risk reduction) corresponds to a proposal for seismic strengthening strategy resourcing to retrofitting techniques for slender masonry structures by minimum intrusion criteria which are intended to improve the seismic performance and to reduce the expected damage. Nepalese Pagoda temples, many of which are considered world classified heritage (UNESCO), are the main focus case study in the implementation of the method.

1.2 Motivation

The study scope is directed towards conservation and retrofitting/strengthening of slender masonry structures, which is one of the major concerns in order to preserve the built heritage for future generations.

The historical slender masonry structures located in seismic prone areas are especially vulnerable to suffer structural damages, due to their geometrical, mechanical and structural features, which could lead to global or local collapse mechanisms. The post–earthquake information from various events (1934 Nepal–Bihar earthquake, 1976 Friuli earthquakes, 1999 Kocaeli and Duzce earthquakes, etc.) reveals that a vast number of such slender structures were destroyed by the quake. Although numerous collapses and heavy structural damage evidence were reported following the earthquakes, not many researchers investigated the seismic behaviour and performance of these structures. Cultural heritage buildings and monuments are, therefore, at risk, and the cultural loss in the consequence of an earthquake is incalculable. Furthermore, typical problems of masonry structures such as material degradation, geotechnical problems, buckling behaviour of slender elements and the nonlinear behaviour of masonry generated by the presence or development of cracks for very low horizontal load levels due to its poor tensile strength are of high importance.

The safeguard of this architectural heritage is a fundamental issue in the cultural life of modern societies. The preservation of the historical construction against the seismic action is of strategic importance, considering incalculable value of its architectural value. Presently, conservation and restoration of cultural heritage are one of the major concerns, since many of them are considered world classified heritage (UNESCO). The need of preserving historical constructions is thus not only a cultural requirement but also an economical and developmental demand.

This research aims to propose a simplified methodology for the seismic vulnerability assessment of slender masonry structures and implement it particularly in Nepalese Pagoda temples as a case study. Moreover, in this research few retrofitting strategy is proposed and a comparative study is carried out between original and retrofitted (assumed) state Pagoda temples to understand its effectiveness in loss estimation.

1.3 Objectives

1.3.1 General objective

The broad objective of this research work is to propose a simplified seismic vulnerability assessment methodology for slender masonry structures.

1.3.2 Specific objectives

The following specific objectives aim to achieve the above mentioned general objective:

- Describe the main features that rule the structural vulnerability of slender masonry structures (specifically for Nepalese Pagoda temples) reported in the literature;
- Identify the major parameters that influence the dynamic properties of slender masonry structures;
- Analyze the seismic sensitivity of the common structural components of Nepalese Pagoda temples;
- Development of a simplified methodology for the seismic vulnerability assessment of slender masonry structures;
- Application of the proposed methodology for Nepalese Pagoda temples as a case study;
- Propose a retrofitting strategy for Nepalese Pagoda temples.

1.4 Organization of the thesis

Chapter 1 presents the introduction of the thesis and identifies the specific contributions to the scientific knowledge in a more general context. This chapter shortly describes the

background and motivation for choosing this research and also provides the overview on the general objective as well as particular objectives to achieve it.

Chapter 2 is an intensive literature review aimed to acquire detailed information and knowledge on slender masonry structures. This extensive state of the art includes both the study of different analytical and numerical based approaches and the analysis of the most relevant experimental campaigns performed. The information regarding damage scenarios due to past earthquakes, as well as repair and strengthening interventions proposed and followed by different researchers are discussed. Moreover, this chapter also presents another important objective of intensive literature review, which was to gather and compile data on slender masonry structures regarding dynamic, geometrical and mechanical characteristics for further use in the developing of a reliable numerical formulation for predicting the fundamental frequency of slender masonry structures.

Chapter 3 corresponds to a second intensive literature review regarding seismic history, seismic performance, construction system and research carried on Nepalese Pagoda temples. Moreover, this chapter also presents the task carried out to analyze particular structural fragilities and characteristics of the historic Nepalese Pagoda temples which affect their seismic performance. For this task three different Nepalese Pagoda temples were selected and numerical modeling using SAP 2000 was done. Among those three temples, one of them was experimentally analyzed for dynamic properties and the model calibration has carried out. Finally the updated model was used for parametric analysis to understand the seismic response of the common structural components of Nepalese Pagoda temples. Outcomes of this task contribute to understand the structural fragilities of Pagoda temple typology and the associated traditional building technology and construction details. It has also aided to identify the most influential structural parameters when assessing seismic vulnerability of such structures.

Chapter 4 presents a simplified methodology for assessing the seismic vulnerability of slender masonry structures based on a vulnerability index evaluation method. Here, 12 parameters (qualitative and quantitative) are defined to evaluate the vulnerability index for slender masonry structures. Nonlinear parametric analysis is carried out to calibrate most of the quantitative parameters, as well as to define the weight of each parameter. Moreover, this chapter also present the implementation of this methodology for different

types of slender masonry structures to develop vulnerability curves for this structural typology.

Chapter 5 started with the descriptions of task carried out on field survey of 78 Nepalese Pagoda temples for gathering sufficient information to support the vulnerability assessment. The information collected in the field survey is crucial for applying the vulnerability index method on Pagoda temples as case studies. This task will be followed with the application of the proposed vulnerability index method on these temple structures. Finally, in this chapter damage and vulnerability mapping of the 78 Nepalese Pagoda temple structures along with loss assessment and proposal of retrofitting strategy for loss mitigation will be presented.

Finally, chapter 6 summarizes and presents the most important conclusions derived from this research work. Moreover, some unsolved issues and recommendations for further research are mentioned.

CHAPTER 2

SLENDER MASONRY STRUTURES: A LITERATURE REVIEW

Summary *This chapter presents detailed information and knowledge on slender masonry structures acquired from an intensive literature review. This chapter is closed with the presentation of four reliable empirical formulations for predicting the fundamental frequency of slender masonry structures.*

Chapter outline

2.1 Introduction

Slender masonry structures such as towers, minarets, chimneys and Pagoda temples (see Figure 2.1) can be characterized by their distinguished architectural characteristics, age of construction and original function, but their comparable geometric and structural ratios yield to the definition of an autonomous structural type. These structures are featured by their notable slenderness and also represent one of the main differences from most of the historic structures or even ordinary buildings [1].

Considering that historical masonry is typically characterized by a complex geometry, irregularities and a high degree of heterogeneity, stress concentrations can occur, thus promoting local collapses. Hence, the structural failure can be driven even by a moderate increase in the stress level, which can occur during seismic events or even with the effects of cyclic loads as wind and temperature variations [2–5]. Moreover, strong earthquakes tensile damage is distributed along the height of the structure, while the shear damage is

concentrated in the lower part [6]. These structures are able to resist gravitational actions, but as they were not explicitly designed to withstand seismic loading, show particularly weakness in regard to horizontal loading induced by strong motion [7]. The limited ductility of the masonry combined the slenderness of theses towers, that behave as a vertical cantilever fixed at the base, generally provides a rather brittle structural behaviour [8]. Therefore, these constructions are particularly vulnerable with respect to seismic action [9].

The dynamic behaviour of a structure is important to define its health status, as well as, to define the restoration intervention, after damage generated by an earthquake [10]. The behaviour of slender masonry structures under seismic loads is generally dominated by the axial stresses that arise from the static vertical loads combined with the dynamic loads induced by the low–intensity earthquake that is often close to the compression strength of the traditional masonry material and also makes them more vulnerable to base settlements [3]. Thus, such structures have long been considered to be particularly susceptible to seismic actions and therefore, it is crucial to understand the dynamic behaviour of these structures to preserve and strengthen them against earthquake excitation.

The knowledge of dynamic properties, together with local site seismicity and stratigraphy, is the starting point for an accurate estimation of the seismic safety of these structures [11]. A reliable evaluation of the dynamic properties of a structure is of importance for the analysis of its dynamic behaviour, in particular under seismic actions [12]. One of the fundamental dynamic properties, so called fundamental frequency, plays a primary role for the assessment of the seismic demand on structures. It can be evaluated by numerical analyses, or even according to empirical formulations provided in building codes. In the case of slender masonry structures, where reliable results are required from the numerical model analyses for precisely calibrating the interventions work, but systematic studies focused on this issue are still missing.

The present chapter is driver to describing an intensive literature review regarding the state of the art on slender masonry structures. The seismic behaviour and failure mechanisms of slender masonry structures are the most important aspects which determine the seismic vulnerability of these structures. Hence, a deep understanding of all these aspects is the basis towards the achievement of their risk reduction, by means of decreasing their seismic vulnerability using an appropriate retrofitting strategy, which is the main

objective of this thesis. Moreover, in this research, a number of literature reviews has been carried out in order to collect a data regarding the dynamic properties, material and geometric characteristics of slender masonry structures. The collected database has been analyzed and correlated to develop a reliable formulation for predicting the fundamental frequency of such structures.

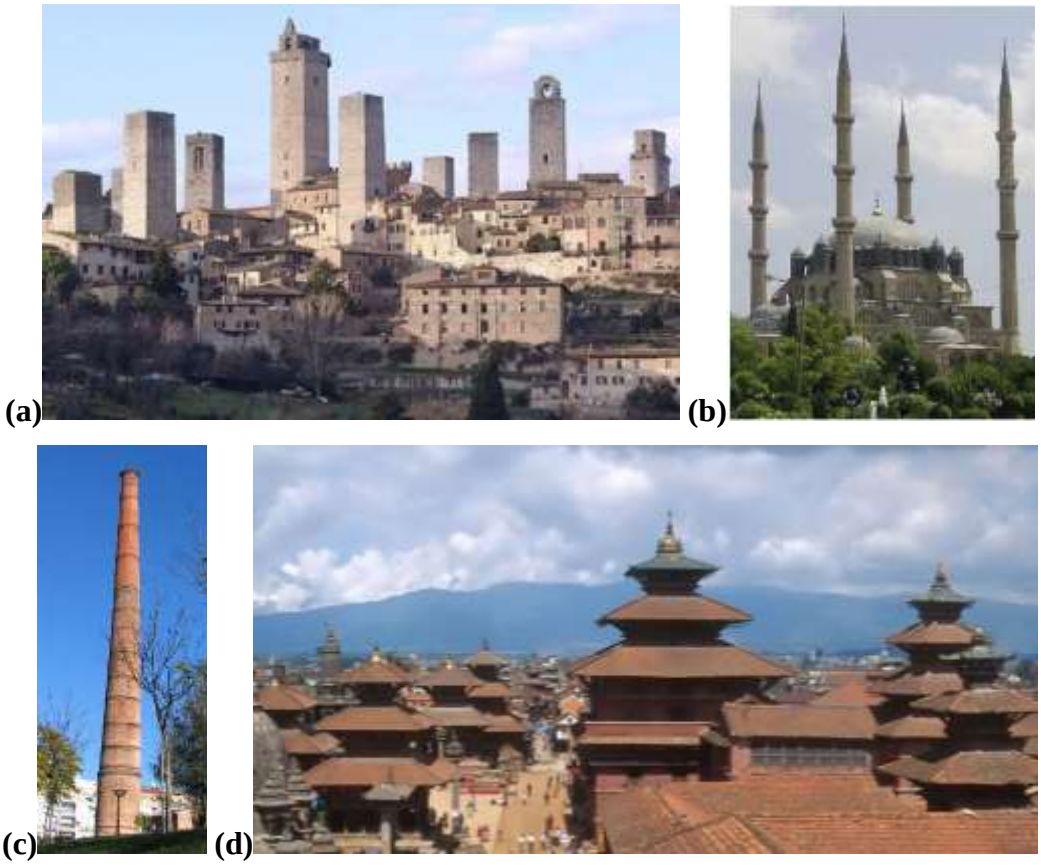

Figure 2.1: Slender masonry structures: a) Towers [13]; b) Minarets [14]; c) Chimney [15]; d) Pagoda temples

2.2 State of the art on slender masonry structures

2.2.1 Damage scenario of slender masonry structures in past earthquake

The historical slender masonry construction, have demonstrated during the past to be susceptible to damage, and prone to partial or total collapse, under earthquake actions, sometimes due to lack or inadequate retrofit [16]. A detailed analysis of the documentation regarding the damages caused by recent and less recent Italian earthquakes [17; 10] allow drawing interesting conclusions on the qualitative behaviour of such structures when they

are subject to seismic action. In particular, the following issues can be considered as relevant:

- In isolated bell tower damage patterns are frequently distributed along the whole height, although they are usually more severe at the base [18] (see Figure 2.2a);
- During strong earthquakes vertical shear cracks are sometimes observed. In this case, the reduction of the cross–section stiffness during the deformation process may have a key role on the overall response of the structure [2] (see Figure 2.2b);
- It can be argued that the damage evolution during a dynamic excitation plays a crucial role in reducing the resisting geometry of the structure, thus activating higher vibration modes which seem to be associated to the damage of the upper part, especially the tower crown and the belfry [19; 20] (see Figure 2.2c).

Curti *et al.* [24] observed in 31 Italian bell towers damaged by the 1976 Friuli earthquakes that the belfry is the most vulnerable part of the tower due to the presence of large openings leading to the pillars to be slender and by the top masses. As well as in the case of towers which share sides with church at different heights are horizontal constraints that increase the seismic vulnerability of the tower by limiting its slenderness and by creating localized stiffening zones that could cause the concentration of important stresses.

The documentation by Firat [25], pointed the location of the failure in the minarets that collapsed during 1999 Kocaeli and Duzce earthquakes (Turkey) was found to be at the near bottom of the cylinder, where a transition was made from circular to square section (see Figure 2.2d). The old masonry minarets were also observed to fail near the bottom of the cylinder, where the minaret connects to the adjacent building or is part of it at the lower section [22]. Few cases of minor damage were also observed, such as the collapse of parts of the balcony (see Figure 2.2e) during Kocaeli earthquake (Turkey) [26].

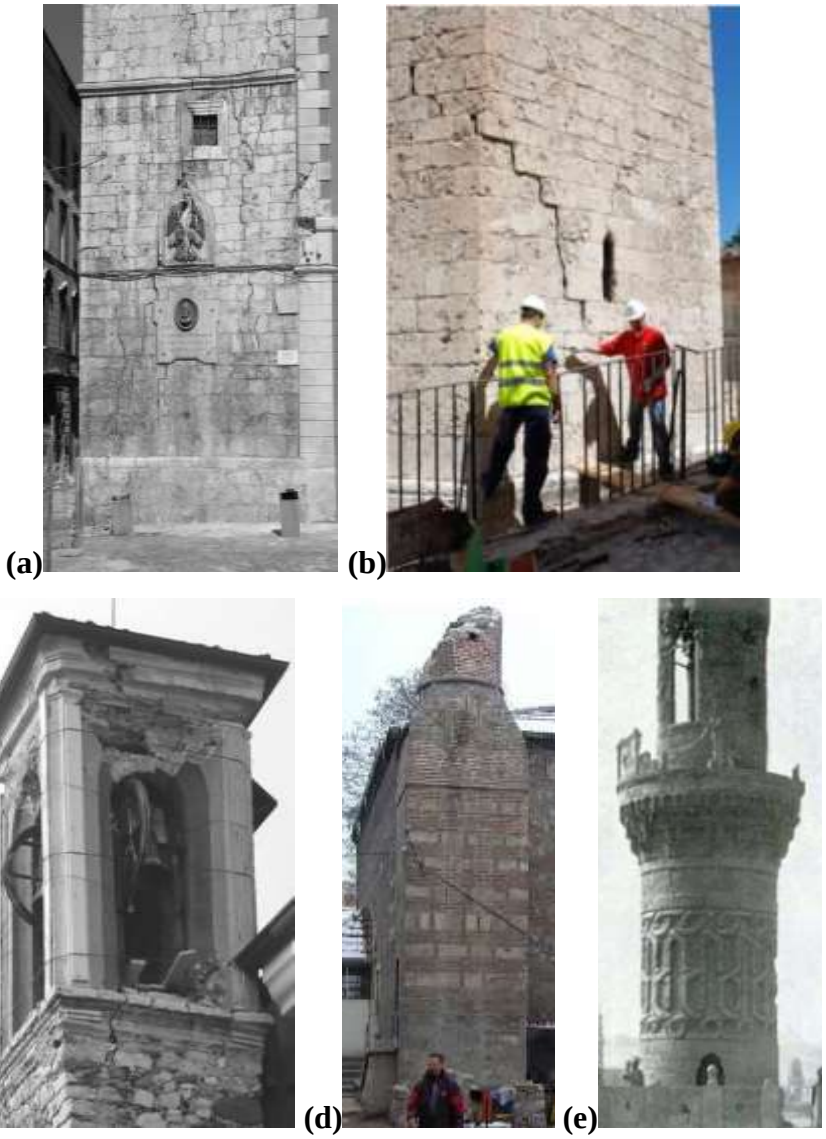

Figure 2.2: Earthquake induced damage on bell tower and minaret: a) vertical cracks at the base [10]; b) shear crack on the stem [20]; c) damage at belfry [21]; d) collapse at transition zone [22]; e) partial collapse of balcony [23]

2.2.2 Analytical and experimental investigation on slender masonry structures

In Italy, the sudden collapse of the Pavia civic tower, in 1989, motivated the development of many investigations concerning these types of structures [27–37]. These investigations involved both analytical and experimental analysis including several tasks: field survey of the ‘‘as built’’ configuration and of the crack pattern, non–destructive testing (e.g. ambient vibration [1; 15; 26; 32; 38–41] or terrestrial laser scanning [15; 42]) and slightly destructive tests (e.g. flat–jack tests [43–45] or sonic pulse velocity tests [46]),

laboratory tests on cored samples, finite element modeling and theoretical analysis [16; 28; 39–40; 47–54].

At present, a number of studies are available in the technical literature dealing with numerical and experimental analyses of slender masonry structures. It can be stated that a wide and consolidated scientific tradition exists is based on the use of a variety of different analysis techniques, as for instance:

- Utilization of non–linear FE codes [36; 48–49; 51–52; 55];
- Combined eigenvalues and experimental identification studies [16; 39];
- 2D limit analyses assuming masonry as either a no–tension or a scarcely resistant in tension material [16; 39; 56];
- 3D nonlinear dynamics of slender towers by specific fiber–element models [57–58];
- Experimental and in–situ tests [29; 59];
- Repairing and rehabilitation proposals [4; 60].

The results of these studies are peculiar to each structure under investigation, but they are the outcomes of a common three–step process that consists of the following: (a) monitoring, (b) diagnosis, and (c) retrofitting. In fact, prevention and rehabilitation can be successfully achieved only if diagnosis of the building is carefully analyzed [61].

According to what reported in the technical literature the majority of the historical big structures has been modelled with a so called macro–modeling strategy, i.e. the heterogeneous masonry is replaced at a structural level by a fictitious material with average mechanical properties (either orthotropic or isotropic) representing the global response of the whole structure under increasing loads. In some cases advanced material models have been used, such as elastic–plastic models with softening and damage, which are the only ones suitable to have an insight into the structural behaviour of a masonry structure. For instance, Buti's bell tower (Italy) was studied by Bernardeschi *et al.* [49] in the presence of two different load conditions: firstly the bell tower was subjected only to its own weight and then to both self–weight and static horizontal loads simulating seismic actions. An 8^{th}–century masonry tower (Sineo in Alba, Italy) was numerically analysed and monitored by Carpinteri *et al.* [55], in order to investigate the causes of dangerous crack patterns

occurring at the base. Several dynamic structural characterizations are also available in the specialized literature, as for instance the study conducted by Ivorra and Pallares [38] on the bell tower of ‘‘Nuestra Sra. de la Misericordia Church’’ (Valencia, Spain). With reference to the geometrical configuration of the bell tower, different numerical models were calibrated, on the basis of dynamic tests, in order to determine the bending and torsion frequencies of the tower. In [4], some remarks regarding the basic design choices and the selection of the most appropriate materials and techniques for the restoration of the Monza Cathedral bell tower are reported. A seismic analysis of the Asinelli Tower in Bologna (Italy) is performed by Riva *et al.* [36]. In this study, an assessment of the tower's stability with respect to seismic events, compatible with the local seismic hazard, is carried out by means of a non–linear dynamic analysis on a simplified model mainly made of beam elements with non–linear stress–strain behaviour. The application of geo–radar techniques to the analysis of three main structural problems concerning the bell tower (Torrazzo) in Cremona is studied by Binda *et al.* [29]. Their study demonstrates the necessity and the great potentialities of a multidisciplinary collaboration in morphological analyses and diagnoses carried out by means of non–destructive investigations.

2.2.3 Proposed and followed repair and strengthening interventions

Nowadays, there is a huge variety of techniques and materials available for the protection of historical masonry constructions. Among them, two main techniques are distinguished, the rehabilitation or restoration works and the retrofitting. The rehabilitation or restoration works aim to use materials of similar characteristics to the originals and to mainly apply the same constructive techniques, in order to locally correct the damage of certain structural elements, e.g. sealed up of cracks and reposition of mortar and units. In general terms, the objective of these works is to preserve the building in good conditions and in its original state, mainly to withstand the vertical loading generated by self–weight. By the other hand, the structural retrofitting intends to use modern techniques and addition of advanced materials in order to mainly improve the seismic performance of the building, by increasing its ultimate lateral load capacity (strength), ductility and energy dissipation. Compatibility, durability and reversibility are the fundamental aspects recommended in literature to be taken into account when retrofitting is applied for the seismic protection of cultural heritage.

In order to improve the structural behaviour of the tower, a series of repair and strengthening techniques are proposed to be executed both at a local and global level. This consisted of the application of [4]:

- Metallic horizontal reinforcing rings on several sections along the height of the tower to confine the masonry and to improve the connection between the contiguous walls;
- The application of the reinforced repointing technique diffused on various portions of the walls to counteract the creep damage, and concentrated on some pilaster strips to strengthen the corners;
- Local interventions of injection, rebuilding and pointing of the mortar joints, to restore the zones having high material deterioration.

The study carried out by Ceroni *et al.* [62] on bell Tower of Santa Maria Del Carmine (Italy), reported the following intervention work on past:

- By the end of the 19th century, several steel tie rods have been inserted connecting the orthogonal walls and placed symmetrically and parallel to the walls (see Figure 2.3a) with various end anchorage systems (plate for strands, horizontal and vertical bars (see Figure 2.3b; 2.3c; 2.3d).
- During the 1970s, several internal steel chains were added and RC injections were conducted in numerous areas corresponding particularly to the connections of the RC staircase in the masonry walls and in the corners.
- After the 1980 Irpinia earthquake, mortar injections, reinforced with steel bars, were carried out in the corners of most floors under the fourth level. The connection was improved with a diffuse system of steel reinforced inclined mortar injections.

In order to stabilize an existing deformed structure and to stop its further unhinging development, prestress cables are suggested by Stavroulaki *et al.* [63] in Torre Grossa at San Gimignano (Italy). The technique of externally placed tendons is widely used for the reinforcement of existing structures, because of several advantages: minimum disturbance of the structure and its users, negligible change of mass, stiffness and dynamic

characteristics of the existing structure, minimum loss of prestressing forces due to friction, and the use of high–quality materials with known properties [62; 64–66].

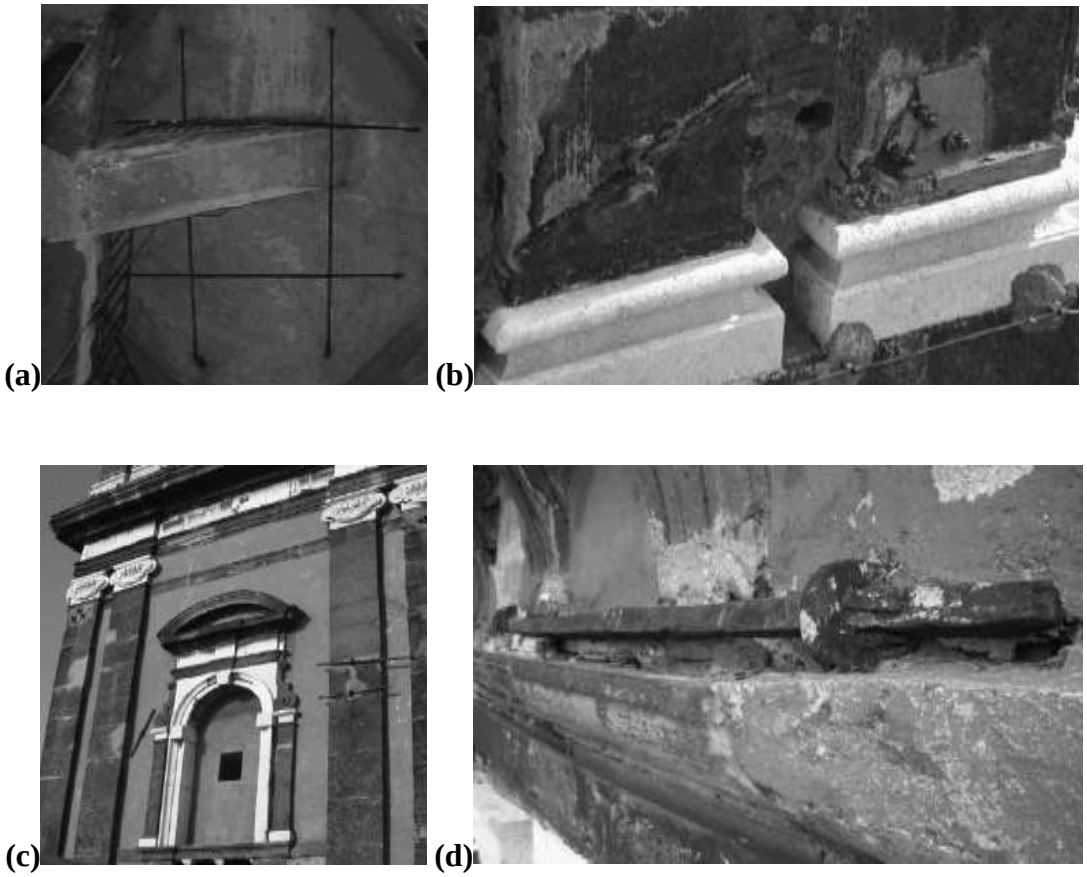

Figure 2.3: Steel tie rods [62]: a) inferior view of system of four tie rods; b) external anchorage for steel strands; c) external anchorages and closure of existing windows; d) external horizontal anchorage

2.3 Database collection and analysis

Slender masonry structures can be characterized by their distinguished architectural characteristics, age of construction and original function, but their comparable geometric and structural ratios yield to the definition of an autonomous structural type. These structures are characterized by their notable slenderness and also represent one of the main differences from most of the historic structures or even ordinary buildings [1]. These structures are scattered over different countries with different densities and features. Database of such structures was compiled through a systematic literature review. Data was acquired from experimental works performed on the determination of dynamic properties and material characteristics.

Tables 2.1, 2.2, 2.3 and 2.4 summarize the database that comprises 59 slender masonry structures, among them 32 are towers, 16 are minarets, 7 are chimneys and 4 are Pagoda temples respectively. The database summarizes the geometric characteristics of slender masonry structures along with theirs dynamic properties. The data base information regarding geometric characteristics indicates the total height of the structures ranging from 10m (shortest) to 87.4m (tallest) and the breadth of the wall at base varying from 1.96m (minimum) to 14m (maximum). Moreover, the minimum slenderness which is considered as the height to minimum breadth of the wall at base ratio ranges from 1.66 (minimum) to 15.67 (maximum).

Table 2.1: Database compiled from the literature review carried out for masonry towers

Reference	Type of masonry	Total height, *H* (m)	Min. breadth at base, *B* (m)	Slenderness, H/B	Experimental natural frequency (Hz)
Tomaszewska [71]	—	22.65	7.70	2.94	1.42
Bonato *et al.* [30]		26.00	3.50	7.43	1.66
Pelella *et al.* [73]		30.00	4.00	7.50	1.95
Casciati and Al–Saleh [79]		39.24	5.96	6.58	1.05
Kohan *et al.* [82]		41.40	7.60	5.45	1.37
Bongiovanni *et al.* [67]	Brick masonry	18.50	3.00	6.17	2.43
Carone *et al.* [69]		20.00	3.50	5.71	2.63
Sepe *et al.* [1]		28.00	8.20	3.41	2.40
Ivorra *et al.* [76]		35.50	7.00	5.07	2.15
Ivorra and Pallares [38]		41.00	5.60	7.32	1.29
D'Ambrisi *et al.* [9]		41.80	6.00	6.97	1.08
Russo *et al.* [16]		58.00	7.60	7.63	0.61
Gentile and Saisi [32]		74.00	6.00	12.33	0.59
Camata *et al.* [68]	Stone masonry	19.00	5.40	3.52	3.78
Ramos *et al.* [70]		20.40	4.50	4.53	2.56
Bayraktar *et al.* [48]		23.00	5.00	4.60	2.59
Guerreiro and Azevedo [72]		30.00	8.00	3.75	1.37
Ceriott *et al.* [74]		31.00	8.00	3.88	1.25
Foti *et al.* [75]		34.70	4.11	8.44	4.57
Gentile and Sais [77]		36.72	5.70	6.44	1.21
Peeters *et al.* [81]		41.00	7.00	5.86	1.57
Buffarini *et al.* [18]		43.00	6.50	6.62	1.48
Ferraioli *et al.* [11]		45.50	14.00	3.25	1.05
Costa [84]		55.00	8.00	6.88	1.05
Diaferio *et al.* [85]		57.00	7.50	7.60	2.04
Pieraccini *et al.* [86]		87.40	14.50	6.03	0.62
Ivorra and Cervera [78]	Stone masonry + Brick masonry	37.19	4.68	7.95	0.73
Balduzzi *et al.* [80]		40.00	4.00	10.00	1.36
Ferraioli *et al.* [11]		41.00	11.30	3.63	1.26
Jaras *et al.* [83]		49.90	12.60	3.96	1.25
Bartoli *et al.* [13]		60.00	9.50	6.32	1.31
Ceroni *et al.* [62]		68.00	11.00	6.18	0.69

Table 2.2: Database compiled from the literature review for masonry minarets

Reference	Type of masonry	Total height, *H* (m)	Min. breadth at base, *B* (m)	Slenderness, H/B	Experimental natural frequency (Hz)
Oliveira *et al.* [26]	Brick masonry	23.02	3.73	6.17	1.68
		38.65	3.68	10.50	0.80
		41.60	3.97	10.48	1.37
		48.70	4.64	10.50	1.18
		51.70	5.12	10.10	0.95
		63.20	4.96	12.74	1.02
		66.55	7.52	8.85	1.32
		66.55	7.52	8.85	1.17
		74.40	6.50	11.45	0.83
Zaki *et al.* [87]	Stone masonry	20.00	3.40	5.88	1.84
El–Attar *et al.* [41]		24.48	3.80	6.44	1.95
Pau and Vestroni [88]		30.00	3.55	8.45	1.45
Turk and Cosgun [89]		40.25	3.00	13.42	0.88
Oliveira *et al.* [26]		44.96	5.28	8.52	1.03
Krstevska *et al.* [90]		47.00	3.00	15.67	1.04
Oliveira *et al.* [26]		54.90	4.80	11.44	0.63

Table 2.3: Database compiled from the literature review carried industrial masonry chimneys

Reference	Type of masonry	Total height, *H* (m)	Min. breadth at base, *B* (m)	Slenderness, H/B	Experimental natural frequency (Hz)
Aoki and Sabia [91]	Brick masonry	15.00	1.96	7.65	2.69
Costa [92]		22.86	2.20	10.39	1.37
Yamamoto and Maeda [93]		23.10	2.34	9.87	1.00
Eusani and Benedettini [95]		36.00	3.40	10.59	0.93
Lopes *et al.* [15]		41.40	3.70	11.19	0.61
Costa *et al.* [96]		45.60	4.30	10.60	0.79
Grande and Açores [94]	Stone masonry	31.00	4.00	7.75	1.13

Table 2.4: Database compiled from the literature review carried Nepalese Pagoda temples

Reference	Type of masonry	Total height, *H* (m)	Min. breadth at base, *B* (m)	Slenderness, H/B	Experimental natural frequency (Hz)
Jaishi *et al.* [97]	Brick masonry	10.00	3.00	3.33	3.10
Shakya *et al.* [98]		12.76	3.48	3.67	2.06
Jaishi *et al.* [97]		16.93	10.20	1.66	2.32
		27.00	6.58	4.10	1.68

The database information regarding dynamic properties shows the frequencies of the reviewed structures. It is noticeable in the database that the fundamental frequency of slender masonry structures is highly influenced by height of the structure and slenderness ratio (i.e. the taller the structure the lower the fundamental frequency and similarly higher the slenderness ratio lower the fundamental frequency). The database reveals that the tower structures have third mode shape as torsion. All the experimental frequency for various

slender masonry structures presented here in database is measured by different authors using ambient vibration test. Note that there is much less information regarding dynamic properties of chimneys and Pagoda temples because research in these types of structures is taking its 1st step.

2.3.1 Formulation for computing the fundamental frequency/period of tower and cantilever structures

The empirical formulation proposed for the prediction of fundamental period/frequency for bell tower/cantilever structures by different codes and authors are taken as a basis for developing new empirical formulae for such structures. Later, the predictive performance between previous author's formulations and newly developed formulation are compared with reference to the experimental fundamental frequency.

A linear relation between the fundamental vibration period (T_1) and the height (H) of the tower proposed by Faccio *et al.* [99] is:

$$T_1 = 0.0187H \tag{2.1}$$

The formulation in Eq. (2.1) better fits the experimental data, for slender structures with a period lower than 1sec, however, it slightly underestimates the period higher than 1sec [12].

An empirical correlation for the prediction of the natural period (T_1) of Italian masonry towers as a function of height (H) has been proposed by Rainieri and Fabbrocin [12]:

$$T_1 = 0.01137H^{1.138} \tag{2.2}$$

Eq. (2.2) leads to an overestimation for low values of the natural period and to an underestimation at the higher values of the natural period [12].

From Eq. (2.3), proposed by the Spanish Standard NCSE–02 [100], the value of the estimated fundamental frequency of towers (f_1) can be obtained by:

$$f_1 = \frac{\sqrt{L}}{0.06\sqrt{\frac{H}{2L+H}}} \tag{2.3}$$

where, L is the plan dimension of the building in the direction of oscillation, H is the height of tower.

Eq. (2.3) leads to an overestimation for low values of the natural period and to an underestimation for higher values of the period [12].

The first frequency of vibration (f_1) for cantilever [101] is given by:

$$f_1 = \frac{1}{2\pi}(1.875)^2\sqrt{\frac{EI}{\overline{m}L^4}} \tag{2.4}$$

where, E is the modulus of elasticity, I the moment of inertia, $\overline{m}$ the mass per unit of length, and L the total length of the cantilever.

2.3.2 Empirical formulae for computing the fundamental frequency of slender masonry structures

On the basis of previous formulations and compiled database, four new empirical formulations are developed for the reliable prediction of fundamental frequency of slender masonry structures. Each formulation is further expressed in three sub formulations depending upon different multiplication factors, for three different structures categories (i.e. all types of slender masonry structures, towers (bell tower, clock tower, civic tower etc.) and minarets). Linear R squared approach is carried out to evaluate the predictive performance of these proposed empirical formulations.

On the basis of power correlation with the experimental fundamental frequency, the first formulation for predicting fundamental frequency (f_1) is developed as a function of height (H), which is presented in Eq. (2.5)

$$f_1 = \frac{1}{\alpha H^{\beta}} \tag{2.5}$$

where,

α = 0.0517 and β = 0.76 (for all types of slender masonry structures); with R^2 = 0.59

α = 0.0151 and β = 1.08 (for masonry tower structures); with R^2 = 0.73

α = 0.1178 and β = 0.533 (for masonry minaret structures); with R^2 = 0.59

On the basis of Eq. (2.3) formulation, here is suggested a second formulation (Eq.(2.6)) for the prediction of the fundamental frequency (f_1) of slender masonry structures as a function of the height *(H)* and the minimum breadth at base *(B)*:

$$f_1 = \frac{(B)^{\varphi}}{CH\left(\frac{H}{B+H}\right)^{\delta}} \tag{2.6}$$

where,

C = 0.038, φ = 0.25 and δ = 1 (for all types of slender masonry structures); with R^2 = 0.89

C = 0.03, φ = 0.17 and δ = 0.5 (for all masonry tower structures); with R^2 = 0.96

C = 0.1, φ = 1 and δ = 1 (for all masonry minaret structures); with R^2 = 0.46

Retaining the basic structures of Eq. (2.4), where fundamental frequency of a slender structure is expected to be a function of the second moment of area *(I)*, height of the structures *(H)*, young's modulus of elasticity *(E)* and the mass per unit of length *($\overline{m}$)*, a third formulation (Eq. (2.7)) for the prediction of the fundamental frequency (f_1) of slender masonry structures is proposed accounting for all these parameters.

$$f_1 = \frac{1}{2\pi}(1.875)^2\sqrt{\frac{XEI}{\overline{m}H^4}} \tag{2.7}$$

where,

X = 1.425 (for all types of slender masonry structures); with R^2 = 0.56

X = 1.375 (for all masonry tower structures); with R^2 = 0.48

X = 1.345 (for all masonry minaret structures); with R^2 = 0.89

On the basis of power correlation with the experimental fundamental frequency, the formulation for predicting fundamental frequency (f_1) is developed as a function of minimum slenderness ratio, i.e. height (H) to minimum breadth at base ratio (B), which is presented in Eq. (2.8).

$$f_1 = Y\left(\frac{H}{B}\right)^{-Z} \tag{2.8}$$

where,

Y = 3.648 and Z = 0.55 (for all types of slender masonry structures); with R^2 = 0.33

Y = 3.58 and Z = 0.57 (for masonry tower structures); with R^2 = 0.20

Y = 8.03 and Z = 0.86 (for masonry minaret structures); with R^2 = 0.58

Here, the newly developed formulations expressed in Eq. (2.5), Eq. (2.6) and Eq. (2.8) are basically function of geometrical characteristics whereas Eq. (2.7) is the function of both geometrical and mechanical characteristics. These formulations have been compared with experimental database and previous formulations by other authors for validation.

2.3.3 Predictive performance compared results

The fundamental frequency predicted by the proposed empirical formulations is compared with previous authors' estimation and also with the experimental fundamental frequency. Moreover, predictive performance of proposed sub–formulations for various types of slender masonry structures is also compared for validation of their reliability.

Figure 2.4 illustrates the comparison between the experimental and empirical fundamental frequency expressed according to different predictive formulations for all types of slender masonry structures. Results reveal that empirical formulation proposed by Faccio *et al.* [99] and Rainieri and Fabbrocin [12], leads to an overestimation of the fundamental frequency for slender structures of height between 15m to 50m, while the values from Eq. (2.5) better fit the experimental fundamental frequency.

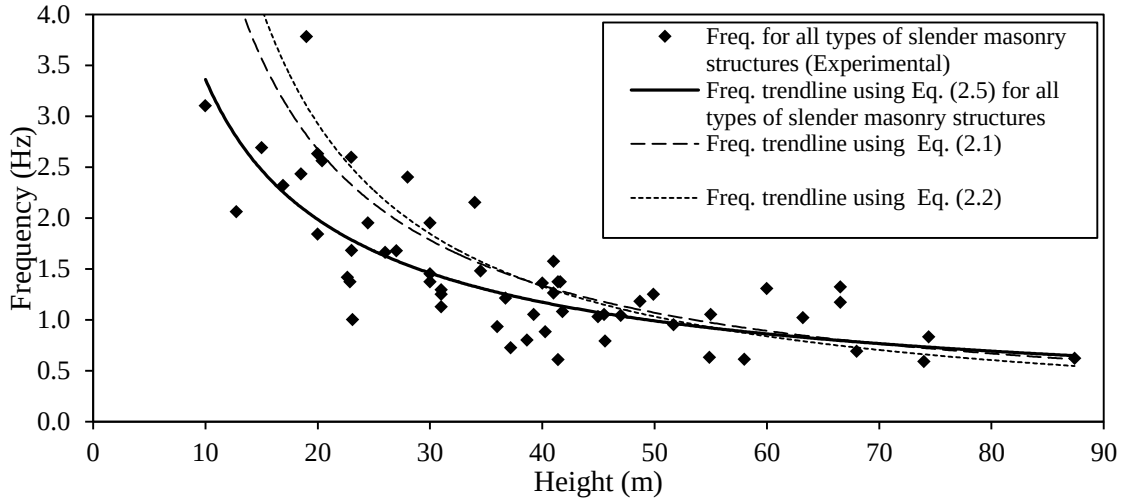

Figure 2.4: Comparison between experimental and predicted values of the fundamental frequency of slender masonry structures according to different formulation

Figure 2.5 illustrates the comparison of empirical fundamental frequency expressed by Eq. (2.5) for different types of slender masonry structures. Results reveal that the fundamental frequency predicted by three different sub–formulations (i.e. for all types of slender masonry structures, towers and minarets) derived from Eq. (2.5), using different numerical values for factor α and β, have different trendlines, which suggest, it is not reliable to estimate the fundamental frequency for all types of slender masonry structures using a single formulation. Therefore, for the better predictive performance, it is better to estimate using individual formulation presented in Eq. (2.5).

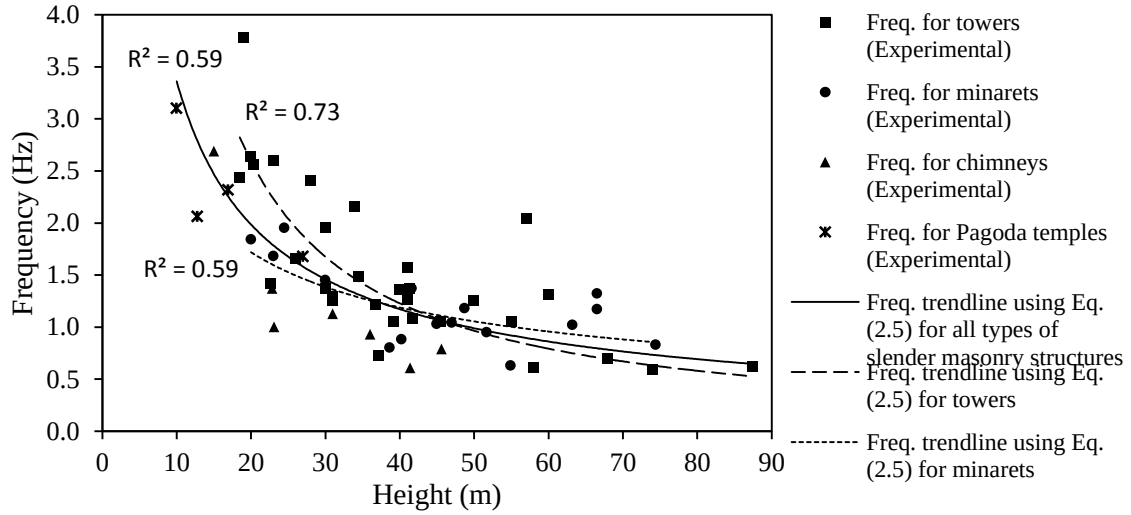

Figure 2.5: Comparison of the fundamental frequencies predicted by three different sub–formulations of Eq. (2.5) for all types of slender masonry structures, towers and minarets

Similarly, Figure 2.6 illustrates the comparison between experimental and empirical fundamental frequency expressed according to NCSE–02 [100] and Eq. (2.6). Results show that empirical formulation proposed by NCSE–02 [100], leads to an underestimation of fundamental frequency for the slender masonry structures 15m to 40m height, while the values from Eq. (2.6) formulation better fit the experimental fundamental frequency.

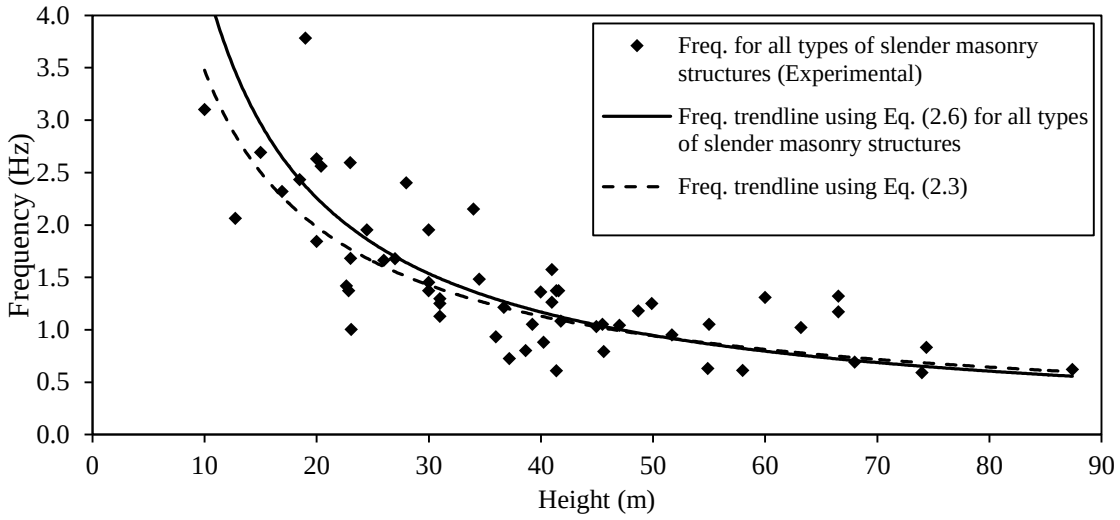

Figure 2.6: Comparison between experimental and predicted values of the fundamental frequency according to Eq. (2.3) and Eq. (2.6) for all types of slender masonry structures

Result of the comparison between empirical fundamental frequencies expressed by Eq. (2.6) for different types of slender masonry structures is shown in Figure 2.7. Here, the result reveals that the fundamental frequency predicted by three different sub–formulations (i.e. for all types of slender masonry structures, towers and minarets) derived from Eq. (2.6), using different numerical values for factor C, φ and δ, have a similar trendline, which suggests that it is reliable to estimate fundamental frequency for all types of slender masonry structures including towers with the same formulation. However, results also show that sub–formulation derived from Eq. (2.6) for the minarets has a different trendline than others, which means that for the better predictive performance, it is better to estimate the fundamental frequency of minaret structures using different formulation presented in Eq. (2.6).

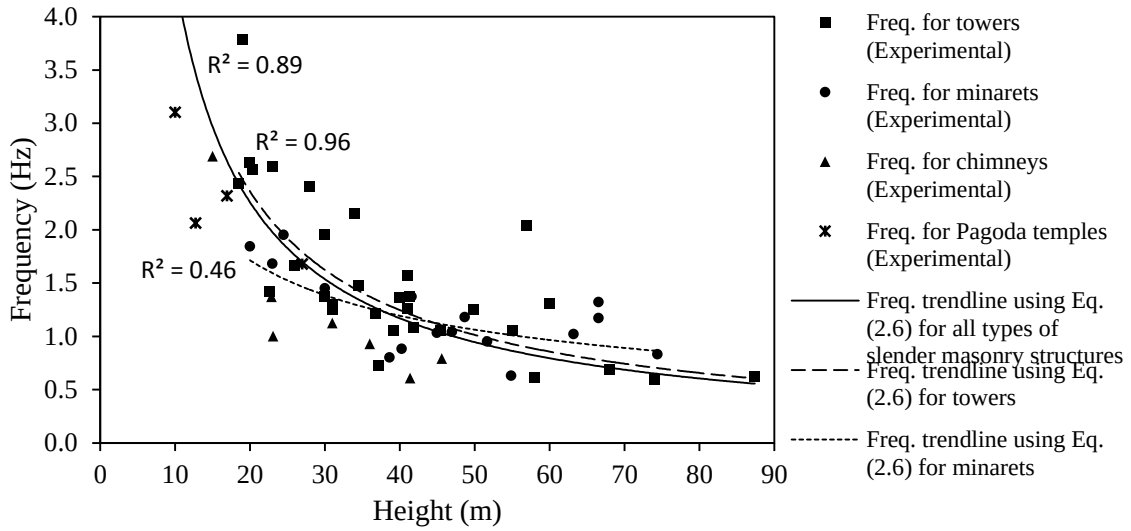

Figure 2.7: Comparison of the fundamental frequencies predicted by three different sub–formulations of Eq. (2.6) for all types of slender masonry structures, towers and minarets

Figure 2.8 illustrates the comparison between experimental and fundamental frequency expressed according Eq. (2.4) and Eq. (2.7). Results show that formulation proposed in Eq. (2.4), leads to an underestimation of fundamental frequency, while the values from Eq. (2.7) formulation better fit the experimental fundamental frequency.

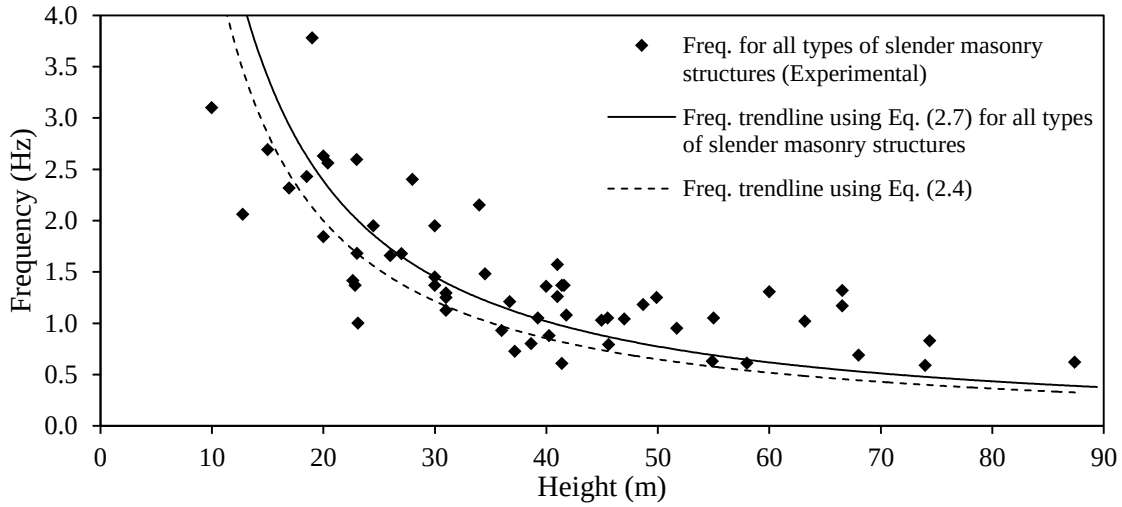

Figure 2.8: Comparison between experimental and predicted values of the fundamental frequency according to Eq. (2.4) and Eq. (2.7) for all types of slender masonry structures

Figure 2.9 illustrates the comparison of empirical fundamental frequency expressed by Eq. (2.7) for different types of slender masonry structures. Result reveals that the

fundamental frequency predicted by three different sub–formulations (i.e. for all types of slender masonry structures, towers and minarets) derived from Eq. (2.7), using different numerical values for factor X, have similar trendlines, which suggest that it is reliable to estimate the fundamental frequency for all types of slender masonry structures including towers and minarets resourcing to a single formulation. But, for the better predictive performance, it is better to estimate using individual formulation presented in Eq. (2.7).

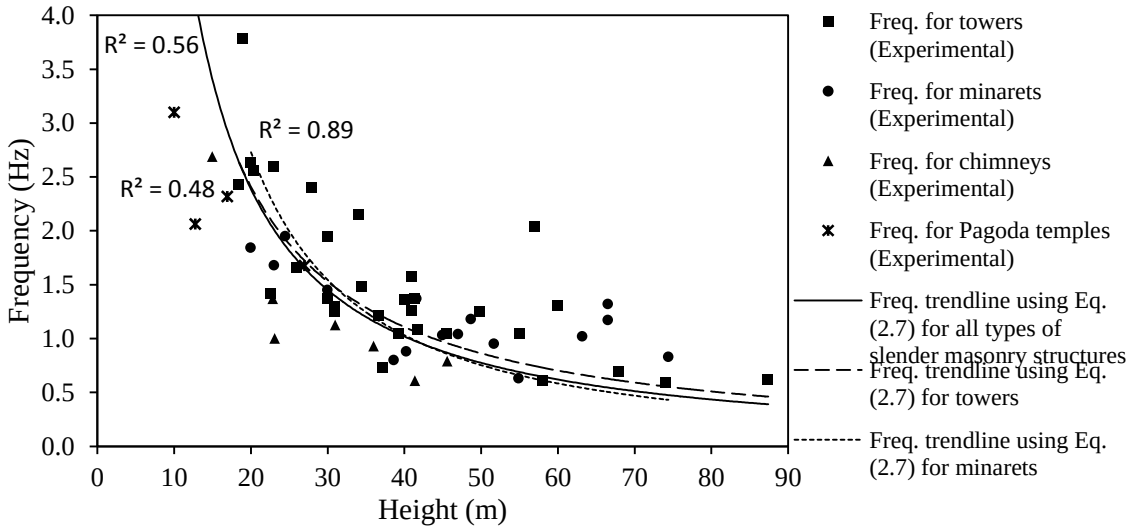

Figure 2.9: Comparison of the fundamental frequencies predicted by three different sub–formulations of Eq. (2.7) for all types of slender masonry structures, towers and minarets

Lastly, Figure 2.10 illustrates the comparison between experimental and empirical fundamental frequency expressed according Eq. (2.8) for all types of slender masonry structures. Result shows that an empirical formulation proposed, lead to better fit the experimental fundamental frequency.

Figure 2.11 illustrates the comparison of empirical fundamental frequency expressed by Eq. (2.8) for different types of slender masonry structures. Result reveals that the fundamental frequency predicted by three different sub–formulations (i.e. for all types of slender masonry structures, towers and minarets) derived from Eq. (2.8), using different numerical values for factor Y and Z, have a similar trendline, which suggest that it is reliable to estimate fundamental frequency for all types of slender masonry structures including towers with the same formulation. However, results also show that sub–formulation derived from Eq. (2.8) for the minarets has a different trendline than others, which means that for the better predictive performance, it is better to estimate the

fundamental frequency of minaret structures using different formulation presented in Eq. (2.8).

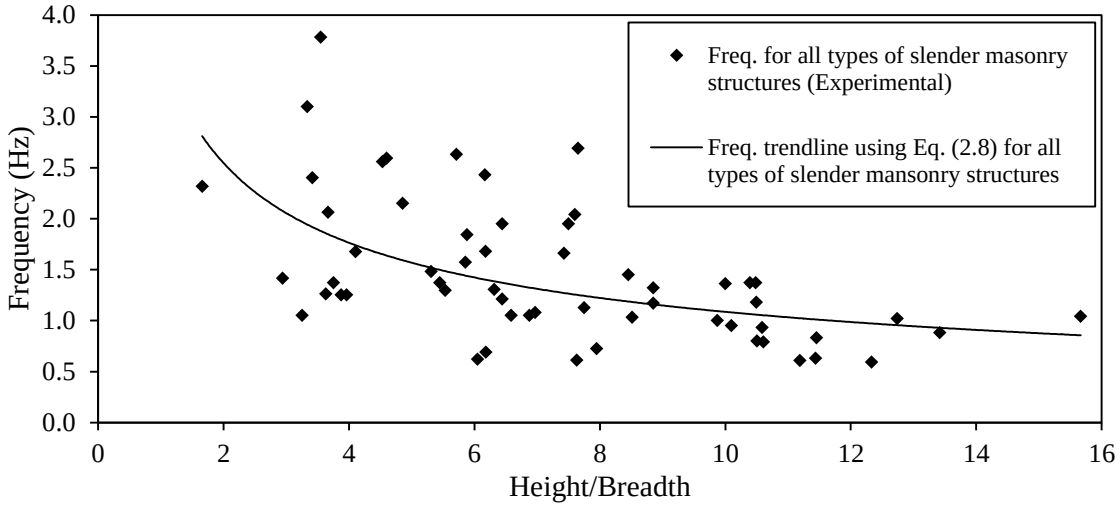

Figure 2.10: Comparison between experimental and predicted values of the fundamental frequency according to Eq. (2.8) for all types of slender masonry structures

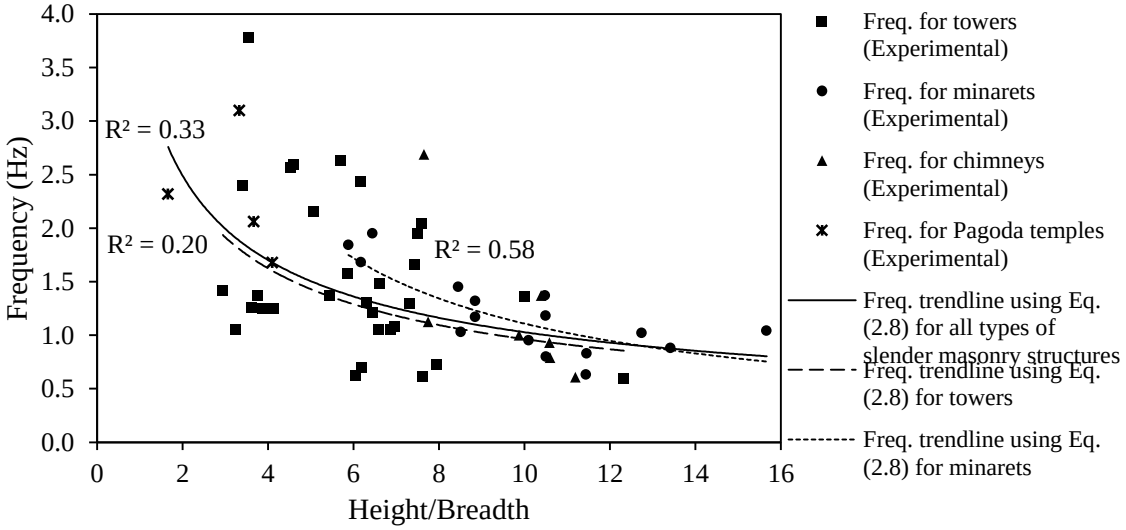

Figure 2.11: Comparison of the fundamental frequencies predicted by three different sub–formulations of Eq. (2.8) for all types of slender masonry structures, towers and minarets

Among all of four empirical formulation proposed, Eq. (2.6) has the highest linear R squared value (R^2), which obviously is the best predictive performance formulation for all types of slender masonry structures.

2.4 Conclusions

Researchers have identified that one of the most important parameters that determines the vulnerability of such kind of structures is its slenderness. At present, many studies are available in the technical literature for the numerical/experimental analysis of slender masonry structures. A main issue in the seismic behaviour of slender masonry structures is the influence of the axial stresses induced by gravity loads, whose values are often of the same order of magnitude as the ultimate compression of the masonry material. This behaviour, combined with the dynamic characteristics of the seismic action represents a major challenge.

In the present chapter the database compiled is the key constituent in the calibration of empirical formulations for the prediction of the fundamental frequency for slender masonry structures. Data was collected through literature review on slender masonry structures regarding experimental natural frequency, geometrical and mechanical characteristics. The experimental fundamental frequencies have been correlated to develop an empirical formulation for the prediction of the fundamental frequency of slender masonry structures. Based on all documented and validated experimental data, reliable empirical formulations for the better prediction of the fundamental frequency for slender masonry structures are proposed. Comparative results confirm that the newly developed formulation has a reliable predictive performance.

CHAPTER 3

NEPALESE PAGODA TEMPLES: A SENSITIVITY ANALYSIS

Summary *This chapter corresponds to a second intensive literature review regarding seismic history, seismic performance, construction system and researches carried on Nepalese Pagoda temples. Moreover, this chapter also presents the task carried out to analyze particular structural fragilities and characteristics of the historic Nepalese Pagoda temples which affect their seismic performance.*

Chapter outline

3.1 Introduction

Nepal is located in a highly active tectonic region of the Himalayan belt, one of the most severe earthquake prone areas of the world. Nepal is lying between the Indian and the Eurasian plate, which are moving continuously, resulting in frequent devastating earthquakes. Cultural heritage buildings and monuments are, therefore, at risk, and the eventual cultural loss in the consequence of an earthquake is incalculable. Post–seismic

surveys of past earthquakes have shown the potential damage that unreinforced masonry structures, particularly Pagoda temples, may suffer in future earthquakes.

Most of the Nepalese Pagoda temples, erected during 14th century, are considered non–engineered constructions that follow very simple rules and construction detailing in respect to seismic resistance requirements and, in some cases, without any concern for seismic action. Presently, conservation and restoration of Nepalese temples is one of the major concerns, since they are considered world heritage with universal value. The present research is devoted to outline particular building characteristics of the UNESCO classified Nepalese Pagoda temples and the common structural fragilities, which may affect their seismic performance. Moreover, based on a parametric sensitivity analysis, structural weaknesses and fragilities of Pagoda temples were identified associated to the local and traditional construction techniques, detailing and common damages.

3.2 State of the art on Nepalese Pagoda temples

3.2.1 History of Nepalese Pagoda temples

Nepalese Pagoda temples, built as a structure reserved for religious or spiritual activities, began to appear around the middle of 14th century during the *Malla* Dynasty (1200–1768) [102]. Almost all the monuments, independence/irrespective of types, such as different tiered roof temples, *pati, sattal, monastris, dhungedhara, chaityas, viharas, stupas*, etc. and traditional private houses that belong to the *Malla* period which is also known as the medieval period. These monuments were constructed when there were no mechanical and technical facilities and were handcrafted to a high quality and in a vast quantity, with the best available materials and skills at the time of their construction [103].

3.2.2 Structural characterization of Nepalese Pagoda temples

The main peculiarities of Pagoda temples in comparison to other traditional masonry structures are their considerable wall thickness, multi–tiered roof, box type configuration, and considerable plinth section and height (see Figure 3.1). These structures are constructed using brick masonry and timber members with tiles or metal roof coverings.

Figure 3.1: Nepalese Pagoda temples

3.2.2.1 Foundations

Conservation works are usually done plinth upwards, therefore, the foundation of existing temples have rarely been studied in depth, and hence the condition of foundations is unknown. After the 1934 earthquake some temples were rebuilt over the old foundation, since those still presented good condition. The foundation of the tiered temple is often just as wide as the plinth platform itself and appears as a masonry mat foundation. This has led many observers (apparently expecting a foundation in the pattern of stepped footings for the main masonry walls) to suggest that tiered temples had no foundation at all [104]. Observations of existing temples with high plinth show that it is usual for the plinth mat to be built directly off the ground level or on a thin brick soling. However, the temples with shallow plinths rise from some depth below ground. As for the foundation and massive plinth (1 to 5m height) in pyramid shape, these yield even more complexity.

Figure 3.2a and Figure 3.2b show schematic examples of the foundation of Nepalese Pagoda temples with low and high plinth, respectively. These expressive plinth base massive foundations will benefit to eliminate the earthquake risks associated with soft soils [105].

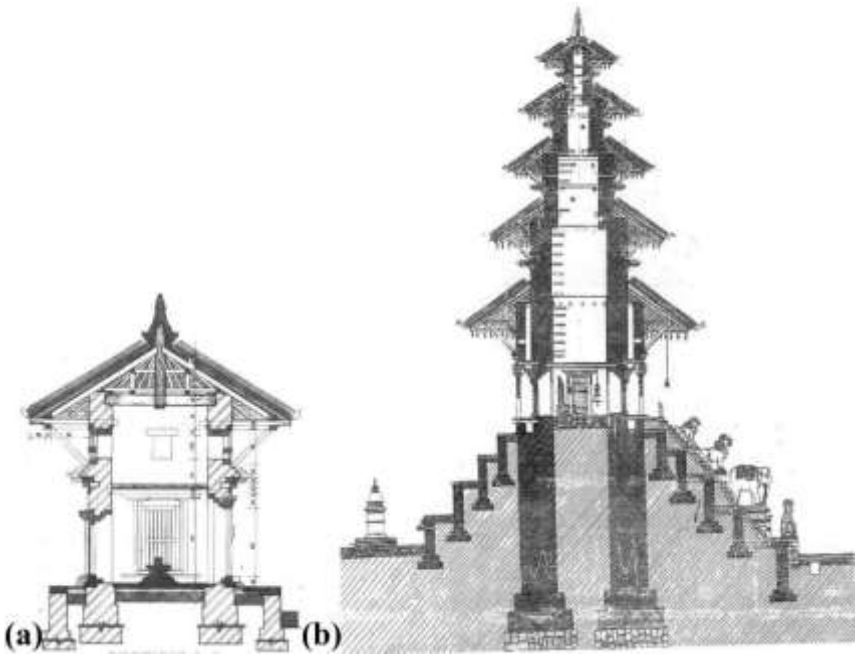

Figure 3.2: Temple section with foundation: a) *Shiva* temple; b) *Nyatopol* temple [106]

3.2.2.2 Masonry walls

Brick masonry walls constructed in the longitudinal and transverse directions are the main load bearing system in these temples. In case of multi–tiered temples, wall thickness is not the same for every storey, it reduces from ground storey to top tower (see Figure 3.2b). The thickness of the masonry walls range from 50cm to 75cm and were constructed with three layers in a single cross–section as shown in Figure 3.3. The outer faces of the walls are made of fired clay bricks with smooth finishing and inner face is made of sun dried bricks [107]. Outer and inner face wall layer was not well connected with the middle core wall. Normally, the middle core is filled with rubble stone, brick fragment and mud, which made the wall very poor to withstand in some cases heavy load from the main structure. Similar multi–leaf masonry walls construction practice in several buildings of the historical city centers of L'Aquila and Castelvecchio Subequo is reported by Indirli *et al.* [108]. The bonding mortar inside the massive walls is not visible from the outside but has a very significant influence on the structural strength and capacity of the temples. In many temples, yellow clay mortar, mud mortar and, more rarely, lime–surkhi mortar was used [109]. The main masonry wall system arrangements and fabric of existing multi–tiered temples are shown in Figure 3.4.

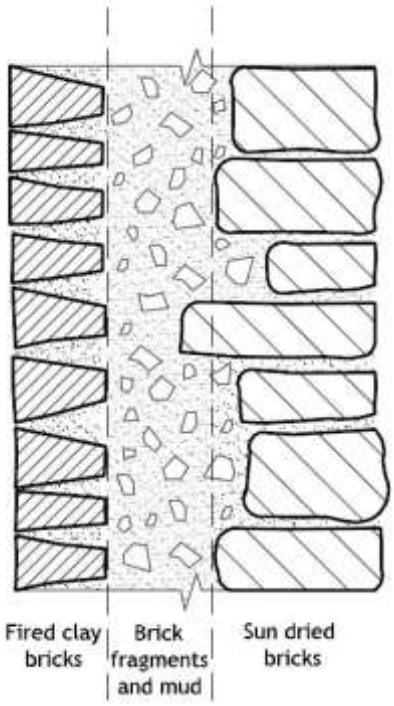

Figure 3.3: Traditional wall section

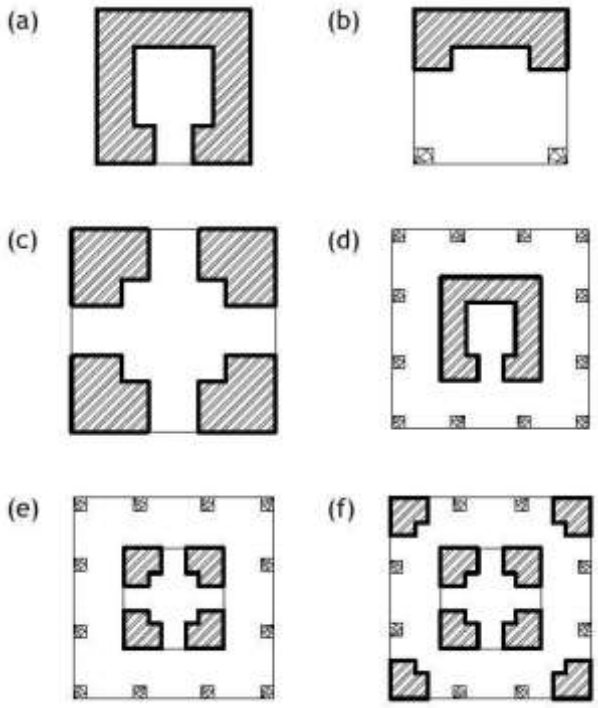

Figure 3.4: Schematic representation of wall system of Nepalese Pagoda temples: a) one sides open; b) three sides open; c) four sides open; d) walk way between outer colonnade and inner wall, inner wall with one door opening; e) walk way between outer colonnade and inner wall, inner wall with four door openings; f) double wall system, walkway between walls, all four sides door openings

3.2.2.3 Timber members

The Pagoda temple height ranges from one to five tier symmetric structures with brick masonry and timber elements. The ground floor consists of a Sal wood (*Shorea Robusta*) timber framing system. These frames arrangements support the wall of 2.5 to 3.5m height above it, which supports the first roofing system and also has decorative features. The sections marked in Figure 3.5 reveal the traditional construction of the top tower, which rest on timber joists and timber columns along with timber beams, supporting the walls above. The timber columns at the base level stand on a stone base with a small pin inserted into the stone and the top of the timber column's pin goes through the beam, as shown in Figure 3.6.

Most of the temples have timber first floors, built using simple battens or joists upon which timber planks are laid. These in turn support the final floor finish. This technique closely resembles to the ancient masonry buildings floor structure construction practice throughout Europe [110]. Given that Nepal is located in an earthquake prone zone, some

carpenters have developed their construction techniques accordingly, providing additional bracing by linking the vertical and horizontal structural components [111]. This practice is very effective in preventing relative slippage effect of the floor structure on the walls in the presence of lateral forces and hence creating a box–type behaviour response. This connection is made using wedges (timber peg) that fix the wall plate along the perimeter through the joists that run inside and outside the building, as shown in Figure 3.7. The wall plate, which runs throughout the perimeter of the wall constituting a type of ring–beam, allows a better distribution of the dead and live loads along the wall length, also allowing a better in plane stiffness and stress distribution [112]. The floor is then joined to the horizontal frame (wall plate) using battens, some of which also run through the wall and are fixed in position using wooden wedges. But, in many of temples structural floor system are constructed by simply laying timber joists in one direction and there is no anchoring scheme of the joist with the walls, as shown in Figure 3.8.

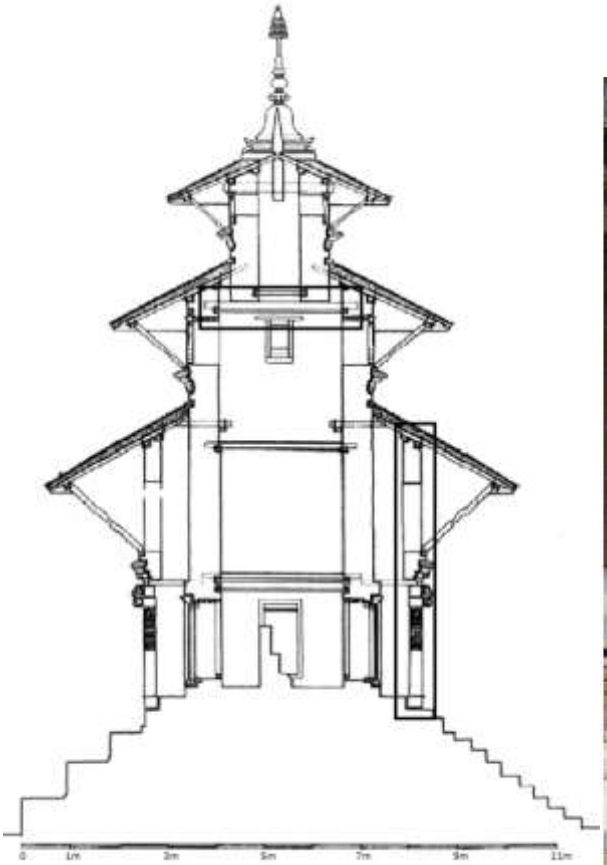

Figure 3.5: Section of *Narayan* temple [106]

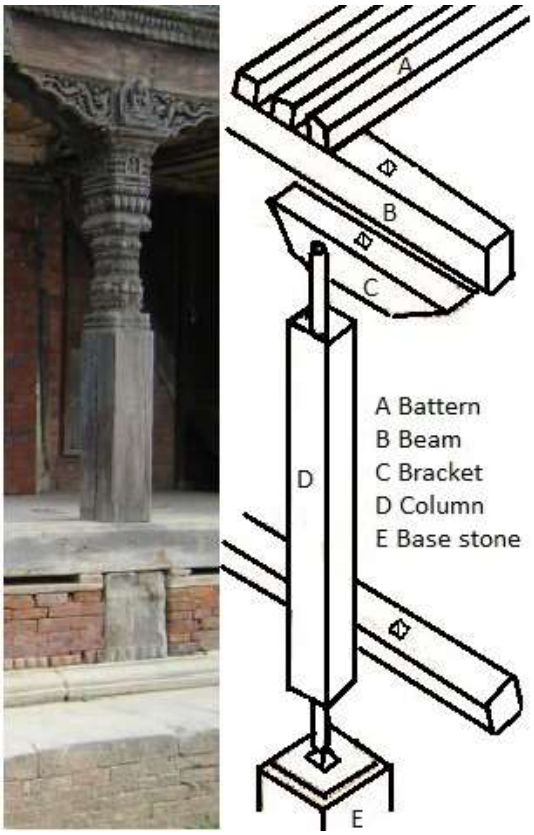

Figure 3.6: Beam–column joint system

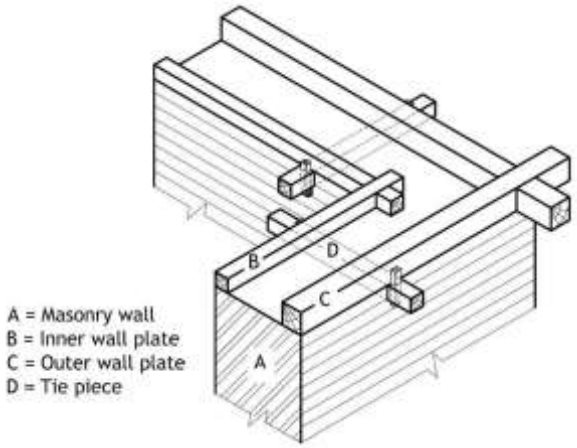

Figure 3.7: Inner and outer wall plate

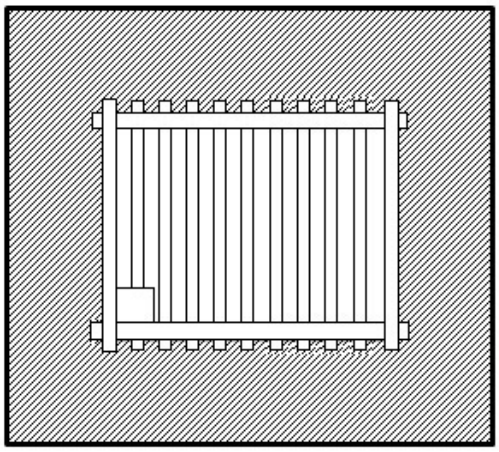

Figure 3.8: Floor system

3.2.2.4 Roof system

In respect to the roofing system, the temples can be distinguished as one roof, two roofs, three roofs up to five roof temple. Similarly, according to roof style, temples can be divided as either Pagoda style or *Sikhara* style. Temple roofs have symmetrical pitches springing from the central point of the inner masonry cell. The pitches are constituted by small rafters that spring from the corners in a radial arrangement [111]. In Figure 3.9 is shown the typical roof construction system of Pagoda temples. The inner end of diagonal rafters connected to the wall plate or to timber post (in case of top roof), at the intermediate length are supported by wall plates laid on the wall, and the outer part rests on the purlins. The whole roof dead load is supported by rafters, which transfer to wall plates and purlins. Simple timber pegs are inserted through roof rafters to brace them against the wall plates and purlins in which they rest, as shown in Figure 3.10 and Figure 3.11 respectively, which is the most common traditional timber joinery detail.

Moreover, the inclined timber struts are the members that hold the roof by transferring load from purlins to the wall section, but there is no rigid connection in between strut with purlin and load bearing masonry wall of the temple, as shown in Figure 3.12. The only rigid connection is with the eaves board at the edge, which are not very strong to sustain large displacements [109]. A huge overhanging roof structure with high dead load, supported by the struts is another weak point of the temple structures. The heavy mud layer under the tiles, combined with the large surface of the roofing system, have a large influence on the total weight of the temple as referred 15–20% and, consequently, a large impact on earthquake demands.

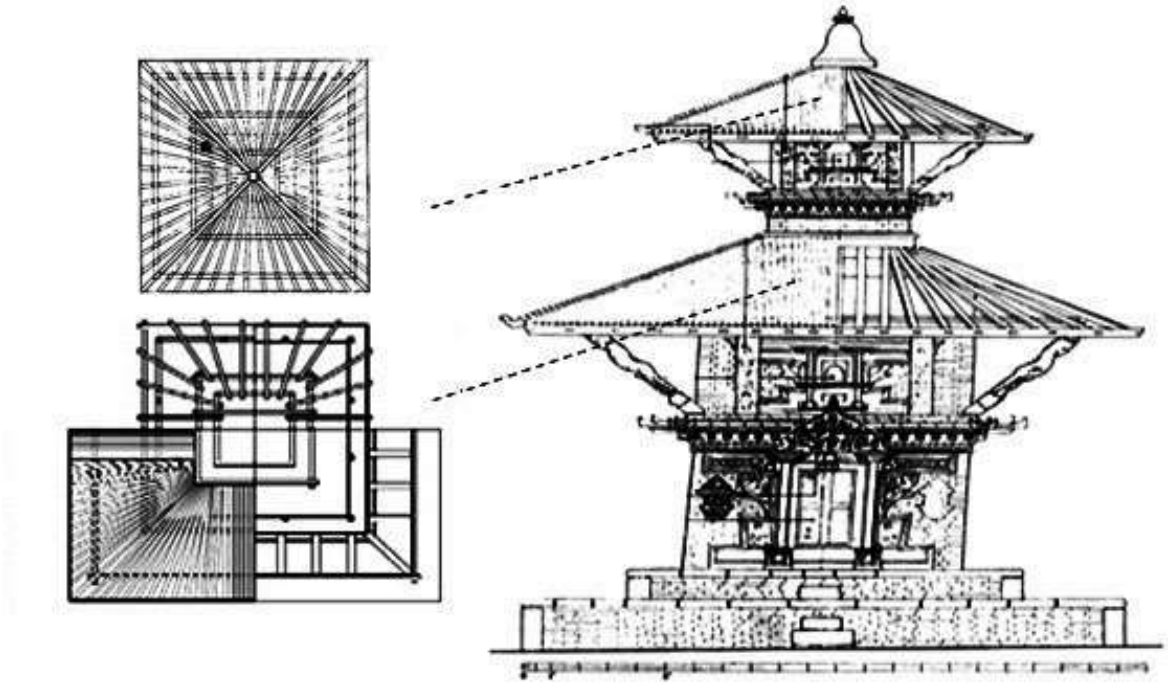

Figure 3.9: Roof construction system in Pagoda temples [106]

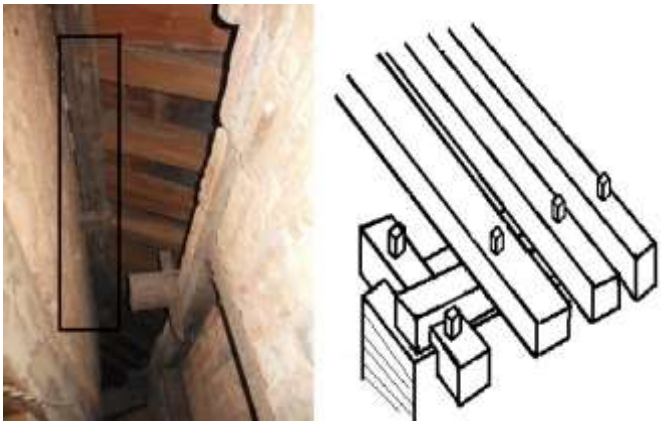

Figure 3.10: Rafter and wall plate joint at upper end (left) and above wall (right)

Figure 3.11: Detail timber peg joint

Figure 3.12: Timber struts

3.2.3 Seismic behaviour of Nepalese Pagoda temples

Nepalese Pagoda temples were constructed when there were no mechanical and technical facilities and were handcrafted to a high quality with the best available materials and workmanship at the time of their construction [103].

The 1934 earthquake post–earthquake photographic information, as shown in Figures 3.13 and 3.14, reveal that a vast number of monuments were destroyed by the quake. Cultural heritage buildings and monuments are, therefore, at risk, and the eventual cultural loss in the consequence of an earthquake is incalculable. Post–seismic surveys of past earthquakes have shown the potential damage that unreinforced masonry structures, particularly Pagoda temples, may suffer in future earthquakes [109].

Figure 3.13: Bhaktapur Darbar Square world heritage site before and after 1934 earthquake [109]

Figure 3.14: Kathmandu Darbar Square world heritage site after 1934 earthquake [109]

The traditionally built temples have evolved through many years of building experience from the 12th to the 18th centuries. Practical earthquake experience has been incorporated in the construction during those centuries. Some important features of traditional construction techniques in respect to Pagoda temples are pointed out by Nienhuys [105]:

- A symmetrical construction (square floor plan) is in general less vulnerable to earthquakes than a unsymmetrical construction;
- A huge massive plinth avoids shear at the foundation level. Such plinth may redistribute shear forces throughout the structure, thus partly absorbing the impact of strong earthquake jolts;
- A conical mass distribution with a wide base is difficult to push over. When a mass needs to be pushed over a leaning support, it will withstand most earthquakes;
- A concentric support structure with interconnected columns will function as a table on slightly movable legs.

On the basis of the above basic mentioned traditional technology features, it can be said that our ancestors have learned by trial and error on earthquake construction techniques. However, most of the Nepalese Pagoda temples were erected following very simple construction rules and details, to comply with seismic resistance requirements [113]. Structural characteristics in the historical design and configuration of the Nepalese Pagoda temples which affect performance in an earthquake are outlined by Theophile *et al.* [114]:

- Lack of vertical structural continuities is created by the resting of upper temple level on timber beams rather than directly on the wall structure below. This configuration puts the temple at risk to withstand the lateral forces of an earthquake;
- Lateral forces of an earthquake are exacerbated by the top heaviness of the structure created by the great mass of mud and tile covered roof;
- Ambulatory–like arcades at base level create a soft ground floor, a weak zone which may fail before it transfers the earthquake's demands from ground to upper areas of the temple;
- Overall looseness of the structure detracts from performance in an earthquake. Lack of rigid connections are found in a poor through–wall bonding of the multi–layer masonry wall, structurally deficient timber joinery and traditional timber pegged joints, rigid in only one direction.

3.2.4 Previous research on Nepalese Pagoda temples

3.2.4.1 Material properties of structural components

In many cases geometry of the structure, or the mechanical characteristic of construction materials, are not sufficiently known to conduct a structural safety assessment problem, so numerical models cannot carry out a reliable simulation of expected on plausible behaviours. Therefore the evaluation of the mechanical properties, especially of masonry is necessary to determine the seismic vulnerability of existing constructions and to eventually design seismic retrofitting strategies. It is crucial to have experimental data collected to characterize old and existing structures [115]. Sufficient research has not been carried out on traditional construction technology and materials used in Nepalese Pagoda temples. However, some experimental research work carried out to derive the mechanical properties of traditional masonry constructions in Nepal, providing valuable information for the numeric modeling of temple structures ahead.

Thapa [107] carried out research work with the objective of determining the various mechanical properties of traditional materials related with brick masonry to apply as input in seismic analysis of historical masonry structures of Nepal. The sample and the testing application used in test process are shown in the Figure 3.15. And the results obtained are summarized in Table 3.1.

Figure 3.15: Test setup on brick masonry wall [107]

Table 3.1: Mechanical properties of traditional masonry materials [107]

Material	Experiment setup and type	Specific weight (kN/m^3)	Young's modulus (MPa)	Shear modulus (MPa)	Average compressive strength (MPa)	Average shear strength (MPa)
Mud mortar	Compression test on cubes	17.5	34.5	–	1.09	–
Brick unit	Compression test on cubes	13.5	–	–	9.18	–
Mud masonry brick wall panel	Compressive test	19	–	–	0.56	–
	Combined loading test	19	632	253	–	0.14
	Diagonal compression test	19	336	172	–	0.14

The above results were obtained from tests carried out on bricks collected from old ruined masonry buildings, which are representative of materials typically used. The tested results on brick masonry and its units represent reliably the characteristics of the existing brick masonry of temple structures, due to the fact that both structures where built in the same period.

In the work of Jaishi *et al.* [97], allowable stresses for brick masonry structures were considered following the values presented in the National Building Code of India (Part VI), as summarized in Table 3.2. Similarly, the elastic properties of the construction materials, as summarized in Table 3.3, were used for finite element modeling of temple structures in previous works, based on material testing at the real site in Kathmandu valley. But the value of Young's modulus for mud–mortar brick masonry adopted by Jaishi *et al.* [97] was taken from the research conducted by Tomazevic *et al.* [116].

Table 3.2: Allowable stresses on brick masonry [97]

Failure mode	Allowable stress (MPa)
Shear	0.201
Tensile	0.050
Compression	0.606

Table 3.3: Material properties adopted in FE modeling of temple structures [97]

Material	Specific weight (kN/m^3)	Young's modulus (MPa)	Poisson's ratio
Timber	8	1250	0.12
Mud–mortar brick masonry	20	800	0.10

Parajuli *et al.* [117] performed non–destructive testing (acoustic emission test), in order to evaluate the properties of masonry in traditional brick masonry houses constructed in the same period that the temples and the results are summarized in Table 3.4. The Results show that the Young's modulus of wall decrease with the increase in wall thickness, this is

due to increase in the joints and voids inside the wall with increase in wall thickness, resulting in sharply reducing its strength [117].

Table 3.4: Young's modulus of traditional brick masonry walls [117]

Thickness of wall (cm)	Young's modulus (MPa)
11	11567
14	10889
23	3000
44	782

Nienhuys [105] in his report "Options for Reconstruction and Retrofitting of Historic Pagoda Temples" calculated the overall weight of *Narayan* temple, adopting for the specific weight of the materials the values summarized in Table 3.5.

Table 3.5: Density of traditional construction materials in temples [105]

Mud–mortar brick masonry (kg/m^3)	Roof timber (kg/m^3)	Roof clay layer 8–20cm thick (kg/m^3)	Roof tiles 6cm thick (kg/m^3)
1400	800	1400	1400

3.2.4.2 Dynamic properties of Nepalese Pagoda temples

The field dynamic testing provides a direct way to obtain the real dynamic properties of a structure. There are mainly three types of structural dynamic testing: (1) forced vibration testing, (2) free vibration testing, and (3) ambient vibration testing. In the first two methods, the structure is excited by artificial means such as shakers or drop weights. In contrast, ambient vibration testing uses the natural or environmental excitation induced by winds and traffics. Ambient vibration tests are usually preferred over the other non–destructive forced vibration techniques since no forced excitation is required and thus the cost of the vibration test project is reduced significantly.

On December 19–30, 2002 an ambient vibration test was carried out by Jaishi *et al.* [97] on three typical temples of Nepal and modal parameter was obtained using peak picking (PP) and advance stochastic subspace identification (SSI), which is tabulated in Table 3.6.

Nepalese Pagoda temples are stiffer with fundamental time period less than 0.6sec. It is also demonstrated that the damping ratios of Nepalese temples lay between 1% and 6% that is lower than those reported elsewhere for historical structures due to stone or brick masonry type of construction [97]. Apart from this, there is no information of research work carried out on Nepalese Pagoda temples for acquiring the dynamic properties.

Table 3.6: Experimental dynamic properties for Nepalese Pagoda temples [97]

Temple	Photographic view	Mode	Frequencies (Hz)		Damping ratio (%)
			PP	SSI	
Nyatopol		First bending (N–S)	1.685	1.677	1.5
		First bending (E–W)	1.709	1.739	5.9
		Second bending (E–W)	3.906	3.872	3.3
		Second bending (N–S)	3.931	3.890	3.0
		Third bending (E–W)	5.105	6.358	2.9
		Third bending (N–S)	6.128	6.194	2.6
Yechheswor		First bending (E–W)	2.310	2.334	1.5
		First bending (N–S)	2.246	2.326	1.7
		Second bending (E–W)	5.762	5.207	3.6
		Second bending (N–S)	5.176	5.172	4.3
		Third bending (N–S)	8.300	8.360	4.4
		Third bending (E–W)	8.207	8.337	4.1
Salan Ganesh		First bending (E–W)	3.003	3.005	1.8
		First bending (N–S)	3.345	3.036	2.1
		Second bending (E–W)	4.907	4.915	1.2
		Second bending (N–S)	6.660	6.756	1.6
		Third bending (E–W)	7.300	6.748	2.0
		Third bending (N–S)	6.660	7.397	2.4

3.2.4.3 Analytical failure modes of Nepalese Pagoda temple

Even though many uncertainties, in the work of Jaishi [118], ten temples were modeled using SAP 2000 shell model. Response analysis using seismic coefficient and response spectrum method were carried out which showed that the most vulnerable parts of masonry temples are as described below.

- The piers between the openings are more flexible than the portion of the wall below or above the openings, so practically all deformations take place in piers that leads to its failure. The masonry piers near door opening fail in tension in most of temples, but in some temples the compression mode of failure is also present;
- In traditional temples, masonry wall is directly above doorframe. This wooden member is safe in all case;
- Most of traditional Nepalese temples possess framing arrangements in ground floor level. This framing arrangement is safe;
- Wall section where reduction in wall thickness in vertical plane occurs shows failure part;

- Analysis of most of the results shows that the corner sections of walls is weaker that middle portion.

The dominant modes of failure in these temples are of tensile and compressive nature. Shear failure is not encountered in most of the temples due to considerable wall thickness. But in some type of temple having bearing core area only on one side, reveals considerable shear stress. In such type of temples, all the three modes of failure are observed. Most dominant mode of failure in Nepalese temples is associated with tensile stress. However, the above mentioned studied was based on a linear analysis, besides recognizing the limitation of the linear approach for modeling complex materials. Hence, a detail nonlinear analysis might be needed to know exact failure mode of such structures.

3.2.5 Strengthening practice on Nepalese Pagoda temples

Normally, most of the strengthening actions carried out for temples in a very simple way, just repairing for quotidian used, resourcing to modern materials, without any concern in terms of seismic strengthening. One of the challenges in the restoration and retrofitting process of such monuments is to achieve a durable compromise between full structural consolidation and the preservation of the historic fabric and appearance [114]. The conservation work on Nepalese Pagoda is carried out by KVPT [119] in cooperation with government of Nepal archeology department. KVPT [119] is the only international non–government agency registered and working in the field of preservation and restoration of cultural heritage in Nepal [118]. The strengthening practices followed by KVPT [119] are pointed below [114]:

- Repair or rebuilding of timber wall plate and tie structure with improved joinery and steel plate reinforcement;
- Concealed bolting of timber joints at strut, purline and rafter location;
- Reinforced concrete ring beam above the wall;
- Steel beams inserted to support the upper temple level (turret);
- Steel collar used for tying joist and timber joist, and inner and outer wall plates together;
- Steel bracing between inner and outer walls at floor level;
- Iron strap above timber cornices;

- Small wall repairs incorporate iron butterflies to increase bonding between wall layers.

These interventions obviously help in low intensity earthquakes but what happens in larger quakes still is to be study. Many technologies were developed for modern steel and reinforced concrete construction which can be expected to resist earthquake tremors without threatening lives. However research or technology has not been developed yet to enhance the resistance of historic building to tremors, at least in Nepal.

Seismic improvement of *Radha Krishna* Temple (see Figure 3.16) was carried out by KVPT [119]. Here, steel I section joist were inserted to hold the upper temple level (turret) and steel collar to tie the timber members as well as concrete ring beam is introduced between rafter and wall plate above the masonry wall.

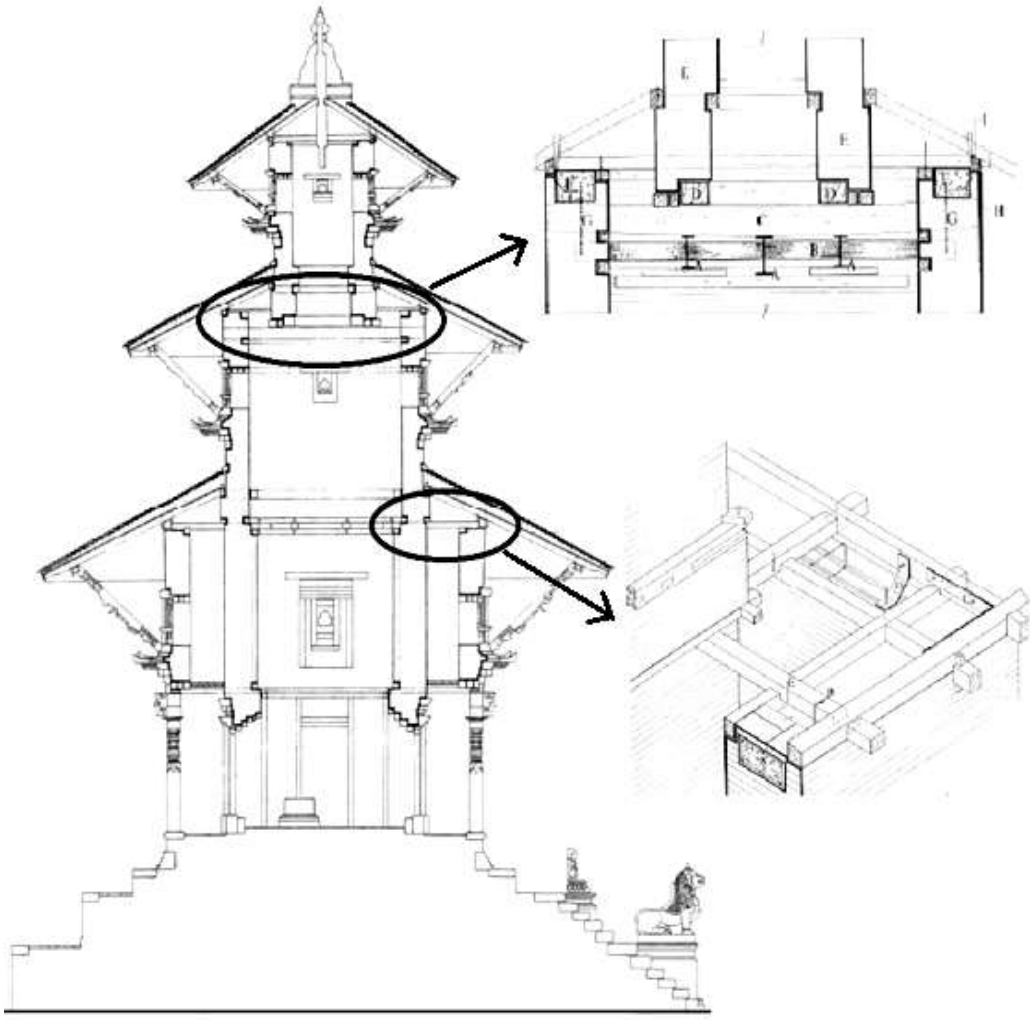

Figure 3.16: Strengthening work on *Radha Krishna* temple [114]

3.3 Seismic sensitivity analysis of the common structural components

3.3.1 Numerical modeling of temples

Every structural problem is primarily aimed to be solved by numerical studies and calibrated by testing. However, because of various difficulties in numerical modeling, some problems may require complicated experimental investigation to calibrate the results. Therefore, an initial numerical analysis is necessary to understand the global behaviour and response of structures. The main difficulties in numeric modeling of historic buildings and, particularly, for temple structures are [120; 121]:

- Lack of data on geometric dimensions;
- Difficulties in identifying the characteristics of construction materials;
- Excessive cost of detailed laboratory testing;
- Variability of the data due to construction techniques and workmanship quality;
- Heterogeneous material properties for the same structural member due to traditional long term construction process.

Even though many uncertainties, the three temples namely (a) *Shiva* temple, (b) *Lashmi Narayan* temple and (c) *Radha Krishna* temple as shown in Figure 3.17, were selected to be modeled for the parametric analysis carried out. The geometrical characteristics of these three temples are listed in Table 3.7. The three temples are selected to be representative of the most common types of Pagoda temples in Nepal. Nevertheless, every temple has different features and many aspects that make it unique.

The first temple selected is Shiva temple, representing one roof plan symmetrical temples, with uniform wall thickness throughout the height and with low plinth level. The second temple is Lakshmi Narayan temple, which represents the majority temples in Nepal. It is a temple with two roofs, having symmetric plan but presenting a vertical load path discontinuity (i.e. top tower resting on timber joists due to walls misalignment in height). Finally, the third selected temple is Radha Krishna temple, which represents a limited number of temples, but which are very precious due to their marvelous architecture. This last temple has a plan symmetrical with an extended gallery at the ground floor and standing on a high plinth. The wall thickness is not uniform throughout the height of the temple. A double wall at the second storey with a walkway floor between walls exists in this type of temple. Also as in the two roof temple, it has a vertical load path discontinuity (wall misalignment).

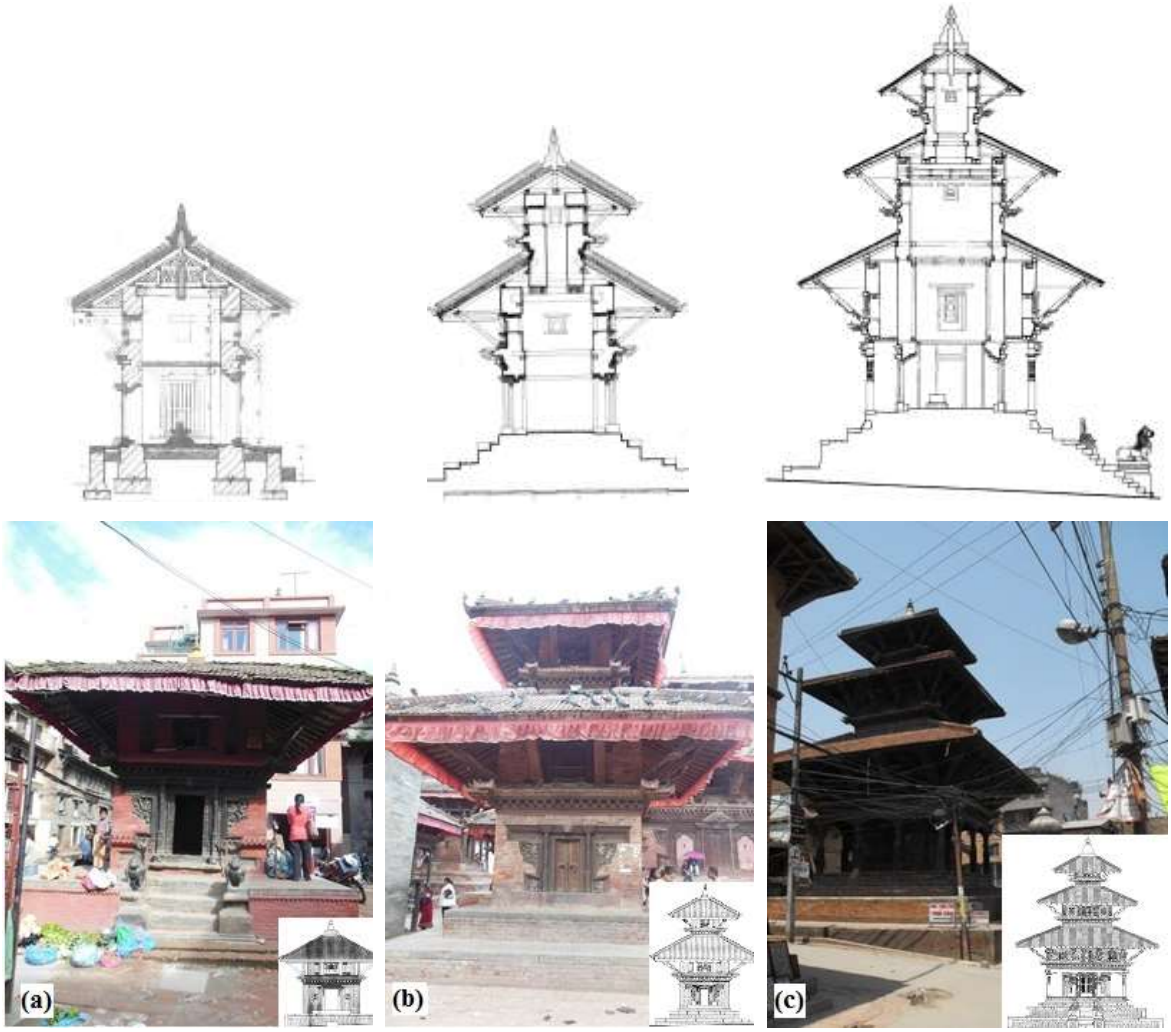

Figure 3.17: Three Nepalese Pagodas: a) *Shiva*; b) *Lakshmi Narayan*; c) *Radha Krishna*

Table 3.7: Dimensions of three selected temples

Temple	Height above plinth (m)	Base cross–section (m^2)	Top cross–section (m^2)	Wall thickness at base (m)	Wall thickness at top (m)
Shiva	4.73	2.82 × 2.82	2.82 × 2.82	0.46	0.46
Lakshmi Narayan	5.92	2.52 × 2.52	1.27× 1.27	0.48	0.40
Radha Krishna	12.76	3.48 × 3.48	1.69 × 1.69	0.64	0.45

In the scope of this research, these three representative temple structures are modeled resourcing to SAP 2000 [122] (see Figure 3.18). For modeling the temple, eight node solid elements are used to model the masonry wall structure, frame elements are used to model the timber structure and shell elements are used to model roof and floors structure. The models take into account the presence of openings and the variation of wall thickness at different levels. The base at the level of plinth was considered rigid since no reliable

information on the foundation was available. Floors were considered rigid in their plane (when timber elements exist in both directions and are attached effectively between them). The pinnacle, door and windows are not considered in the modeling. Moreover, the materials of structural components are assumed homogeneous, isotropic and linearly elastic.

The 3D finite element model of *Shiva* temple consists of 992 solid elements, 512 shell elements and 513 frame elements with a total of 2323 nodes, resulting in 6717 active degrees of freedom. *Lakshmi Narayan* temple consists of 832 solid elements, 524 shell elements and 713 frame elements with a total of 2043 nodes, resulting in 5877 active degrees of freedom. Similarly, *Radha Krishna* temple consists of 9572 solid elements, 1960 shell elements and 3136 frame elements with a total of 16171 nodes, resulting in 47817 active degrees of freedom.

It is difficult to ensure the optimized model without comparing the analytical results with some experimental values obtained from test. Thus, the model calibration was carried out for *Radha Krishna* temple, comparing the analytical modal parameters with the experimentally identified. In the absence of ambient vibration measurements on the *Shiva* and *Lakshmi Narayan* temples, the same mechanical properties and modeling parameters founded for *Radha Krishna* temple were used. The calibrated numerical models are used for a parametric analysis studying the effect of stiffness variation over the fundamental frequency of temple structures.

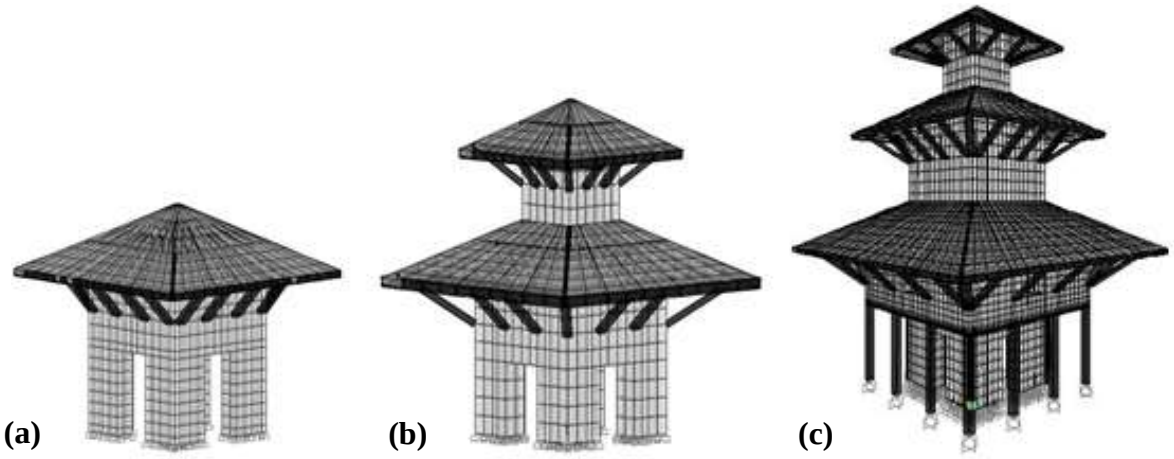

Figure 3.18: FE models: a) *Shiva* temple; b) *Lakshmi Narayan* temple; c) *Radha Krishna* temple

3.3.2 Experimental modal identification and model updating

3.3.2.1 Ambient vibration test of *Radha Krishna* temple

An ambient vibration test was conducted on *Radha Krishna* temple to measure the dynamic response. The goal of the measurements consisted in identifying the natural frequencies and corresponding mode shapes, with the purpose of calibrating the finite element model. Figure 3.19 shows a schematic representation of the sensors distribution. The test was conducted using a 6 channel data acquisition system with 6 uniaxial accelerometers. These accelerometers were used to record acceleration responses in two directions (i.e. xx which corresponds to E–W and yy which corresponds to N–S directions) simultaneously. For each channel, the ambient time histories (acceleration vs. time) were recorded for 180 s at intervals of 0.005 s, which resulted in a total of 36,000 data points.

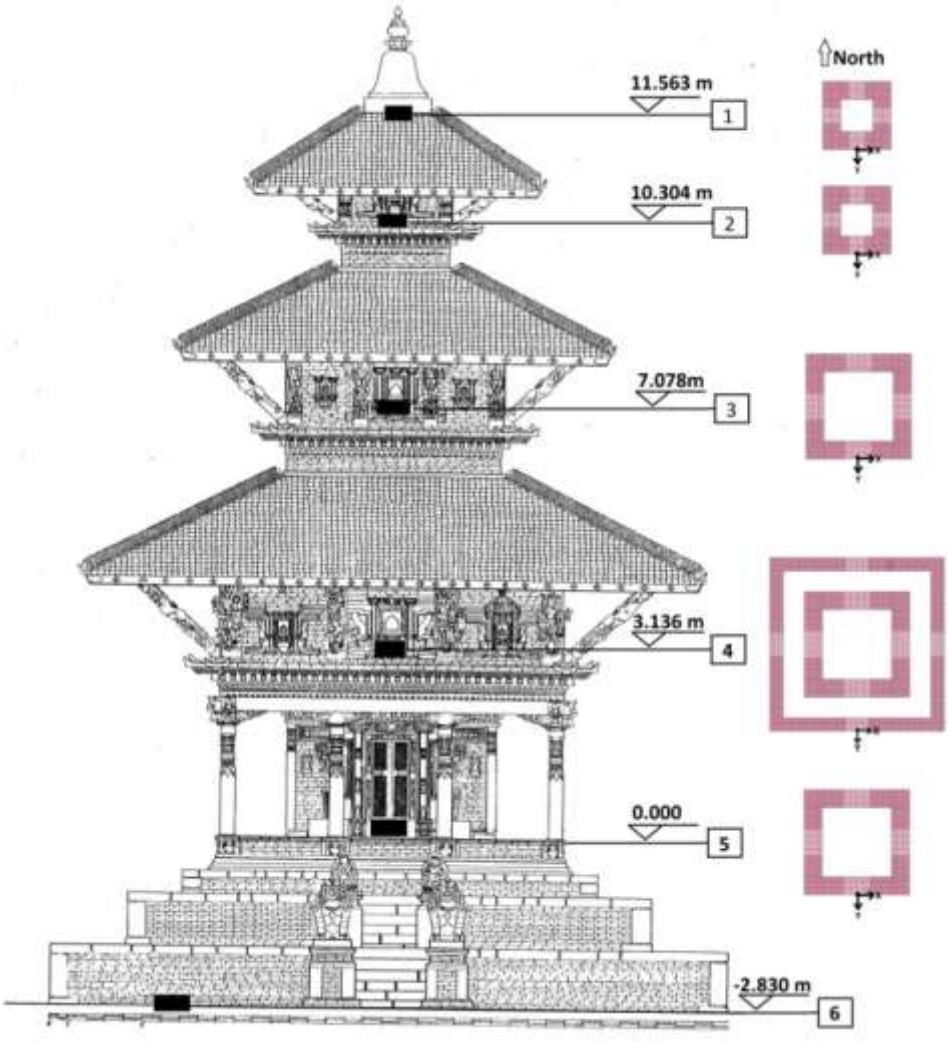

Figure 3.19: Location of accelerometers used in experimental modal identification of *Radha Krishna* temple

The modal identification was performed using peak picking techniques of modal extraction in the frequency domain (Frequency Domain Decomposition (FDD), Enhanced Frequency Domain Decomposition (EFDD) and Curve–fit Frequency Domain Decomposition (CFDD)) implemented in ARTeMIS [123] software. These techniques allow the estimation of not only the natural frequencies and modal damping but also each mode shape [124; 48; 125; 75]. The power spectral densities for the set of performed measurements are presented in Figure 3.20.

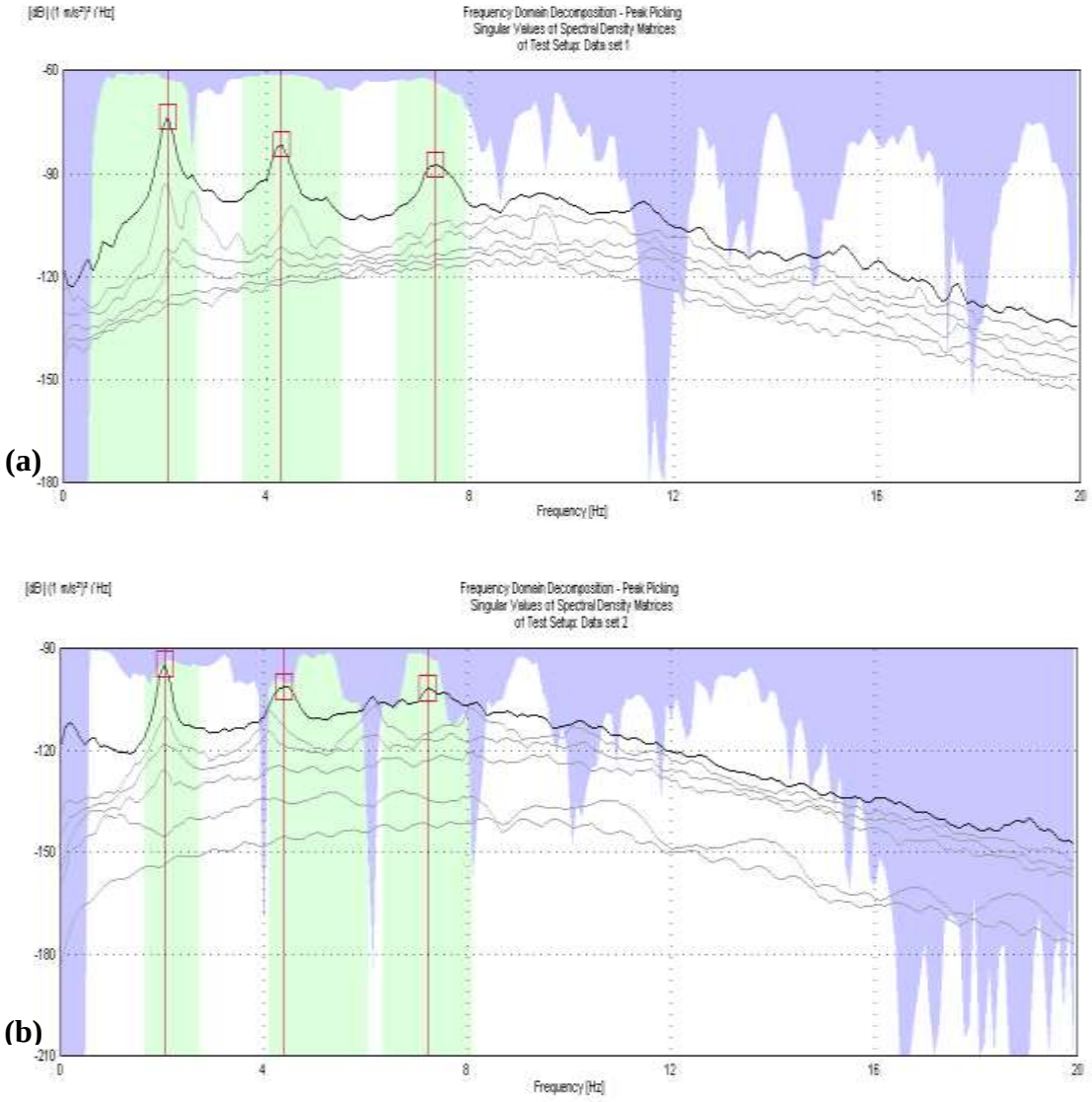

Figure 3.20: Identification of spectral peaks (FDD): a) E–W direction; b) N–S direction

Figure 3.21 shows the first six vibration mode shapes (2D model) estimated from the recorded measurements and, in Table 3.8, the corresponding natural frequencies and modal damping values are presented.

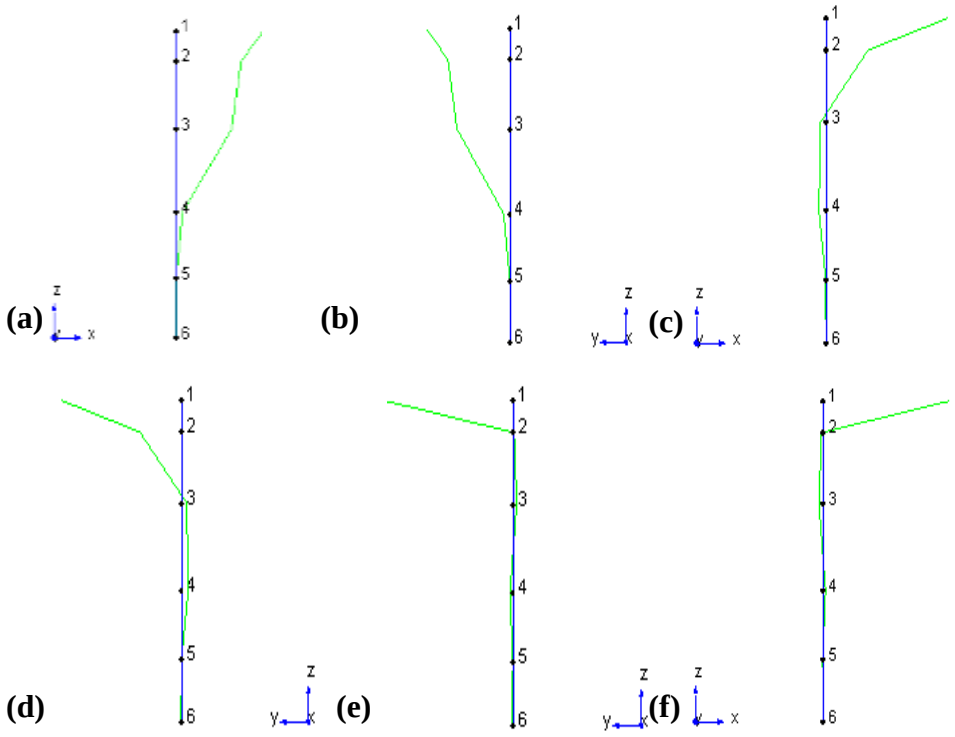

Figure 3.21: Vibration modes identified from ambient vibration measurement: a) first bending xx; b) first bending yy; c) second bending xx; d) second bending yy; e) third bending yy; f) third bending xx

Table 3.8: Natural frequencies and modal damping from ambient vibration measurement

Mode	FDD (Hz)	EFDD (Hz)	CFDD (Hz)	Mean value (Hz)	Damping (%)
First bending xx (E–W)	2.051	2.043	2.089	2.061	3.540
First bending yy (N–S)	2.051	2.046	2.090	2.062	3.302
Second bending xx (E–W)	4.297	4.277	4.275	4.283	3.025
Second bending yy (N–S)	4.395	4.395	4.491	4.427	2.864
Third bending yy (N–S)	7.227	7.336	7.304	7.289	1.382
Third bending xx(E–W)	7.324	7.359	7.359	7.347	1.933

3.3.2.2 Calibration and validation of numerical model

The parameters selected for the calibration procedure are the equivalent Young's modulus of masonry walls and of the timber members. The experimental values from previous research works on material properties were trialed for the calibration of the equivalent Young's modulus values assigned to the masonry walls and timber members of the temple structure. The adaptation of experimental mechanical properties provided by Thapa [107] for masonry walls and by Jaishi *et al.* [97] for timber members result in minimum differences between the frequencies and mode shapes obtained numerically, and those resulting from the measurements performed on site. In Table 3.9, the mechanical

properties obtained after calibration of the finite element model to accurately reflect the dynamic characteristics of the *Radha Krishna* temple are reported. In Table 3.10, the comparison between the natural frequencies from dynamic identification and those from the numerical model are shown. In Figure 3.22 the comparison between the analytical mode shapes (3D model) obtained with FEM and the experimental obtained with FDD is reported. But, the number and location of the sensors during environmental vibration measurements were not satisfactory to catch the third mode shapes of the temple (torsional). As can be observed in the result, the correlation between the measured and calculated modes reveals a good match. In fact, when considering the modal frequencies, a good approximation for the first six frequencies (excluding torsional frequency) with a maximum error of 7.19% is observed.

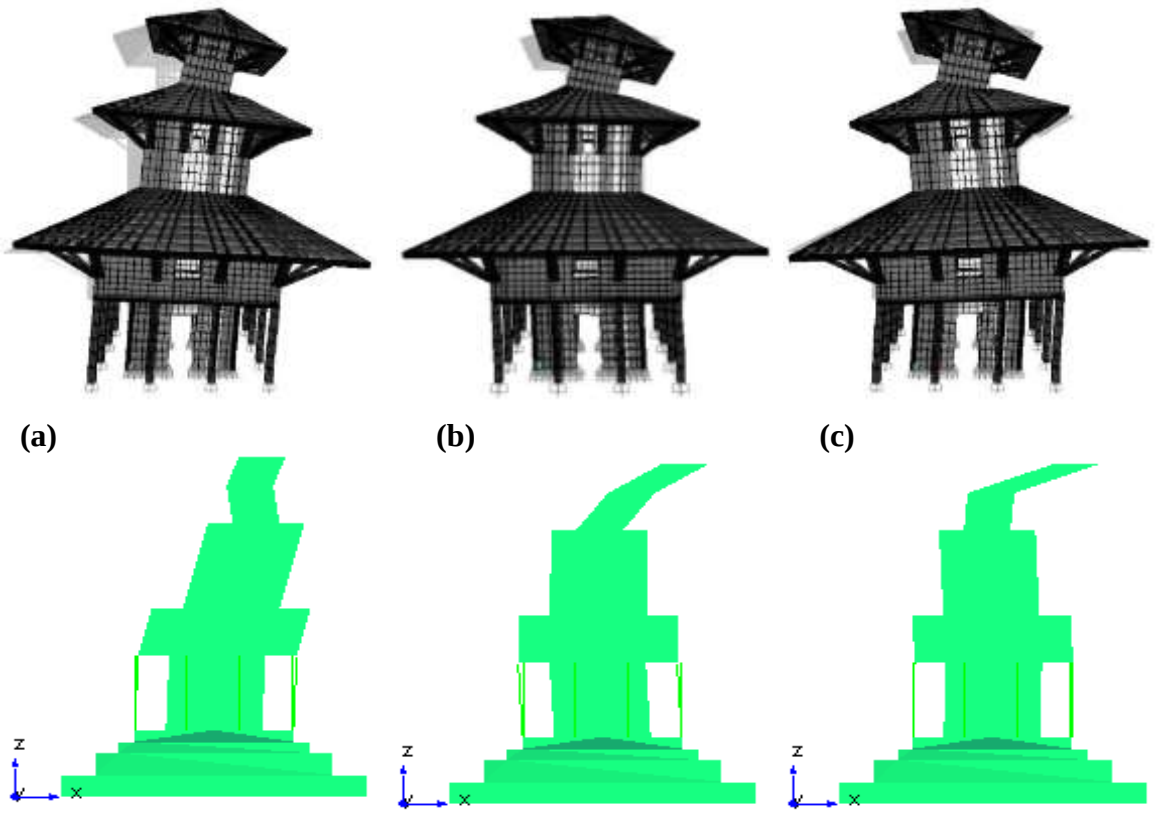

Figure 3.22: Comparison between measured and computed vibration mode shape: a) first bending xx; b) second bending xx; c) third bending xx

Table 3.9: Material properties used in FE modeling

Material	Specific weight (kN/m^3)	Young's modulus (MPa)	Poisson's ratio
Timber	8	1250	0.12
Mud–mortar brick masonry	19	632	0.25

Table 3.10: Comparison between measured and computed frequencies

Mode	Measured frequency (Hz)	Computed frequency (Hz)	Error (%)
1^{st} (first bending xx)	2.061	2.034	1.31
2^{nd} (first bending yy)	2.062	2.034	1.37
3^{rd} (torsional)	–	3.354	–
4^{th} (second bending xx)	4.283	4.413	–3.04
5^{th} (second bending yy)	4.427	4.413	0.32
6^{th} (third bending yy)	7.289	6.810	6.57
7^{th} (third bending xx)	7.347	6.819	7.19

3.3.3 Parametric analysis and results

In order to study the change of the fundamental frequency of the three temple structures (*Shiva*, *Lakshmi Narayan* and *Radha Krishna* temple), due to variation in the stiffness simulating in a simple manner, damage or degradation of vulnerable members, a number of parametric analyses were carried out. Stiffness variation is carried out to simulate damage or degradation of timber or masonry elements. Damage or degradation of members was simulated, by reducing the Young's modulus of elasticity (*E* value) of those members [32; 126; 127]. Linear elastic parametric analysis was carried out to study the decrease in global stiffness of the temple structures. These results were revealed in terms of change in fundamental frequency of temple structures.

Modal analysis results reveal that, due to symmetry of the three structures in both directions, the first and second modes, as well as fourth and fifth modes, have the same frequency and are flexural mode shapes (bending), while the third mode shape is torsional for all models (see Table 3.11).

Table 3.11: Analytical frequency of the three temples

Temple	Frequency (Hz)				
	First mode (bending xx)	Second mode (bending yy)	Third mode (torsion)	Fourth mode (bending xx)	Fifth mode (bending yy)
Shiva	5.499	5.499	7.998	17.604	17.604
Lakshmi Narayan	4.205	4.205	7.911	9.158	9.158
Radha Krishna	2.034	2.034	3.354	4.413	4.413

The parametric analyses were carried out to understand the effect of damage or degradation of structural elements in fundamental frequencies of the temple structures. The timber members selected for these parametric analyses are struts, columns and floors, which are elements to which potential damage may occur. Similarly, masonry wall portions were selected for these parametric analyses, namely: i) masonry wall corners, ii) one–third height of the wall at base storey, and also iii) the wall section where timber joists are inserted. Lastly, analyses are also made with the accumulation of all type of damages or degradation/decay issues studied singularly. The percentage change in the fundamental frequency calculated, due to damages or degradations, for the various potential vulnerable members are summarized in Table 3.12.

Damages in vulnerable members decrease the fundamental frequency of the structures, due to reduction of stiffness. The results of the parametric analyses show that the damages in masonry walls are the major cause bringing change in fundamental frequency, when compared to the damages in timber elements.

The results for all three temples modeled reveal that the damages to the one–third of the base storey height of the masonry wall is the most vulnerable scenario among the studied, since the percentage of fundamental frequency decreases by twice, for each 20% reduction in the *E* value. The percentage decrease due to this damage is similar for *Shiva* and *Lakshmi Narayan* temples, and it is noticeable that *Radha Krishna* temple has the lowest relative decrease.

From the parametric analysis in the case of damage at masonry wall corners, results reveal nearly the same decrease in the fundamental frequency for all three temples, but *Lakshmi Narayan* (2 roof) temple shows slightly higher reduction than the other two temples.

Similarly, the results of the parametric analysis carried out to understand the effect of insertion of timber joists in the masonry walls, show a significant decrease in percentage of the fundamental frequency in the *Shiva* and *Lakshmi Narayan* temples. Comparatively, *Radha Krishna* temple, with the highest surface area, has lowest relative decrease of frequencies. Regarding masonry wall damages, the large wall thickness of *Radha Krishna* temple plays a fundamental role in the good structural response, resulting in the lowest reduction in percentage of the fundamental frequency than the other two temples.

Table 3.12: Reduction in the fundamental frequency due to various damage scenarios

Degraded member	Phenomenon (cause)	Temple	Reduction of E value				
			10%	30%	50%	70%	90%
 Base storey wall	Bulging of outer layer of wall when water penetrates and leads to erosion due to up splashing rain water or insufficient damp proof course.	*Shiva*	2.13%	7.29%	14.31%	24.88%	46.32%
		Lakshmi Narayan	1.83%	6.44%	13.10%	23.92%	47.41%
		Radha Krishna	0.88%	3.13%	6.54%	12.33%	25.64%
 Wall corner joint	Corner cracks or separating of wall faces due to lack of seismic bands and poor interlocking.	*Shiva*	1.42%	4.55%	8.16%	12.48%	18.03%
		Lakshmi Narayan	1.95%	6.24%	11.21%	17.33%	26.49%
		Radha Krishna	1.20%	3.79%	6.80%	10.53%	16.03%
 Timber inserted wall	Reduction in cross–section of masonry wall, where the timber joists are inserted, to hold wall plates in position.	*Shiva*	0.46%	1.55%	3.30%	6.68%	17.60%
		Lakshmi Narayan	0.68%	2.48%	5.34%	10.72%	26.70%
		Radha Krishna	0.15%	0.57%	1.26%	2.72%	8.53%
 Timber strut	Reduction in cross–section due to material decay, degradation, fungal attack, moisture attack, etc.	*Shiva*	0.00%	0.00%	0.01%	0.01%	0.02%
		Lakshmi Narayan	0.00%	0.01%	0.01%	0.02%	0.05%
		Radha Krishna	0.00%	0.01%	0.01%	0.02%	0.04%
 Floor joist	Moisture and/or fungal attack, particularly, where joists are inserted into walls.	*Shiva*	No relevant effect				
		Lakshmi Narayan					
		Radha Krishna					
 Timber column	Rapid decay due to lack of damp proof course and up–splashing rain water.	*Radha Krishna*	1.01%	3.35%	6.38%	10.34%	15.87%
Cumulative of all above effects		*Shiva*	3.07%	10.01%	18.84%	31.28%	54.16%
		Lakshmi Narayan	3.19%	10.50%	19.68%	32.48%	55.49%
		Radha Krishna	2.75%	9.07%	17.04%	28.17%	48.59%

The parametric analysis for the evaluation of the effect of damages to the timber strut shows no appreciable change in fundamental frequency. The timber columns, in case of *Radha Krishna* temple, definitely show important influence. The damage simulated in floor timber battens show no relevant change in the fundamental frequency.

Results regarding the analysis carried out simultaneously considering the entire phenomenon (represented by equal percentage of *E* value reduction) reveal, as expected the highest percentage decrease in the fundamental frequency than for individual damages. The percentage decrease due to this damage phenomenon is similar for *Shiva* and *Lakshmi Narayan* temples. The percentage decrease due to cumulative damage for Radha Krishna temple is twice to thrice (depending upon percentage reduction of the *E* value) in respect to base storey masonry wall damage phenomenon, while in the case of *Shiva* and *Lakshmi Narayan* there is no significant difference. Similarly, the percentage decrease due to cumulative damage for *Shiva* and *Lakshmi Narayan* is twice to thrice (depending upon percentage reduction of *E* value) in respect to masonry wall corners damage phenomenon, while the decrease is thrice for *Radha Krishna* temple.

3.4 Conclusions

The chapter presents the ambient vibration based investigation carried out to assess the dynamic behaviour of the *Radha Krishna* temple. The good match between measured and predicted modal parameters was reached while updating the numerical model which increases the reliability on adopting material properties for the structural components. Due to the good correlation between experimental and theoretical models for *Radha Krishna* temple, the updated model seems to be adequate to provide reliable prediction to assess the structural behaviour.

The results of parametric analysis carried out on the three Nepalese Pagoda temples chosen as representative show that the masonry wall structure (which represents 70–80% of total mass of temple) as the most vulnerable structural component to be safeguarded from damages and conserved. More precisely, damage or degradation to one–third height of the base storey masonry wall and masonry wall corners is fundamental in the reduction of stiffness of the temple structures. Considerable wall thickness of temples over with roofs has made these structures stiffer. The results reveal no effect of the timber strut and floor damage in the overall stiffness of the temple structures. In summary, it can be concluded that more local modeling is needed to understand the local behaviour of timber components and structural vulnerability. These numerical analyses have allowed for better

understanding the main structural fragility and influence of damage or degradation phenomenon over these architectural valued monuments.

Nepalese Pagoda temples are unique cultural heritage standing on seismic prone area. These structures were built with best available material and skill of that time, but following very simple construction rules and details, to comply with seismic resistance requirements. There is lack of sufficient research and conservation works on these structures. So, it is essential to carry out vulnerability assessment and strengthening work to preserve built heritage from future earthquakes.

CHAPTER 4

SEISMIC VULNERABILITY ASSESSMENT METHODOLOGY

Summary *This chapter presents a simplified methodology for assessing the seismic vulnerability of slender masonry structures based on vulnerability index evaluation method. Moreover, this chapter also present the implementation of this methodology in different types of slender masonry structures to develop vulnerability curves for these structure types.*

Chapter outline

4.1 Introduction

At present, a number of studies are available in the technical literature dealing with numerical and experimental analyses of slender masonry structures. However, there is no sufficient research work carried out on developing the relevant seismic vulnerability assessment tools for such structures. It is fact, seismic vulnerability assessment of these types of historical constructions is a difficult task due to the complexity of several factors involved, including the heterogeneity and uncertainty typical of the constituent materials, the intricate geometry configurations, often modified by previous structural or architectural interventions, and the cultural and artistic importance of this type of structure [62].

In general terms, seismic vulnerability measures the amount of damage caused by an earthquake of given intensity over a structure. However, “amount of damage” and “seismic intensity” are concepts without a clear and rigorous numerical definition [128]. According

to Sandi [129], seismic vulnerability is an intrinsic property of the structure, a characteristic of its own behaviour due to the action of an earthquake described trough a law of cause–effect, where the cause is the seismic action and the effect is the damage. However, the amount of damage identified in the seismic vulnerability assessment of buildings depends on many factors such as intensity of the seismic action, soil conditions, constructive materials, structural elements and conservation state.

In 2005, Speranza *et al.* [130] developed a vulnerability assessment method for towers known as VULNeT which was further modified by Sepe *et al.* [1] in 2008, based on GNDT II level approach [131]. This method is commonly used to identify and to characterize the potential seismic deficiencies of a building or group of buildings by means of a qualification by points for every significant component of the structure. This allows the user the determination of a seismic vulnerability index, I_v. One of the most famous methods usually found in the relevant literature corresponds to the developed by Benedetti and Petrini [132] and the GNDT–1990 [133]. This method has been widely used in Italy during the last years and has been upgraded as a result of the continuous experimentation and observed damage of certain types of structures (mainly unreinforced masonry buildings) after earthquakes of different intensities, resulting in an extensive database of damage and vulnerability.

In this chapter a simplified methodology for seismic vulnerability assessment of slender masonry structures is proposed. This methodology evaluate of the seismic vulnerability index for the structure. The evaluated vulnerability index can then be used to estimate structural damage after correlation to a specified intensity of a seismic event. Here, qualitative as well as quantitative parameters are defined to evaluate the vulnerability index. Nonlinear parametric analyses are carried out to calibrate most of the quantitative parameters and weight of each parameter. Finally, this methodology is applied to different types of slender masonry structures, as developing vulnerability curves for these structures.

4.2 Proposed methodology for the vulnerability assessment

There are a variety of methodologies proposed by different authors for the seismic vulnerability assessment of buildings. The selection of a certain methodology of evaluation depends on the next aspects: nature and objective of the study, available information,

characteristics of the building or group of buildings under study, suitable methodology of assessment (qualitative or quantitative) and the organism which will receive the results of the study (e.g. government, scientific organizations, companies and so on). Corsanego & Petrini [134] classified methodologies for the evaluation of structural vulnerability in four groups:

(a) Direct, which estimate in a simple way the damage caused in a structure by a given earthquake (for example FaMIVE [135] and the vulnerability functions or damage probability matrices (DPM) developed by Whitman *et al.* [136]);
(b) Indirect, which determines first a vulnerability index of the structure and then assesses the relationship between damage and seismic intensity (for example ATC–21 [137]);
(c) Conventional, which is essentially a heuristic method, introducing a vulnerability index independent of the damage prediction (ATC–13 [138] and HAZUS [139] are example of this type);
(d) Hybrid, which combines elements of the previous methods with expert judgments (Macroseimic Method devised by Giovinazzi and Lagomarsino [140] is an example of this type).

Dolce *et al.* [141] classifies the methodologies of seismic vulnerability evaluation in four main groups depending on the available information:

(a) Empirical, which evaluates by means of a questionnaire of evaluation and visual inspection (examples are EMS–98 [142] and GNDT–SSN–1994 [131]);
(b) Analytical, which evaluates by means of a numeric analyses on 3D model of structure developed by computational tools;
(c) Experimental, which evaluates by means of tests determining the mechanical and dynamic characteristics of an existing structure;
(d) Hybrid, which corresponds to the combination of the empirical, analytical and experimental.

Here, Corsanego and Petrini [134] classify the methodologies based on the type of approach followed for the evaluation of seismic vulnerability, whereas, the classification by Dolce *et al.* [141] is based on the nature of the methodology. It is possible to assess the

seismic vulnerability of a large group of buildings in a quite general manner (roughly) following simple methodologies (qualitative), or to only evaluate one building in a detailed way by means of refined methodologies (quantitative). Qualitative methodologies allow obtaining a qualification of the buildings or group of buildings in terms of seismic vulnerability that could range from low to high, whereas the quantitative ones in numerical terms (e.g. ultimate force and displacement capacity). However, the selection of one of these methods depends on the objectives of the study, the type of the results required and on the available information. On the other hand, fragility functions, damage probability matrices and vulnerability functions obtained from observed structural damages during past earthquakes in a seismic area were the preferred tools in seismic risk studies performed in the past [132].

The vulnerability index formulation adopted here is based essentially on the GNDT II level approach, presented in GNDT–SSN–1994 [131], for the vulnerability assessment of residential masonry buildings. In this approach, the overall vulnerability is calculated as the weighted sum of 12 parameters (see Table 4.1) used in the formulation of the seismic vulnerability index. These parameters are related to 4 classes of increasing vulnerability: A, B, C and D.

Table 4.1: Vulnerability index (I_v)

Parameter group	Parameter	Class (K_i)				Weight (W_i)	Vulnerability index
		A	B	C	D		
1. Structural system	P1: Type of resisting system	0	5	20	50	1.00	$I_v^* = \sum_{i=1}^{12} K_i W_i$
	P2: Quality of the resisting system	0	5	20	50	1.50	
	P3: Conventional strength	0	5	20	50	1.50	
	P4: Slenderness ratio	0	5	20	50	1.50	
	P5: Location and soil conditions	0	5	20	50	0.75	
2. Irregularities and interaction	P6: Position and interaction	0	5	20	50	1.50	$0 \leq I_v^* \leq 650$
	P7: Irregularity in plan	0	5	20	50	1.00	
	P8: Irregularity in elevation	0	5	20	50	1.50	
	P9: Number, size and location of wall openings	0	5	20	50	1.00	
3. Horizontal structure and roofing	P10: Flooring and roofing system	0	5	20	50	0.50	Normalized index $0 \leq I_v \leq 100$
4. Conservation status and other elements	P11: Fragilities and conservation state	0	5	20	50	1.00	
	P12: Non–structural elements	0	5	20	50	0.25	

Depending on the parameter and the selected class, the method assigns a numerical value (K_i) ranging from 0 to 50, which is affected by a coefficient of importance (Weight

'W_i'). A weight (W_i) is assigned to each parameter, ranging from 0.25 for the less important parameters (in terms of structural vulnerability) up to 1.5 for the most important as shown in Table 4.1. It reflects the importance of each parameter in the evaluation of the seismic vulnerability of the slender structure. As a final stage the seismic vulnerability index (I_v) of the structure will be obtained with the use of equation presented in Table 4.1. The vulnerability index obtained as the weighted sum of the 12 parameters initially ranges between 0 and 650, with the value then normalised to fall within the range $0 \leq I_v \leq 100$. The calculated vulnerability index can then be used to estimate structural damage after a specified intensity of a seismic event. The definition of each parameter class and weight is proposed taking into account the literature for similar methodology, the opinion of experts and parametric analyses results.

4.3 Modeling strategy adopted for parametric analysis

In order to define and calibrate the parameters used for assessing vulnerability, a number of parametric pushover analyses were carried out. Different vulnerability scenarios were introduced in FE model and its analysis results were analysed and compared to define different class and weight for each parameter. The majority of slender masonry structures have square or circular cross–section. The walls are thick, but normally thickness reduction in height. Openings are few and of small separate dimension. Hence, the reference structure is modeled as a vertical hollow cantilever of constant thick–walled with square cross–section, as shown in Figure 4.1. The geometric and mechanical properties adopted are an average value, based on an extensive literature review on such structures. Literatures reviewed were related to the experimental and analytical studies on historical slender masonry structures (among 59 literatures 32 were on towers, 16 on minarets, 7 on chimneys and 4 on Nepalese Pagoda temples) (see chapter 2). For the numerical analyses of the present study, the geometric and mechanical characteristics of the reference structure are tabulated in Table 4.2 and Table 4.3, respectively.

Figure 4.1: FE model of the reference structure

For modeling the reference slender masonry structure, eight node solid elements are used resourcing to Midas FEA v 1.1 (2013) [143]. The model is based on the macro–modeling approach (see Figure 4.2), which is considered as appropriate for the seismic assessment of historical constructions at this scale of analysis [144]. Among many of the other, the important advantages of this approach is that it simplifies the generation of the structural model, and due to the reduction of the degrees of freedom, less calculation effort is required. The macro–modeling, also named smeared, continuum or homogenised model, considers masonry as an isotropic composite material [145].

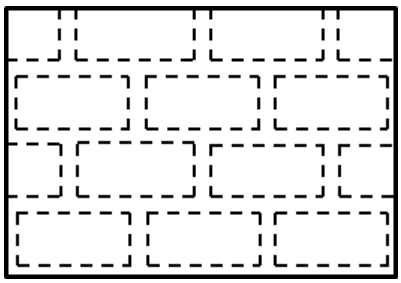

Figure 4.2: Macro–modeling for masonry walls

In order to assess the seismic performance of a certain historical construction, the engineer is required to develop constitutive material models to represent the mechanical behaviour of the materials under analysis, as well as the generation of the structural model mainly based on the monitoring and diagnosis campaigns [146]. Relatively to other structural materials, masonry exhibits nonlinear behaviour since very low demand levels

due to the nonlinear material properties and its poor tensile and shear strength. Moreover, the anisotropic behaviour of masonry is determined by the physical and mechanical characteristics of its components (mortar joints and units). The nonlinear and anisotropic behaviour of masonry imposes the use of seismic analyses based in nonlinear rules to better represent the real behaviour of this material.

This research work does not intended to develop a constitutive material model for masonry or to extend and existing one. Here, the constitutive material model named total strain crack model introduced by Vecchio and Collins [147] is applied, which is integrated in the program Midas FEA. This constitutive material model is based on total strain where stress is described as a function of the strain and follows a smeared crack approach. The basic concept of the total strain crack models is that the stress is evaluated in the directions which are given by the crack direction. Following the explanations of Chen [148] and Lourenço [149], the tension uniaxial behaviour is characterized by post–peak exponential softening and the compressive uniaxial behaviour is characterized by a linear stress–strain relation until one–third of the compressive strength, followed by a parabolic relation for the hardening regime until reaching the compressive strength and another parabolic for post–peak softening (see Figure 4.3a and Figure 4.3b). When total strain fixed crack model is used also the shear retention needs to be defined. In the case of masonry, constant shear retention is used, where the factor β defines the amount of shear stiffness that remains after cracking (see Fig 4.3c). Moreover, the module adopted for the crack bandwidth h is left as the default value, i.e. square root of total in–plane area of the 3D element.

Table 4.2: Geometrical characteristics of the reference structure

Characteristics	Dimension
Total height (H)	40m
External side (B×L)	6×6m^2
Mean wall thickness (t)	1m

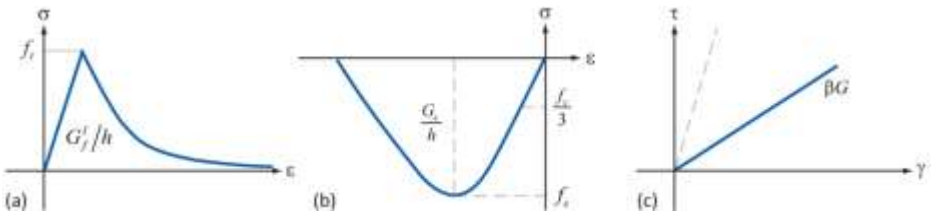

Figure 4.3: Stress–Strain relations applied to the total strain crack model: a) behaviour of material with softening under uniaxial tension; b) behaviour of material with hardening/softening under uniaxial compression; c) behaviour of material with constant shear retention factor under uniaxial shear [143]

Table 4.3: Masonry mechanical properties used as input for FE modeling

Parameters	Symbol	Value
Young's modulus (N/mm^2)	E	3500
Specific weight (kN/m^3)	γ	19
Poisson's ratio	ν	0.19
Compressive strength (N/mm^2)	f_c	3.50
Compressive fracture energy (N/mm)	G_c	0.35
Tensile strength (N/mm^2)	f_t	0.35
Tensile fracture energy (N/mm)	G_f	0.07
Shear retation factor	β	0.01

4.4 Calibration of proposed methodology for vulnerability assessment

4.4.1 Definition of vulnerability assessment parameters

Overall vulnerability is calculated as the weighted sum of 12 parameters used in the formulation of the seismic vulnerability index. These 12 parameters are grouped into four groups. The first group includes parameters that characterize the building resisting system (P1) and the type and quality of masonry (P2), from the material (size, shape and stone type), masonry fabric and arrangement and quality of connections amongst walls, shear strength capacity of the structure (P3), slenderness ratio of the structures (P4) and the soil foundation conditions (P5). The second group of parameters is mainly focused on the buildings relative location and on its interaction with other buildings (P6), evaluates the irregularity in plan (P7) and elevation (P8) and identifies the wall openings number, size and location (P9). The third group of parameter evaluates horizontal structural systems (P10), namely the type of connection of the timber floors and the impulsive nature of the pitched roofing systems. Finally, the fourth group of parameters evaluates the structural fragilities and conservation state of the structures (P11), as well as the negative influence of non–structural elements (P12) with poor connection conditions to the main structural system. Definition and calibration of each parameter is carried out considering the literature for similar methodology, the opinion of experts and parametric analyses results. Definition and calibration of each parameter is detailed in the following sections:

P1: Types of resisting system

This parameter measures the resilient type of system, in terms of organization and quality of the wall design and distribution of the structure, the efficiency of connections between walls. It is essential to evaluate the distribution of walls, as well as connections

between orthogonal walls and their connection to horizontal diaphragm, without regard to the constitution of the masonry (which will be evaluated by another parameter).

To assess the level of connection between orthogonal walls particular attention should be given to the corner angles, identifying the size and arrangement of the units. The interlocking between the units of the masonry wall is particularly vulnerable to detachment, which may be simply triggered by aging or by temperature and moisture variation (temperature cycles). The definition of classes of vulnerability for this parameter is presented in Table 4.4. Figure 4.4 shows some typical retrofitting solutions connecting orthogonal walls.

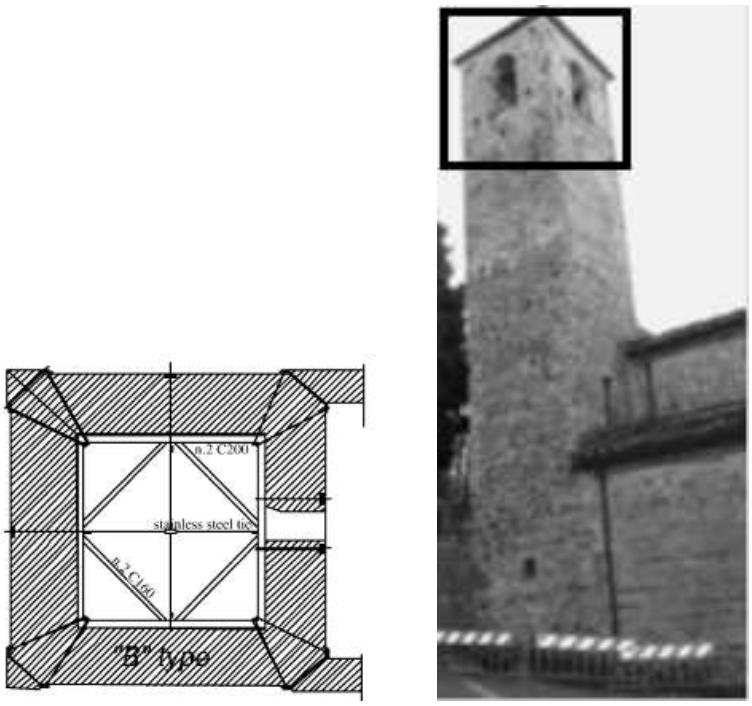

Figure 4.4: Different aspects of the link between orthogonal walls [4; 150]

Table 4.4: Definition of the vulnerability classes for parameter P1

Class	Description
A	Structures built according to earthquake resistant construction codes. Strengthening or consolidation of the building masonry complying to rules earthquake resistance codes, thus ensuring the connection requirements and efficient connection between orthogonal walls.
B	The structure has good links and bonding between orthogonal walls. Existence of ring beams and/or steel ties well distributed in sufficient number with good anchorage, thus ensuring the conditions for binding and effective connection between the vertical elements.
C	The structure does not have the effective connections defined in class B, however it presents good connection quality between orthogonal walls, guaranteed by the appropriate bonding or interlocking units in all the walls.
D	The structure does not present effective connection of loadbearing walls. Total absence of steel tie rods and/or ring beams.

P2: Quality of resisting system

The masonry found in traditional structures is very heterogeneous, with different material components, and techniques for nesting dimensions, which give different levels of resistance and durability. This parameter assesses the quality of masonry walls, according to three features: (a) homogeneity of the material, shape, size and nature of the units (bricks, blocks or stones); (b) unit laying configuration and arrangement of the masonry units; (c) type of cross–linking elements.

The first aspect is to identify the type of material (natural or artificial origin). The resistant characteristics are very dependent on the type of unit or material, and its size. The type of mortar is also an inseparable aspect, as it influences the bearing capacity of masonry. The second aspect relates to the homogeneity and regularity in the arrangement of units masonry, which is essentially of two types: a settlement with units carved with vertical and horizontal joints well defined. The third part analyses the possible presence of cross–connecting elements such as rows, which usually joins the two pieces of wall (internal and external), giving it a degree of monolithic nature. The definition of vulnerability classes is described in Table 4.5. Particular description of class A, B, C and D type masonry with examples are presented in Table 4.6, Table 4.7, Table 4.8 and Table 4.9 respectively.

Table 4.5: Definition of the vulnerability classes for parameter P2

Class	Description
A	Brick masonry of good quality. Well cut stone masonry units (squared) with homogeneous and uniform in size throughout the length of the walls. Irregular stone masonry well mortared and locked/arranged, existence of cross–connection between the two sides of the wall.
B	Brick masonry of average quality and carved stone masonry units with homogeneity over the whole extension of the walls. Stone masonry with irregular cross–link elements between the two sides of the wall.
C	Brick masonry of low quality with irregularities in laying and bonding. Masonry stone units, not squared and heterogeneous dimensions. Irregular stone masonry without cross–linking elements, and average mortar quality.
D	Brick masonry of poor quality with inlay of stone fragments. Stone masonry with very irregular units, nesting irregularly and without locking care (creating gaps). Irregular stone masonry without cross–connection and poor mortar quality.

Table 4.6: Description of the masonry Class A [151]

Description of the masonry	Examples of masonry Class A
Stone masonry consisting of homogeneous units (in terms of material and dimensions), and well cut (parallelepiped form) with good laying techniques and use of good quality mortar, good filling vertical and horizontal joints.	
Stone masonry of low porosity with good laying techniques and locking with well–arranged vertical and horizontal joints. Mortar of good quality.	
Masonry units with perforated clay brick or cement blocks (15 to 45% voids) with well–arranged vertical and horizontal joints, with good quality mortar.	
Stone masonry with timber structure, or frontal walls, under good storage conditions with efficient connections between elements of wood and without apparent deterioration of wood by biological attack or by the action of water.	–
Masonry of solid brick or solid blocks well layed and locked with vertical and horizontal joints filled with mortar of good quality.	
Consolidated masonry and reinforced masonry with appropriate techniques.	–

Table 4.7: Description of the masonry Class B [151]

Description of the masonry	Examples of masonry Class B
Stone masonry units consisting of non–homogeneous (in terms of dimensions), but well locked and arranged longitudinally and transversely. Mortar of good quality.	
Stone masonry (slightly worked) with the use of stone or ceramic elements with dimensions similar to wall thickness, so that the wall confers one cross–linking unit throughout its thickness. Mortar of good quality.	
Adobe masonry, with single or one and a half adobe thick, mortar with good quality.	
Perforated brick masonry or concrete blocks with good laying techniques but arranged only with horizontal joints. Mortar of average quality.	–
Stone Masonry of low porosity, with good laying techniques and locking with vertical and horizontal arranged joints. Mortar of average quality.	–
Stone masonry with wood or frontal walls in good repair with efficient connections, with signs of wood decay by biological attack or rain water. This will include the cases where there is disruption of wood elements.	–

Table 4.8: Description of the masonry Class C [151]

Description of the masonry	Examples of masonry Class C
Coarsely carved stone masonry, irregularly shaped, with poor locking and irregular laying. Mortar of average quality.	
Irregular stone masonry and rounded, with cross–connection. Mortar of average quality.	
Masonry of brick, poor laying techniques and mortar with poor quality.	
Irregular stone masonry without cross–linking elements. Irregular laying and weak mortar quality.	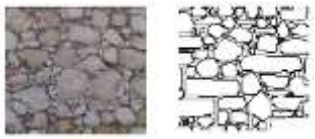
Masonry of two or three panels and composed of irregular stone or brick fragments, with a core of reasonable consistency. Irregular laying with average quality mortar.	
Adobe masonry layed at half of adobe width, with mortar of average quality.	

Table 4.9: Description of the masonry Class D [151]

Description of the masonry	Examples of masonry Class D
Rammed earth.	
Irregular stone masonry not worked high and medium porosity. Settlement deficient (formation of voids) without elements or rows of cross–linking. Mortar weak quality.	
Clay brick masonry of poor quality, using fragments and settlement locking disabled. Mortar of poor quality.	
Masonry of two panels, with core partially empty and unstable (no consistency). Mortar of poor quality.	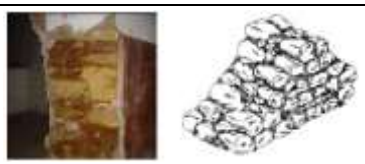

P3: Conventional strength

This parameter is a meaningful assessment of conventional shear resistance capacity of a structure as a function of characteristic shear strength of material. The calibration of this parameter is carried out by performing a pushover analysis. The reference FE model described in section 4.3 was defined with various characteristic shear strength values, adopted from the literature, for modeling models. Since, the total strain crack material model is used, a Mohr–Coulomb failure criteria was used to derive the equivalent tensile and compressive strength of material to be introduced in the analytical models for the respective conventional shear strength value of material. According to this criteria, the tangent of the friction angle (Ø) is the ratio between shear strength and tensile strength, where tensile strength is considered as 10% of compressive strength value. Friction angle is adopted as 30 degrees, which is the average value adopted from the literature on masonry structures of similar type.

The result of the pushover analysis is shown in the Figure 4.5, which is a plot showing the reduction of the maximum global drift capacity compared to a reference structure. In literatures, the characteristic shear strength values for masonry ranges between 20kPa to 200kPa. Hence, the shear strength capacity of 20kPa and 200kPa are considered as lower limit and upper limit for vulnerability classes classification, respectively.

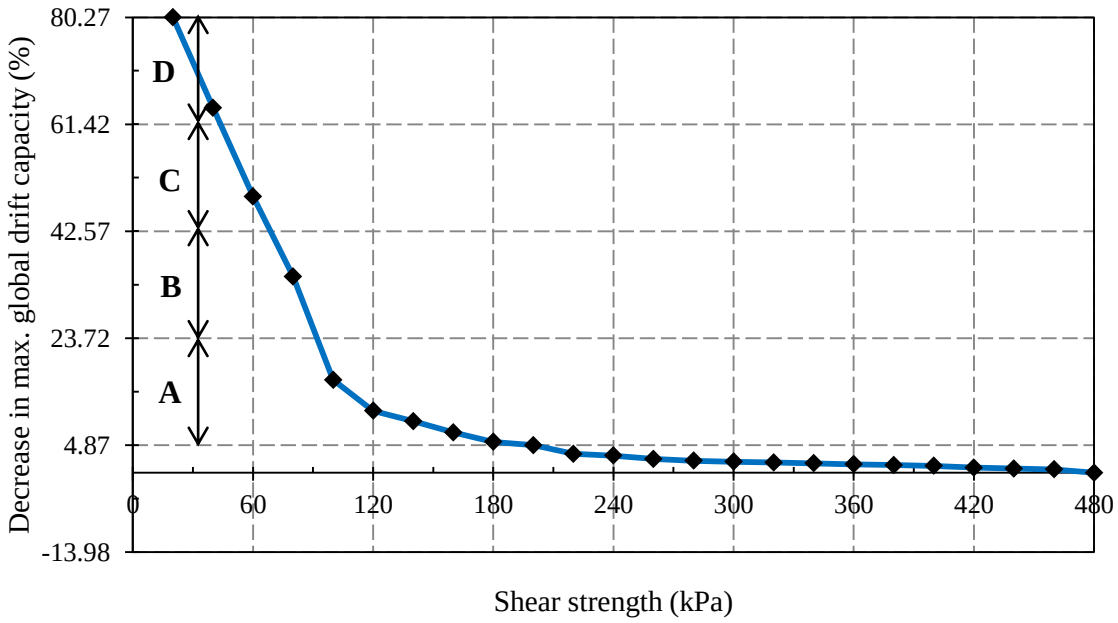

Figure 4.5: Pushover analysis results for different shear strength capacity

The percentage of decrease in maximum global drift capacity between upper limit (80.27%) and lower limit (4.86 %) is divided equally into two divisions (i.e. 4.86%–23.71%, 23.71%–42.56% , 42.56%–61.42% and 61.42%–80.27%) and the relative shear strength capacity is defined as the limiting range for the vulnerability classes B and D respectively (see Table 4.10).

Table 4.10: Definition of the vulnerability classes for parameter P3

Class	A	B	C	D
Limit	τ >100kPa	80kPa< τ ≤100kPa	60kPa< τ≤80kPa	τ≤60kPa

In the absence of experimental characteristic shear strength $'\tau'$ value for assessing structure, it can be sought to some literature values (see Tables 4.11). It is recalled that the shear strain resistant is dependent on the type of units, the nature of the material, the laying and the type of mortar used.

Table 4.11: Characteristic values of shear strength capacity (GNDT–SSN–1994 [131] and González [152])

Types of masonry wall	τ (kPa)	
Solid brick with poor laying mortar	60–120	GNDT–SSN–1994 [131]
Blocks with poor laying mortar	80	
Concrete or cellular concrete block with poor mortar	180	
Stone in poor condition (irregular format)	20	
Stone (in the case of having cross–linking elements the value be increased 30%)		
Simple stone well layed	70–90	
Irregular stone in good condition	40	
Volcanic tuff block	100	
Two leafs masonry	40	
Masonry of volcanic tuff	70	González [152])
Stone masonry rounded	40	
Solid clay brick of average quality	60–120	
Solid clay brick of good quality	180	
Solid cement block	180	
New masonry of solid clay brick	200	
Hollow clay brick masonry	180	
Limestone masonry of regular dimension	100	

P4: Slenderness ratio

Slenderness ratio is the ratio of the effective length of a structural member to its least radius of gyration (as expressed in Eq. (4.1)) and generally is considered as height to breadth ratio. This parameter evaluates the slenderness of the structures which is crucial to

evaluate, since, it highly raises the stresses produced by static and dynamic loads at the base, particularly with regard to horizontal loading induced by a strong–motion. This parameter is vital to define the vulnerability of slender masonry structures.

The definition of vulnerability classes for this parameter is carried out by calculating the maximum top displacement assuming the slender masonry structures as vertical cantilever hollow beam members, as expressed by Eq. (4.2). In this study, the lateral load assumed was 18% (design value of horizontal seismic coefficient) of its self–weight which was distributed linearly as an inverted triangular distribution throughout its height. The design value of horizontal seismic coefficient (α_h), in the Response Spectrum methods (according to IS–1893 [153]) is computed as given by the Eq. (4.3).

$$\text{Slenderness ratio } (\lambda) = \frac{2H}{k} \tag{4.1}$$

$$\text{Maximum top displacement } (\delta_{max}) = \frac{11 w_o H^4}{120 E I_{min}} \tag{4.2}$$

$$\text{Horizontal seismic coefficient } (\alpha_h) = \beta I F_o \frac{S_a}{g} \tag{4.3}$$

where,

H is the height of the structure;

k is the radius of gyration $= \sqrt{\frac{I_{min}}{A}}$;

A is the cross–sectional area ;

I_{min} is the minimum moment of inertia;

E is the young's modulus;

W_o is the lateral load intensity ;

β is a coefficient depending upon the soil foundation = 1.5 (considering un–reinforced strip foundations);

I is a factor depending upon the importance of the structures = 1.5 (considering monumental structures);

F_o is a seismic zone factor for average acceleration spectra = 0.4 (considering zone V);

$\frac{S_a}{g}$ is an average acceleration coefficient = 0.2 (considering natural period of vibration 0.7sec with 2% damping).

The maximum global drift is calculated for different types of slender masonry structures (i.e. 78 Pagoda temples, 72 towers, 32 minarets and 8 chimneys) using the information gathered from the literature review, whereas for Pagoda temples geometric characteristics were obtained from field survey. Maximum global drift versus slenderness ratio and height to breadth ratio is shown in Figure 4.6 and Figure 4.7 respectively for each type of structure.

The definition of vulnerability classes is carried out using the following procedure:

(a) Firstly, structures of same type are sorted in increasing order in respect to maximum global drift percentage (for example maximum global drift for 72 towers ranges from 0.013% to 1.987%);

(b) Secondly, these sorted structures are divided into 4 groups, with equal number of structures in each group (for example, 4 groups of 72 towers consist of 18 in each group and with limiting value of maximum global drift ranging from 0.013% to 0.087%, 0.087% to 0.17%, 0.17% to 0.357% and 0.357% to 1.987%);

(c) Finally, the corresponding value of the slenderness ratio and height to breadth ratio for limiting the value of maximum global drift percentage of each group following the trendline defines the vulnerability classes A, B, C and D for that structure type (see Table 4.12).

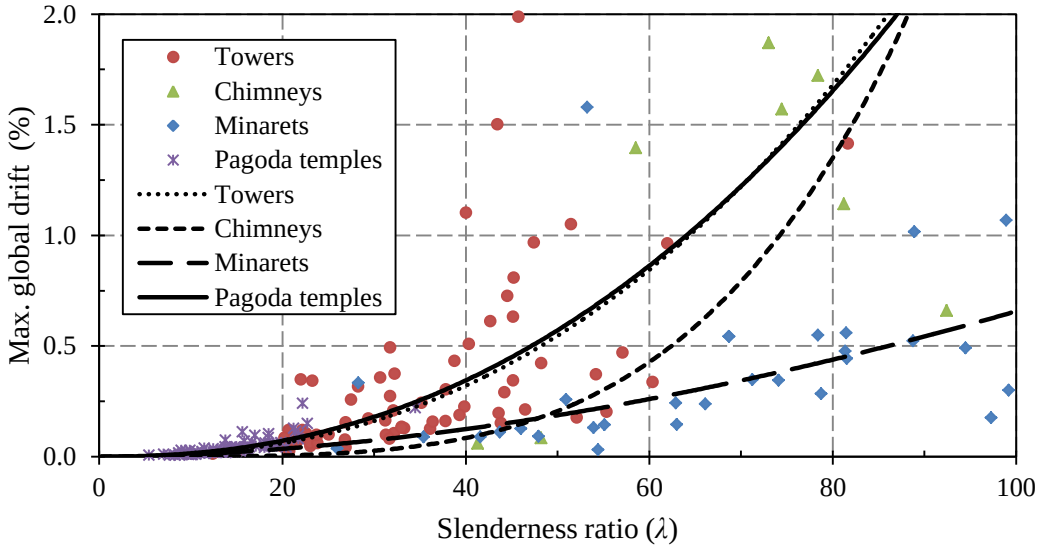

Figure 4.6: Comparison between slenderness ratio vs max. global drift percentage for different types of slender masonry structures

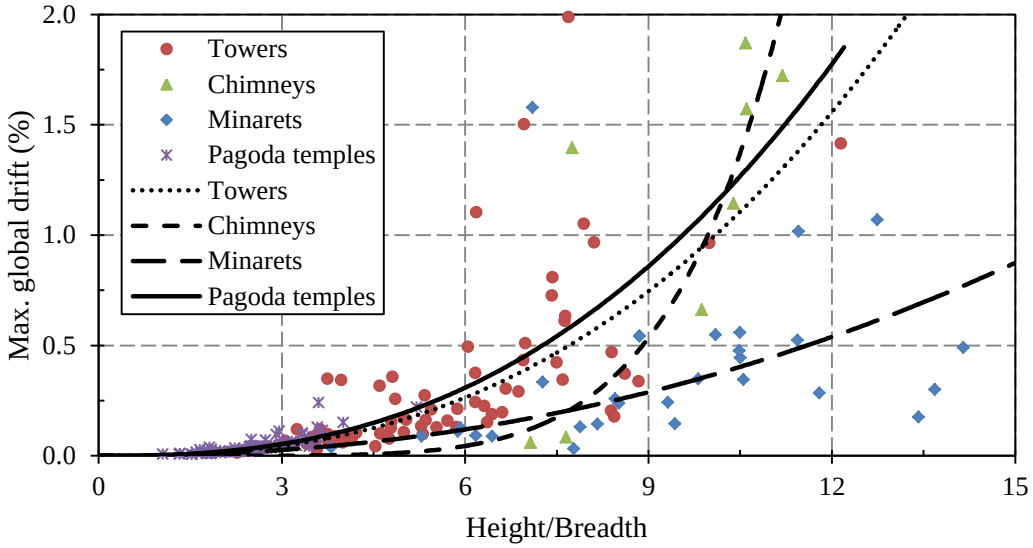

Figure 4.7: Comparison between height/breadth ratio vs max. global drift percentage for different types of slender masonry structures

Table 4.12: Definition of the vulnerability classes for parameter P4, in function of slenderness ratio and height/breadth ratio (according to their influence over the global drift)

Class	Type of structure							
	Bell tower		Chimney		Minaret		Pagoda temple	
A	$\lambda \leq 23$	 [11]	$\lambda \leq 38$	 [91]	$\lambda \leq 40$	 [26;41]	$\lambda \leq 11$	
	$\frac{H}{B} \leq 3.75$		$\frac{H}{B} \leq 6$		$\frac{H}{B} \leq 6$		$\frac{H}{B} \leq 2$	
B	$23 < \lambda \leq 32$	 [48; 70; 76]	$40 < \lambda \leq 66$	 [93]	$40 < \lambda \leq 64$	 [26]	$11 < \lambda \leq 15$	
	$3.75 < \frac{H}{B} \leq 5.25$		$6 < \frac{H}{B} \leq 9.5$		$6 < \frac{H}{B} \leq 9$		$2 < \frac{H}{B} \leq 2.5$	
C	$32 < \lambda \leq 44$	 [82; 81; 38]	$66 < \lambda \leq 84$		$64 < \lambda \leq 90$	 [26]	$15 < \lambda \leq 18$	
	$5.25 < \frac{H}{B} \leq 7$		$9.5 < \frac{H}{B} \leq 10.5$		$9 < \frac{H}{B} \leq 12$		$2.5 < \frac{H}{B} \leq 3$	
D	$\lambda > 44$	 [3;154]	$\lambda > 84$	 [15]	$\lambda > 90$	 [26; 89]	$\lambda > 18$	
	$\frac{H}{B} > 7$		$\frac{H}{B} > 10.5$		$\frac{H}{B} > 12$		$\frac{H}{B} > 3$	
Here, λ: Slenderness ratio, H: Height of the structure and B: Wall breadth at the base (minimum)								

P5: Location and soil conditions

This parameter assesses the importance of factors such as the topography, type and consistency of the ground foundation and also evaluates the risk of landslide or slipping of foundation soils, when subjected to seismic action (see Figure 4.8). In this procedure, the difficulty of assessing the ground–structure interaction is simplified in each case.

It is common in old structures only an extension of the wall depth, a situation that is not classifiable as a foundation. However, it is considered that the typical "thickening" of the base of the wall structure can be classified as a foundation. If existing geophysical reconnaissance elements (geology soil stratification) that allow more accurate identification of the soil foundation types, also allowing their classification assessing the definition of the vulnerability classes as indicated in Table 4.13.

The designation used for the type of soil is proposed in Eurocode 8 (EC8) (i.e. A, B, C, D, E, S1, and S2) [155]. The class assignment is made in respect to the worst conditions identified. It is not considered in the classification in Table 4.13, the risk of other phenomena, such as liquefaction slip and drop. If the study area is recognized to have potential occurrence of liquefaction of saturated granular soils (soil type S1 and S2 according to the EC8 classification) when subjected to an earthquake, it should be considered a vulnerability class D. Note that it is not integrated in this methodology to evaluate the possibility of an effect of soil amplification.

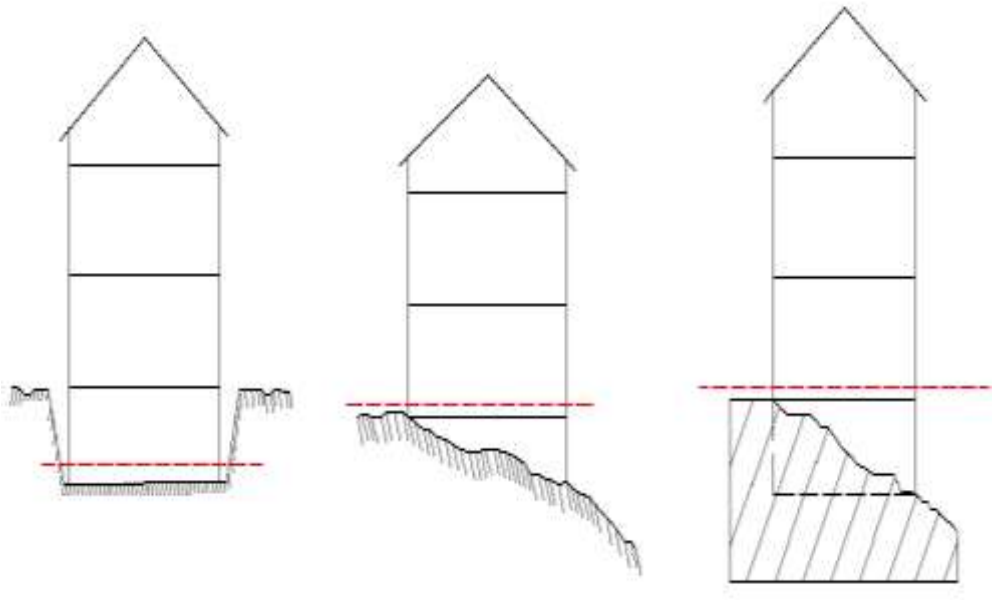

Figure 4.8: Location of the structure in various slope of the land [151]

Table 4.13: Definition of the vulnerability classes for parameter P5

Foundation soil	Foundation land slope 'p' (%)	Class
Soil type A with or without the foundation or soil type B and C with the foundation	$p \leq 10$	A
	$10 < p \leq 30$	B
	$30 < p \leq 50$	C
	$p > 50$	D
Soil type B and C without the foundation	$p \leq 10$	A
	$10 < p \leq 20$	B
	$20 < p \leq 50$	C
	$p > 50$	D
Soil type D and E with the foundation	$p \leq 50$	C
	$p > 50$	D
Soil type D and E without the foundation	$p \leq 30$	C
	$p > 30$	D

P6: Position and interaction

The evaluation of the regularity of slender structures, built in with or adjacent to other buildings, should not be analysed individually. One must take into account the interaction with the adjacent structure to which it is connected, that limits its seismic response (i.e. to the deformation requirements due to the interaction point or section).

The response of the structure to horizontal action is influenced by its position, confinement and interaction, which can produce a high stress concentration at the point of connection and contact with adjacent structures. Figure 4.9 shows the damage occurred in slender structures due to interaction with adjacent structures. Figure 4.10 shows the possible position of such type of structures and vulnerability classes according to location and interaction as described in Table 4.14.

Figure 4.9: Earthquake damage at the bond provided by the adjacent structure [21]

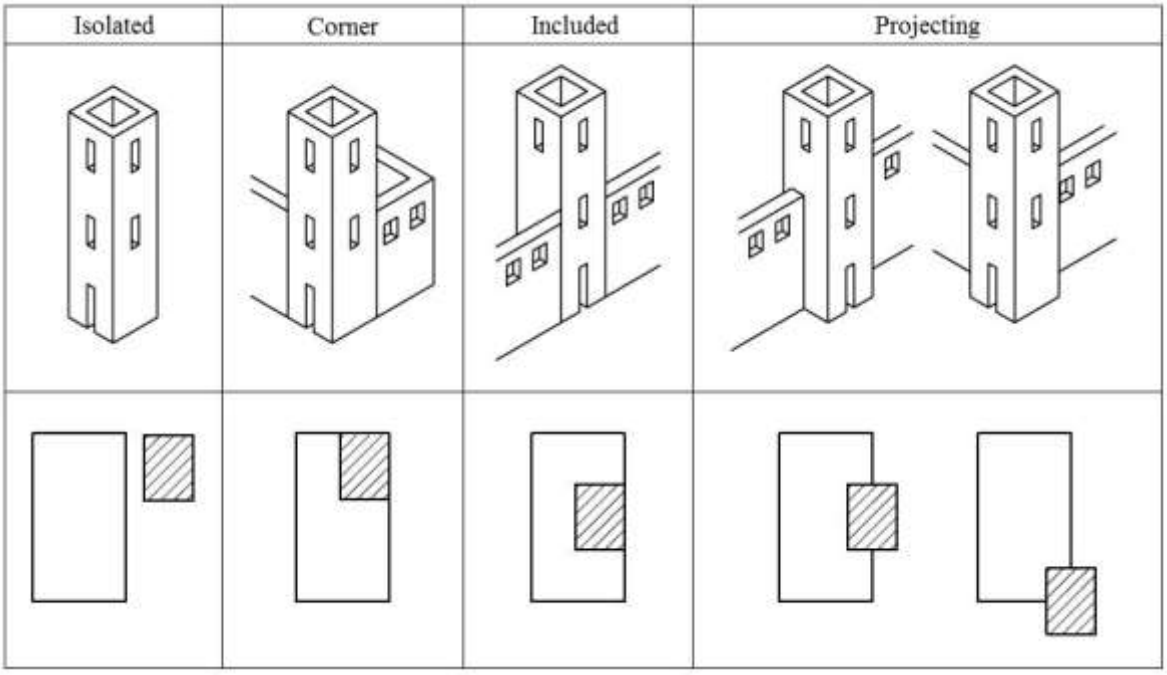

Figure 4.10: Position of the tower in the urban context

Table 4.14: Definition of the vulnerability classes for parameter P6

Class	A	B	C	D
Position of the tower	Isolated	Corner	Included	Projecting

P7: Irregularity in plan

The shape and arrangement in plan of the resistant system of the structures are aspects that influence the structural performance and, consequently, the seismic vulnerability associated to the global torsional effect. The approach followed in this parameter was based on the assessment of the eccentricity between the centre of mass and the centre of rigidity. The eccentricity is considered dependent of size and number of opening sides at base.

The parametric pushover analyses were carried out in numerous analytical models, with different possible plan irregularity scenarios, in order to define the vulnerability classes for this parameter. Irregularities in plan scenarios were introduced in the models by varying the size of openings and number of opening sides at base. The size of openings considered were one–third, half and two–thirds of the wall breadth at the base. Similarly, the number of opening sides was one, two and three with only one in each side and at base. Moreover, the openings were centrally located in each side. The size adopted for all openings in one

model was equal, if it has more than one opening. The results of parametric pushover analyses, in terms of maximum global drift capacity, from these models were compared with the results of the reference structure. Figure 4.11 shows the influence of size of openings and number of opening sides at base in the decrease of maximum global drift capacity (in percentage) in comparison to the reference structure.

Here, the model with one side opening and opening size of two–thirds of wall breadth at the base shows the highest decrease in maximum global drift capacity (i.e. 48%). Result of pushover analysis carried out on model by increasing the size of openings further shows that it could not withstand any lateral load. Hence, 48% decrease in maximum global drift capacity was considered as upper limit for vulnerability classes classification. Based on this upper limit, the percentage decrease in maximum global drift capacity was divided equally into four ranges (i.e. 0%–12%, 12%–24% , 24%–36% and 24%–48%) and the relative opening size at base is defined as the limiting range for the vulnerability classes A, B, C and D, respectively (see Table 4.15). Similarly, the relative eccentricity (e_R) of the structures with openings' size as defined above was estimated. These estimated values define the vulnerability classes in function of the relative eccentricity as shown in Table 4.16.

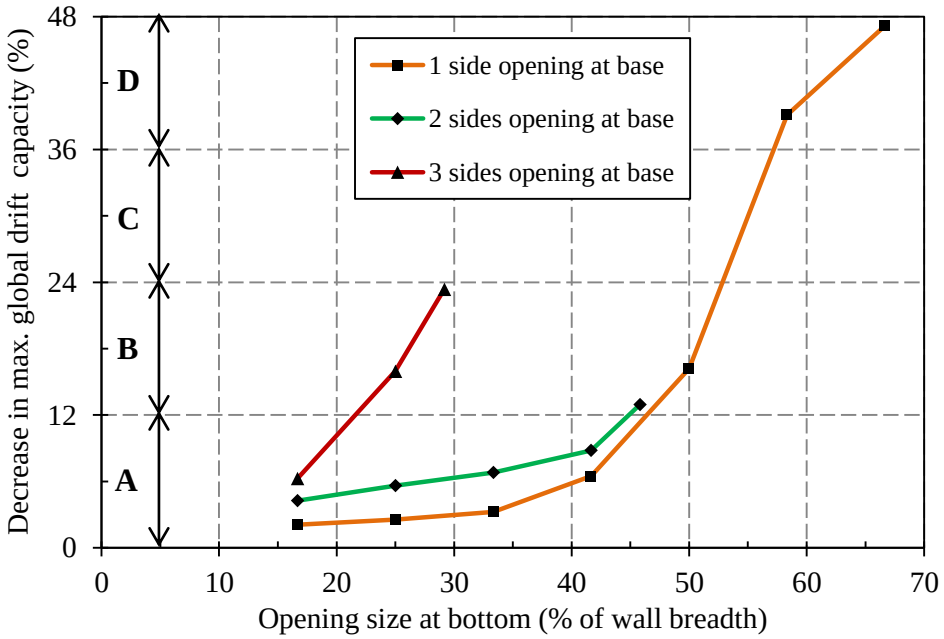

Figure 4.11: Influence of size of openings and number of opening sides at base in the max. global drift capacity

Table 4.15: Definition of the vulnerability classes for parameter P7, in function of the size of openings and number of opening sides at base (dimension of openings are considered centered and equal in all sides)

		Class	Size of openings at base 'OB'		Location	Example
			Square section (% of breadth at base)	Circular section (% of diameter at base)		
Number of sides with opening	1	A	OB ≤46%	OB ≤39%		 [11]
		B	47%< OB ≤53%	40%< OB ≤45%		 [80; 63; 38]
		C	53%< OB ≤57%	45%< OB ≤49%		 [28]
		D	OB >57%	OB >49%		–
	2	A	OB ≤45%	OB ≤38%		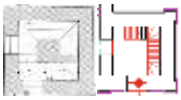 [156; 157]
		B	45%< OB ≤46%	38%< OB ≤39%		–
		D	OB >46%	OB >39%		–
	3	A	OB ≤22%	OB ≤20%		–
		B	22%< OB ≤29%	20%< OB ≤25%		–
		D	BO>29%	BO>25%		

Table 4.16: Definition of the vulnerability classes for parameter P7, in function of the max. relative eccentricity (% of wall breadth)

	Class	A	B	C	D
Number of sides of opening	1	e_R ≤15%	15%< e_R ≤22%	22%< e_R ≤25%	e_R >25%
	2	e_R ≤12%	12%< e_R ≤13%	–	e_R >13%
	3	e_R ≤6%	6%< e_R ≤12%	–	e_R >12%

P8: Irregularity in elevation

This parameter assesses the vulnerability associated to the irregularity in elevation. The irregularity in elevation was defined as a function of stiffness variation along the height of the structure. The approach followed in this parameter is based on the assessment of discontinuity in masonry wall regarding: (a) reduction in the wall thickness (see Figure 4.12a) and (b) presence of non–supported wall portion (see Figure 4.12b).

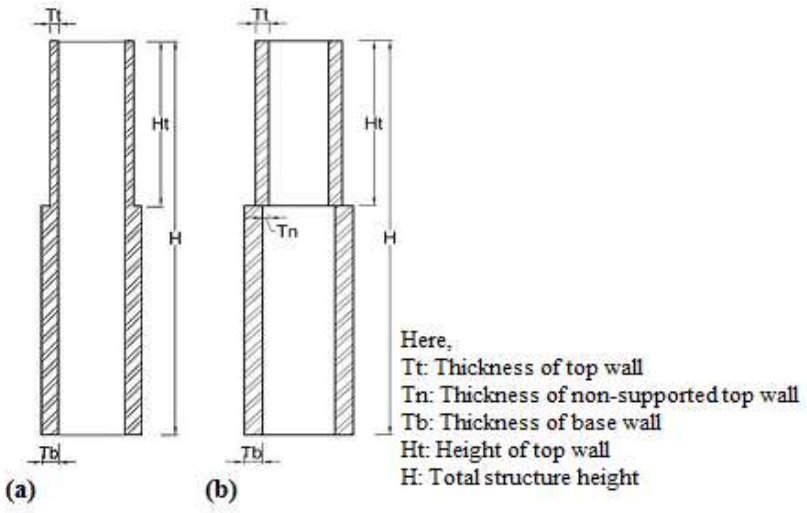

Figure 4.12: Vertical irregularity scenario: a) reduction in wall thickness; b) presence of non–supported wall portion

The parametric pushover analyses were carried out in numerous analytical models, modeled with different possible scenarios of irregularity in elevation, to define the vulnerability classes for this parameter. Firstly, models were considered with an internally, both ways and externally reduction of the wall thickness (i.e. 25%, 50% and 75%) above different levels (i.e. one–fourth, half and three–fourths of total height) as shown in Figure 4.13. Secondly, models were considered with the non–supported wall portion, i.e. thickness of wall portion equal to 25%, 50%, 75% and 100% of its own thickness was not supported by the continuous base wall beneath as shown in Figure 4.14. Furthermore, the non–supported wall portion was accumulated with reduction in the wall thickness (i.e. 25%, 50%, and 75% of base wall thickness) above different levels (i.e. one–fourth, half and three–fourths of the total height). The results of these parametric pushover analyses, in terms of maximum global drift capacity, obtained with these models were compared with the results for the reference structure.

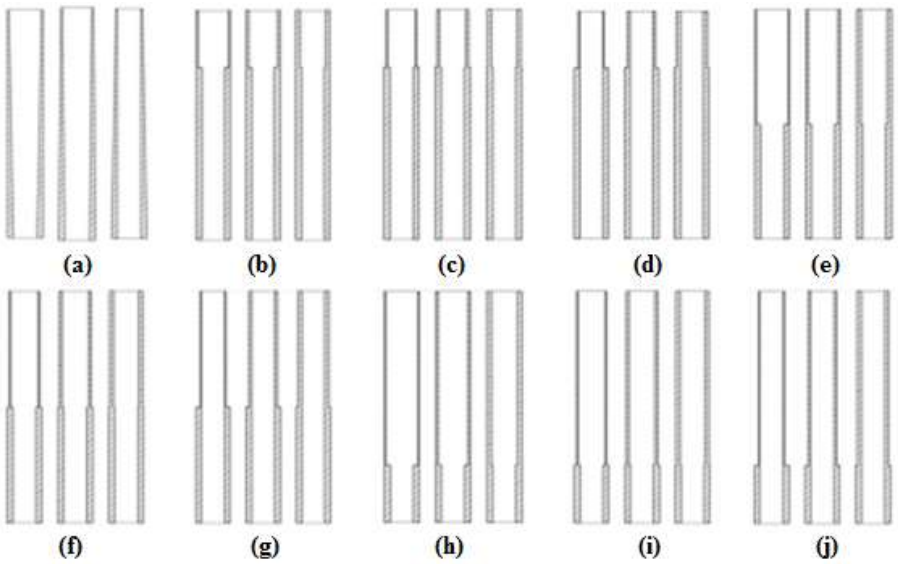

Figure 4.13: Reduction in wall thickness scenario for parametric analysis: a) linearly thickness reduction through overall height internally, both way and externally; b), c), d) 75%, 50% and 25% thickness reduction above 1/4th of overall height internally, both way and externally; e), f), g) 75%, 50% and 25% thickness reduction above 1/2 of overall height internally, both way and externally; h), i), j) 75%, 50% and 25% thickness reduction above height 3/4th of overall height internally, both way and externally

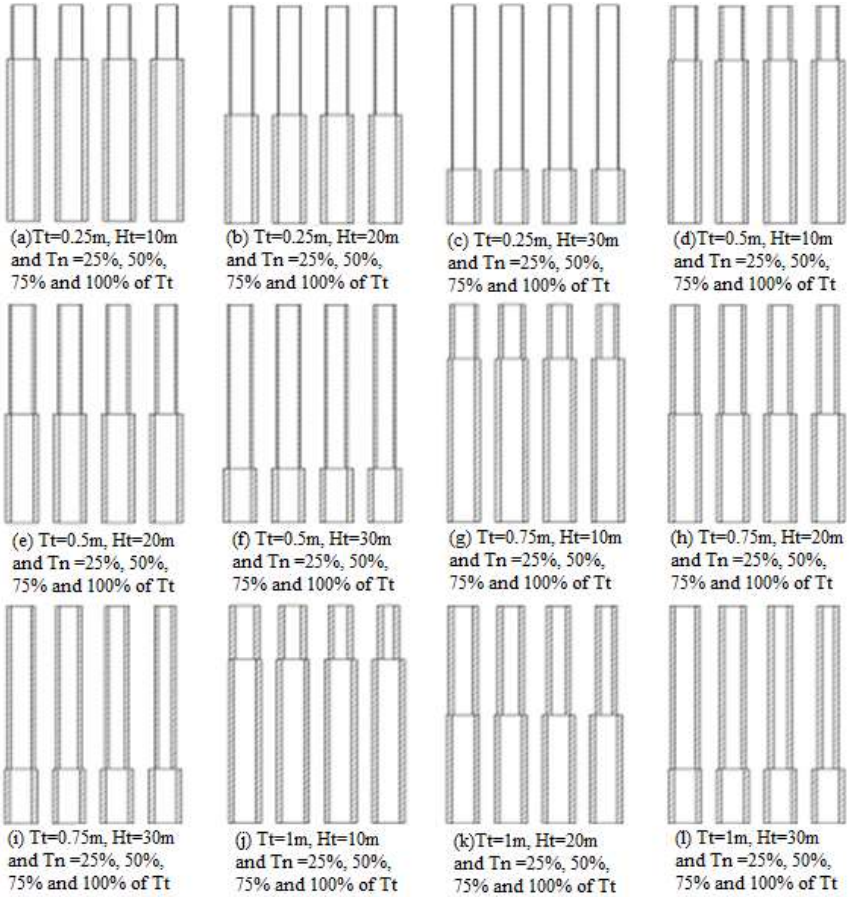

Figure 4.14: Discontinuous scenario in masonry wall section for parametric analysis

Figure 4.15 shows the influence of reduction in the wall thickness in the decrease of maximum global drift capacity in comparison with the reference structure. Here, the model with wall thickness reduction of 75% externally and above half of the height shows a highest decrease in the maximum global drift capacity (i.e. 60%). Result of pushover analysis carried out on model by decreasing its wall thickness further shows that it could not withstand any lateral load. Hence, 60 % decrease in maximum global drift capacity was considered as upper limit for vulnerability classes classification. Based on this upper limit, the percentage decrease in maximum global drift capacity was divided equally into four ranges (i.e. 0–15%, 15–30%, 30–45% and 45–60%) and the corresponding opening size at base is defined as the limiting range for the vulnerability classes A, B, C and D, respectively (see Table 4.17).

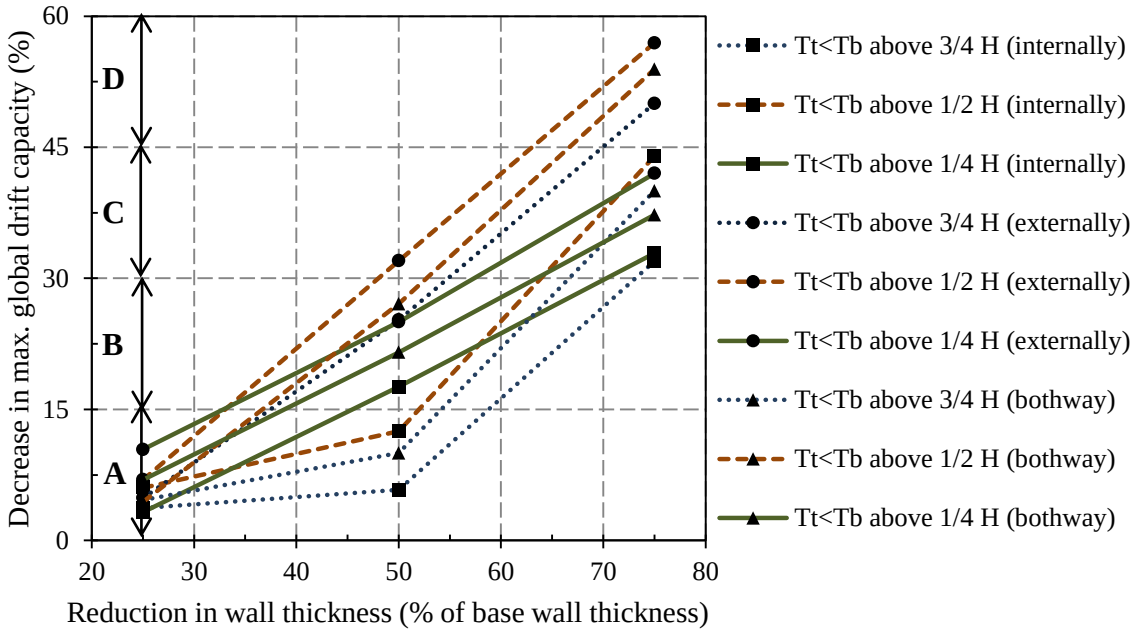

Figure 4.15: Influence of the reduction in wall thickness in the max. global drift capacity

Figure 4.16 shows the analyses results of the influence of the presence of non–supported wall portion in the decrease of the maximum global drift capacity relatively to the reference structure. Here, the model with fully unsupported wall portion with wall thickness reduction by 75% relatively to base wall thickness and above half of the height shows the highest decrease in maximum global drift capacity (i.e. 72%). Result of pushover analysis carried out on model by decreasing its wall thickness further shows that

it could not withstand any lateral load. Hence, 72% decrease in maximum global drift capacity was considered as upper limit for vulnerability classes classification. Based on this upper limit, the percentage decrease in maximum global drift capacity was divided equally into four ranges (i.e. 0–18%, 18–36%, 36–54% and 54–72%) and the relative opening size at base is defined as the limiting range for the vulnerability classes A, B, C and D respectively (see Table 4.18).

Table 4.17: Definition of the vulnerability classes for parameter P8 due to variation of wall thickness

Class	Constant thickness up to 3/4th of height and above that thickness reduction section				Constant thickness up to 1/2 of height and above that thickness reduction section				Constant thickness up to 1/4th of height and above that thickness reduction section				
	Internally or Both ways		Externally		Internally		Externally or Both ways		Internally		Both ways	Externally	
A	$T_t \geq 0.46T_b$	[79]	$T_t \geq 0.63T_b$	[124]	$T_t \geq 0.48T_b$	[20]	$T_t \geq 0.67T_b$	[13]	$T_t \geq 0.55T_b$	[67]	$T_t \geq 0.61T_b$	$T_t \geq 0.67T_b$	[11]
B	$0.46T_b > T_t \geq 0.33T_b$	[62]	$0.63T_b > T_t \geq 0.45T_b$	[32]	$0.48T_b > T_t \geq 0.36T_b$	[158]	$0.67T_b > T_t \geq 0.52T_b$	[22]	$0.55T_b > T_t \geq 0.30T_b$	[91]	$0.61T_b > T_t \geq 0.37T_b$	$0.67T_b > T_t \geq 0.43T_b$	[22]
C	$T_t < 0.33T_b$	[11]	$0.45T_b < T_t \geq 0.30T_b$	[159]	$T_t < 0.36T_b$	[74]	$0.52T_b > T_t \geq 0.37T_b$	[87]	$T_t < 0.30T_b$	–	$T_t < 0.37T_b$	$T_t < 0.43T_b$	[16]
D	–		$T_t < 0.30T_b$	–			$T_t < 0.37T_b$	[26]	–				

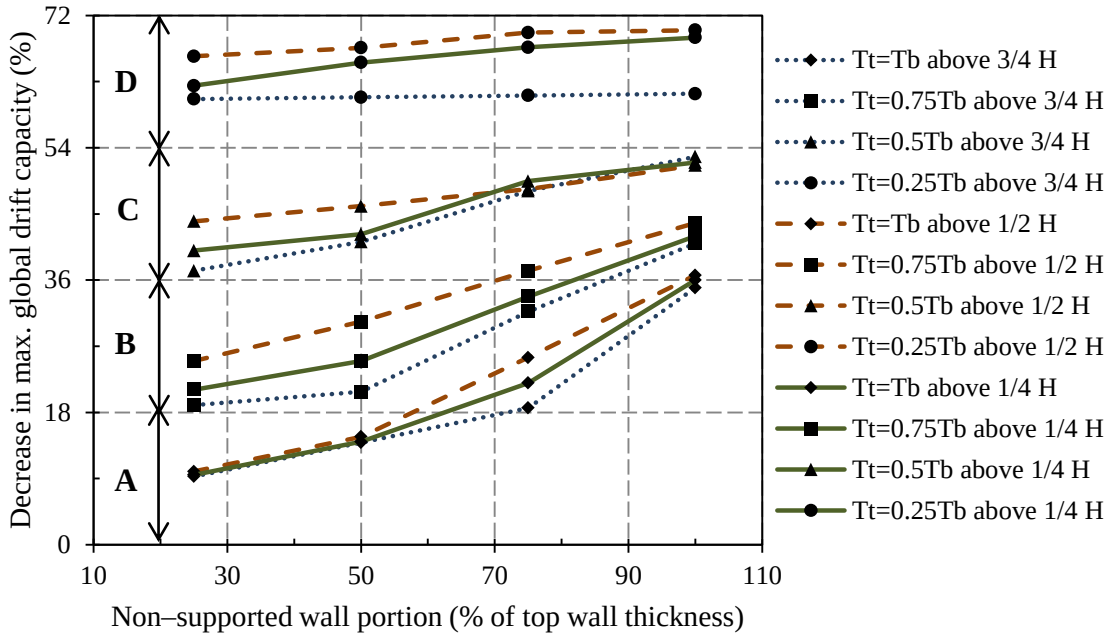

Figure 4.16: Influence of the presence of non–supported wall portion in the max. global drift capacity

Table 4.18: Definition of the vulnerability classes for parameter P8 due to the presence of discontinuities in wall (i.e. non–supported wall portion)

Class	Discontinuous wall above 3/4th of height		Discontinuous wall above 1/2 of height		Discontinuous wall above 1/4th of height	
A	Tn≤0.72Tt and 0.75Tb<Tt≤Tb	[78]	Tn≤0.58Tt and 0.75Tb<Tt≤Tb	[160]	Tn≤0.63Tt and 0.75Tb<Tt≤Tb	[82]
B	0.72Tt<Tn≤Tt and 0.75Tb<Tt≤Tb or Tn≤0.87Tt and 0.5Tb<Tt≤0.75Tb	[60]	0.58Tt<Tn≤Tt and 0.75Tb<Tt≤Tb or Tn≤0.70Tt and 0.5Tb<Tt≤0.75Tb	[106]	0.63<Tn≤Tt and 0.75Tb<Tt≤Tb or Tn≤0.82Tt and 0.5Tb≤Tt<0.75Tb	[106]
C	0.87Tt<Tn≤Tt and 0.5Tb<Tt≤0.75Tb		0.70Tt<Tn≤Tt and 0.5Tb<Tt≤0.75Tb		0.82<Tn≤Tt and 0.5Tb<Tt≤0.75Tb	[106]
	Tn≤Tt and 0.25Tb<Tt≤0.5Tb					
D	Tn≤Tt and Tt≤0.25Tb					[106]

The structures with constant thickness throughout the height or linearly reduction in wall thickness are considered as belonging to the vulnerability class A. The irregularity in elevation is evaluated on the basis of geometrical criteria (variation of wall thickness or presence of a non–supported wall portion). However, the variation of masonry wall arrangement/fabric and material is also important and may limit the structural performance to horizontal actions. Therefore, if a variation of wall masonry material is observed, the vulnerability class should be downgraded by one class.

P9: Wall openings number, size and location

Vulnerability of slender masonry structures is influenced by its mass and stiffness distribution in height, links to adjacent structures, material properties, aspect ratio and its slenderness. The area and location of structural openings in the walls highly influence the damage mechanisms in–plane or out–of–plane of the wall.

Parametric pushover analyses were carried out in numerous analytical models, to define the vulnerability classes for this parameter. The models were considered with openings of different sizes (i.e. one–third, half and two–thirds of wall breadth) and number (i.e. one, two and three), which were located at different levels (i.e. base, middle and top) (see Figure 4.17). Here, openings in the opposite façades are considered identical making the model symmetric in X and Y direction. The results of the parametric pushover analyses, in terms of maximum global drift capacity, obtained with these models were compared with the results for the reference structure.

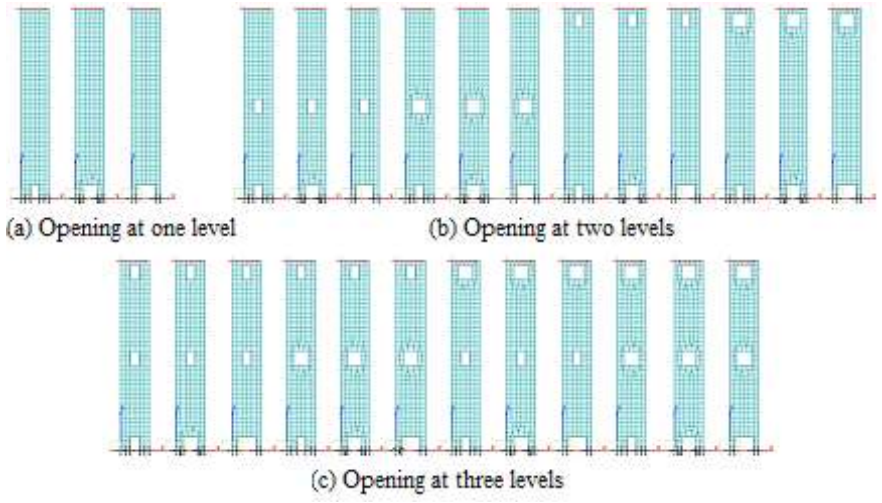

Figure 4.17: FE models for parametric analysis

Figure 4.18 shows the influence of number, size and location of openings in the decrease of maximum global drift capacity relatively to the reference structure. Here, the scenario corresponding to openings size greater than 50% of wall breadth is considered as the cut–off value for defining the vulnerability classes. The structures with opening size greater than 50% of wall breadth are considered as belonging to the vulnerability class D. Hence, 39% decrease in maximum global drift capacity (corresponding to opening size greater than 50% of wall breadth) was considered as upper limit for vulnerability classes classification. The percentage of decrease in maximum global drift capacity between upper limit (39%) and lower limit (0%) is divided equally into four ranges (i.e. 0%–3%, 13%–26% and 26%–39% and the relative opening size at base is defined as the limiting range for the vulnerability classes A, B and C, respectively (see Table 4.19). In the Table below, OB refers as size of opening at base and OA as size of opening above base.

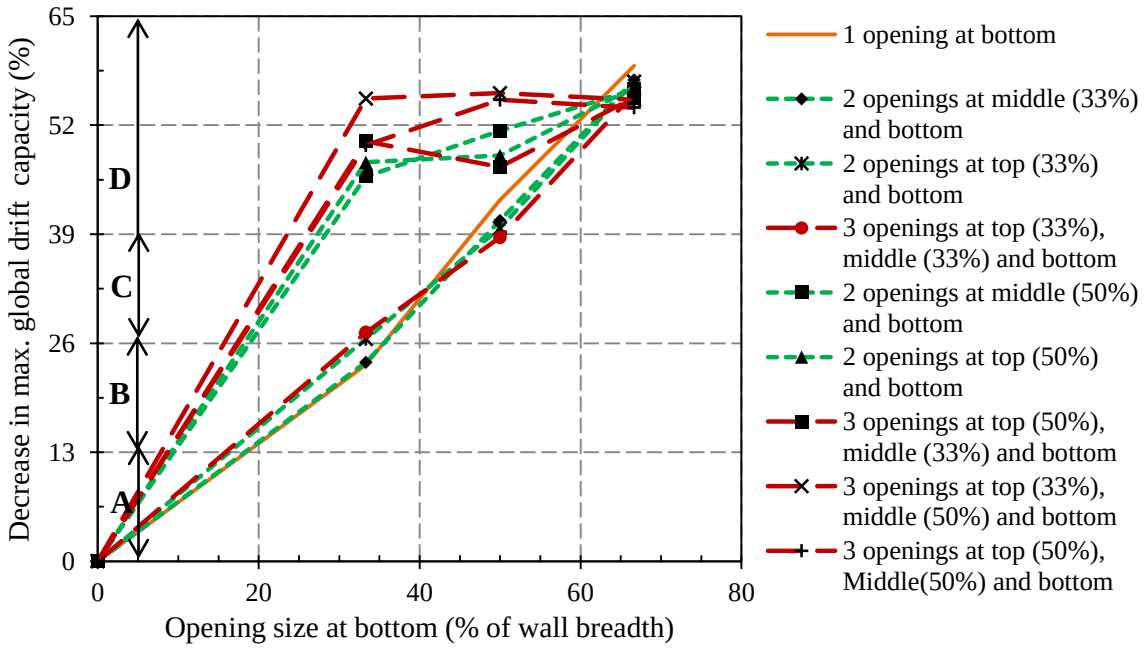

Figure 4.18: Influence of number, location and dimensions of openings in the max. global drift capacity

Tables 4.19: Definition of the vulnerability classes for parameter P9, in function of the number, location and size of openings (according to their influence in the global drift)

Class	Opening at one level			Openings at two level			Openings at three or more level		
	Square cross–section (% of wall breadth)	Circular cross–section (% of diameter)	Example	Square cross–section (% of wall breadth)	Circular cross–section (% of diameter)	Example	Square cross–section (% of wall breadth)	Circular cross–section (% of diameter)	Example
A	OB≤18%	OB≤16%	 [42]	OB≤17% and 0%≤OA≤33% or OB≤9% and 33%≤OA≤50%	OB≤15% and 0%≤OA≤28% or OB≤8% and 28%≤OA≤43%	 [16]  [70]	OB≤16% and 0%≤OA≤33% or OB≤8% and 33%≤OA≤50%	OB14% and 0%≤OA≤28% or OB≤7% and 28%≤OA≤43%	 [32]
B	18%<OB≤36%	16%<OB≤31%		17%≤OB≤34% and 0%≤OA≤33% or 9%≤OB≤18% and 33%≤OA≤50%	15%≤OB≤29% and 0%≤OA≤28% or 8%≤OB≤16% and 28%≤OA≤43%	 [161]  [162]	16%≤OB≤32% and 0%≤OA≤33% or 8%≤OB≤17% and 33%≤OA≤50%	14%≤OB≤27% and 0%≤OA≤28% or 7%≤OB≤15% and 28%≤OA≤43%	  [11]
C	36%<OB ≤50%	31%<OB≤43%		34%≤OB≤48% and 0%≤ OA≤33% or 18%≤OA≤27% and 33%≤OA≤50%	29%≤OB≤41% and 0%≤OA≤28% or 16%≤OB≤23% and 28%≤OA≤43%	  [49]	32%≤OB≤46% and 0%≤OA≤33% or 17%≤OB≤26% and 33%≤OA≤50%	27%≤OB≤39% and 28%≤OA≤43% or 15%≤OB≤22% and 28%≤OA≤43%	 
D	OB>50%	OB>43%		OB>48% and 0%≤OA≤33% or OB>27% and 33%≤OA≤50%	OB>41% and 0%≤OA≤28% or OB>23% and 28≤OA≤43%	  [163]	OB>46% and 0%≤OA≤33% or OB>26% and 33%≤OA≤50%	OB>39% and 0%≤OA≤28% or OB>22% and 28%≤OA≤43%	  [164]

P10: Flooring and roofing system

The quality and type of structural system of the floors and roof has a remarkable influence on the overall structural behaviour. It is proposed in this parameter the definition of the classes according to the state of conservation of floors and roofs, as this affects their connection conditions to the walls, as well as its own. It is important that the floors are well connected to the walls, so that, they transmit vertical and horizontal loads (see Figure 4.19). The deficiency of these connections creates instability in structure, the floor losing its ability to lock the walls (increasing its slenderness, and hence reducing its carrying capacity). Floors with insufficient stiffness in its plane induce a brittle behaviour of the structure, not mobilizing the response of the walls globally.

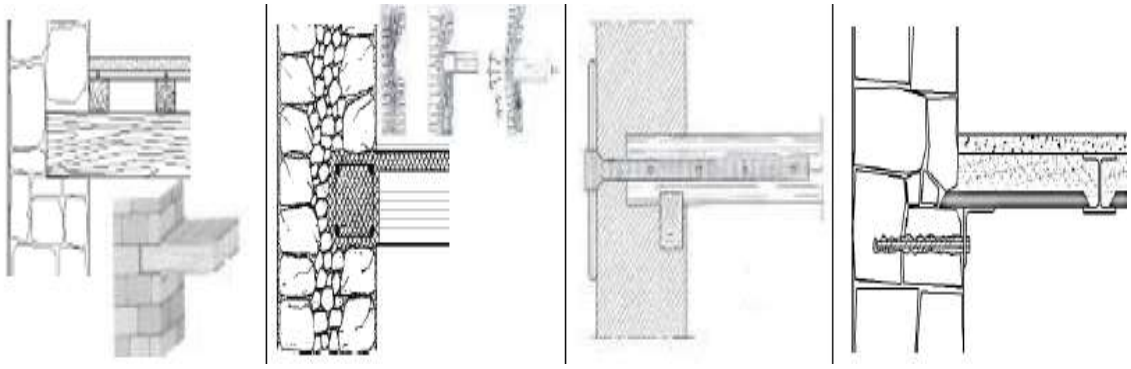

Figure 4.19: Different aspects of the link between wall and floor [151]

This criteria also considers the configuration of roofing. The possibility of coverage triggering lateral impulses to walls is undoubtedly an aspect in conditioning performance of the structures. The existence of elements connecting the roof to the wall, the possible presence of a perimetral beam or tie rods, and also their conservation status may influence the seismic performance of the structures. The impulsive nature of the roof is especially important because it may increase the seismic forces on the walls, eventually causing out–of–plan collapse (see Figure 4.20). Definitions of classes of vulnerability for the parameter P10 are presented in Table 4.20.

Types of roof structures	Example
Flat / No thrusting	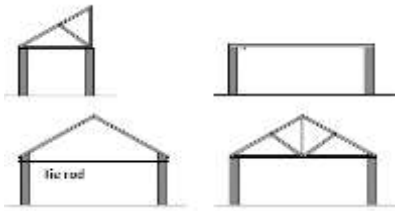
Semi thrusting	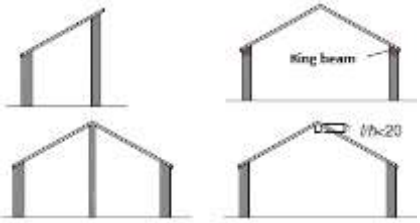
Thrusting (Including vaults)	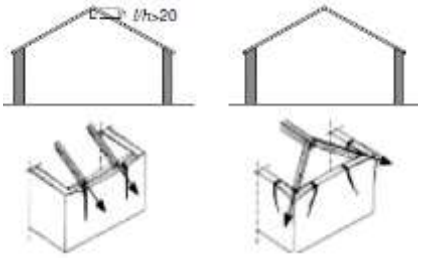

Figure 4.20: Types of roof structures according to its thrusting behaviour [151]

Table 4.20: Definition of the vulnerability classes for parameter P10

Class	Structural type and connection condition of flooring and roofing	Poor conservation state of flooring and roofing system	Roof structure with thrusting nature
A	Rigid or semi–rigid and well connected	Downgrade by 1 class	Downgrade by 1 class
B	Deformable and well connected		
C	Rigid or semi–rigid and improperly connected		
D	Deformable and poorly connected		

P11: Fragilities and conservation state

This parameter intends to evaluate the weaknesses observed in the structure that may aggravate damage eventually resulting from the occurrence of an earthquake. The classes of vulnerability are defined by the severity of structural defects and its origin (an action can be caused by previous seismic event) that can trigger certain mechanisms more adversely. Table 4.21 identifies, class by class, problems and defects that increase substantially the risk of constructions suffer damage, showing in particular the degree of cracking and degradation of materials: cracks along the corners, detachment of orthogonal walls, bulging and deformation, signs of crushing, etc.

Table 4.21: Definition of the vulnerability classes for parameter P11 [151]

Class	Description
A	Masonry walls in good condition with no visible damage.
B	Walls with small cracks (less than 0.5mm), was not widespread. Signs of moisture problems which deteriorates the characteristics of the masonry and lead to degradation or decay of wood.
C	Walls crack opening of about 2 to 3mm. Structures with a state of poor conservation of masonry walls. Serious problems of deformability in the structural members.
D	Walls with deterioration and even if not widespread severe cracking. Walls with physical features and materials that show very poor or severe decrease of resistance. Cracking in locations, such, as near the corners (signs of disconnection between orthogonal walls). Damage introduced by thrusts transmitted by the roof, bulging of load–bearing walls, cracking due to settlement of foundations. Slip wooden framework with respect to the walls of the framework. Decomposition and degradation of wood along the walls. Signs of rotation and walls out of plumb.

P12: Non–structural elements

This parameter measures the effect of elements that are not part of the structural system, such as bells, pinnacles, cornices, parapets, balconies or other projecting members that are attached to the structure (see Figure 4.21). During the seismic event, there connections with the structure weaken and increase the level of damage in structural elements. The definition of vulnerability class of this parameter is classified only as classes A, B and C, as presented in Table 4.22.

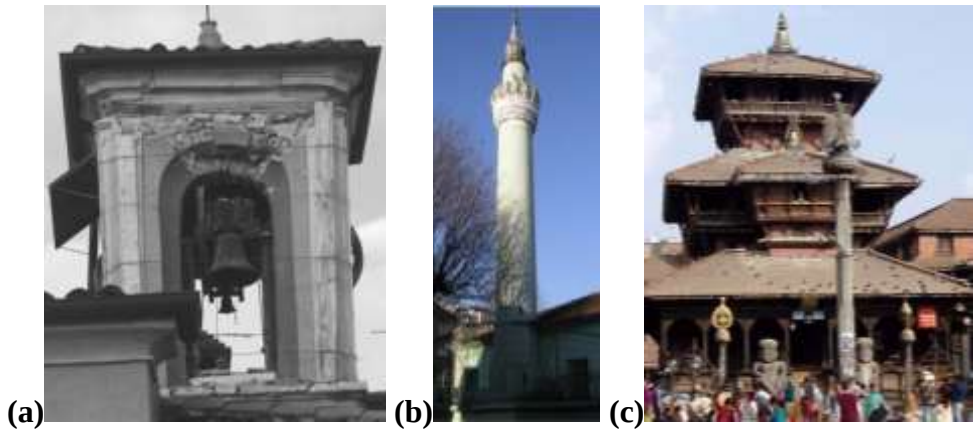

(a) **(b)** **(c)**

Figure 4.21: Non–structural elements: a) bells on bell towers [21]; b) balcony in minarets [26]; c) pinnacles in Pagoda temples

Table 4.22: Definition of the vulnerability classes for parameter P12

Class	Description
A	No hanging or emerging elements such as bells, pinnacles, cornices, parapets, balconies, turrets, etc.
B	Structure with hanging or emerging elements well connected to the walls, turrets with reduced size and weight.
C	Structure with hanging or emerging elements poorly connected to the walls, slender turrets with considerable weight.

4.4.2 Definition of parameters weight

Parameter weight (W_i) is the coefficient multiplying the vulnerability class numeric value (K_i), depending upon its importance, ranging within 0.25 to 1.5. It reflects the importance of each parameter in the seismic vulnerability of the structure. This coefficient is assigned taking into account values proposed in the literature for similar methodology, the opinion of experts and parametric analyses results. To collect information of weight from expert, a questionnaire survey was carried out. The survey response relatively to the weight for each parameter obtained from 18 experts (all over the world and precisely working in similar types of structures), then were tabulated and analysed. Similarly, to define the weight using parametric analyses, numerous models were constructed and pushover analyses were carried out (see Table 4.23).

The result corresponding to the worst scenario in terms of maximum global drift and base shear force for each parameter, in comparison to results for the reference structure is considered as the upper limit for that parameter (see Figure 4.22). The highest change in maximum global drift (i.e. nearly 190%) and in base share force (i.e. nearly 98%), among all the 9 parameters analysed, was divided into three ranges as presented in Table 4.24. Each range corresponds to the numeric value (weight) of 0.75, 1 and 1.5. For each parameter the weight corresponding to its maximum changes in global drift or base shear force was adopted. For all parameters except P2, P3, P6 and P8, the weight is determined by both criteria (global drift or base shear force) matches. For parameters P2, P3, P6 and P8, it was adopted the greater weight among the obtained with the both criteria.

The final weight adopted for each parameter was defined after comparing the weight assigned according to values proposed in the literature, opinion of experts and results of the parametric analyses done, as shown in Table 4.25. For each parameter, it was adopted the most coherent weight amongst all source of information except for parameter P1 and P10. For parameters, P10 (Flooring and roofing system), P11 (Fragilities and conservation state) and P12 (Non–structural elements), parametric pushover analysis were not carried out due to wide range of scenarios and difficulties associated in modeling them.

Table 4.23: Sensitivity analysis performed and results obtained

Parameter	Strategy adopted for the sensitivity analysis carried out with non–linear numerical analysis by varying	Worst scenario (corresponding to scenario when structure can't withstand any lateral load beyond it)	Pushover analysis results (relatively to the reference structure)	
			Max. change in global drift	Max. change in base shear force
P1: Type of resisting system	Young's modulus (*E*) of masonry wall section at corner angles	*E* value = 30% of the reference structure's *E* value	16.68%	15.87%
P2: Quality of the resisting system	Young's modulus (*E*) of masonry wall section	*E* value = 30% of the reference structure's *E* value	189.74%	11.48%
P3: Conventional strength	characteristic shear strength (τ) capacity of masonry wall section	τ value = 20kPa	80.27%	97.98%
P4: Slenderness ratio	slenderness ratio (height to breadth ratio, $\frac{H}{B}$) of the structure	$\frac{H}{B}$ value = 225% of the reference structure's $\frac{H}{B}$ value	109.95%	85.43%
P5: Location and soil conditions	slope angle of foundation of the structure	foundation slope angle = 40˚	20.05%	18.39%
P6: Position and interaction	different restraining scenarios with the adjacent building, as described in section 4.4.1	two sided projecting nature	29.28%	56.01%
P7: Irregularity in plan	the results from vulnerability classes defined in section 4.4.1 were adopted	structure with only one opening at base and size of two–thirds of wall breadth	47.18%	44.86%
P8: Irregularity in elevation		wall portion above half the height of structure, un–supported by base wall and having thickness of 25% of base wall	70%	79.17%
P9: Wall openings number, size and location		structure with only one opening at base and its size of two–thirds of wall breadth	59.07%	46.27%

Table 4.24: Definition of weights as a function of the results for two criteria (global drift and base shear force)

Parameter weight (W_i)	Maximum change in global drift (%)	Maximum change in base shear force (%)
0.75	–47.5 to 47.5	0 to –24.5
1.00	–47.5 to –95 or 47.5 to 95	–24.5 to –49
1.50	95 to 190	–49 to –98

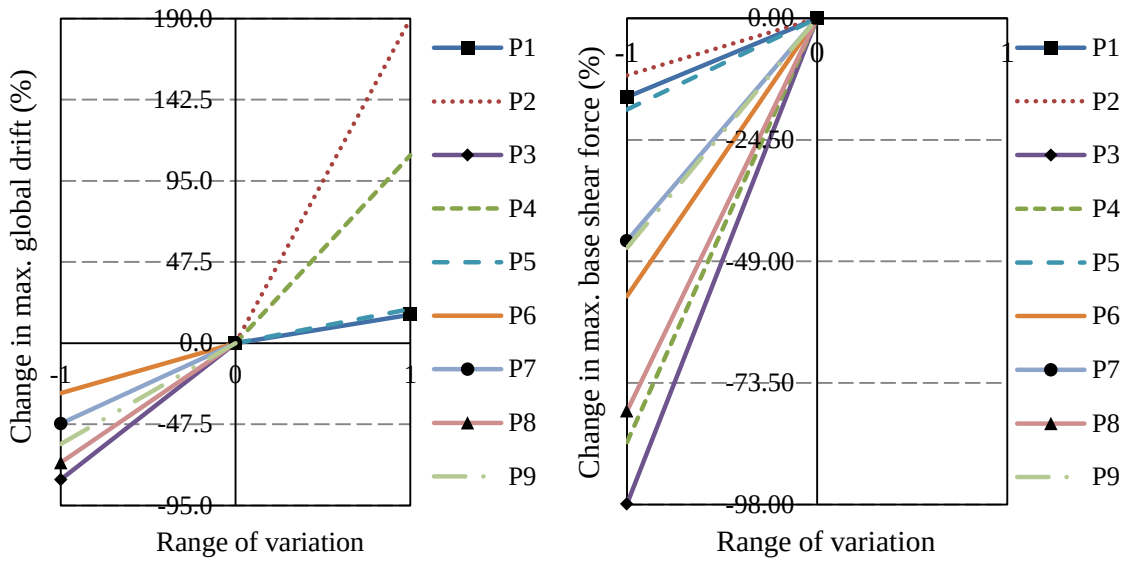

Figure 4.22: Percentage change in max. global drift (left) and base shear force (right)

Table 4.25: Comparison of weight (W_i) for vulnerability assessment parameters

Parameter	Parameter weight (W_i)						
	Similar methodology			Expert opinion	Parametric analysis		Value adopted
	GNDT–SSN–1994 [131]	Vicente *et al.* [165]	VULNeT [1]		Considering the % change in max. top displacement	Considering to % change in max. base shear force	
P1: Type of resisting system	1.00	0.75	1.00	1.41	0.75	0.75	1.00
P2: Quality of the resisting system	0.25	1.00	0.50	1.49	1.50	0.75	1.50
P3: Conventional strength	1.50	1.50	0.80	1.14	1.00	1.50	1.50
P4: Slenderness ratio	–	–	–	1.05	1.50	1.50	1.50
P5: Location and soil conditions	0.75	0.75	0.75	1.00	0.75	0.75	0.75
P6: Position and interaction	–	1.50	–	0.64	0.75	1.50	1.50
P7: Irregularity in plan	0.50	0.75	–	1.05	1.00	1.00	1.00
P8: Irregularity in elevation	0.50–1.00	0.75	1.50	1.27	1.00	1.50	1.50
P9: Wall openings number, size and location	–	0.05	–	0.98	1.00	1.00	1.00
P10: Flooring and roofing system	0.50–1.00	1.00	0.80	0.86	–	–	0.50
P11: Fragilities and conservation state	1.00	1.00	1.00	0.90	–	–	1.00
P12: Non–structural elements	0.25	0.50	0.40	0.25	–	–	0.25

4.5 Implementation of proposed methodology on slender masonry structures

4.5.1 Vulnerability assessment of slender masonry structures

The proposed vulnerability assessment methodology was implemented on different types of slender masonry structures. In case of towers, minarets and chimneys the information collected from literatures was used to assess the vulnerability class for each parameter.

4.5.1.1 Nepalese Pagoda temples

For the implementation of proposed vulnerability assessment methodology, a field survey was done and required information was gathered on 78 Nepalese Pagoda temples. The method proposed here is considered robust, taking into account that the inspection of all the Pagoda temples was carried out in detail and accurate geometrical information was available. Therefore, uncertainty in the assignment of vulnerability classes to each parameter is considered low. Figure 4.23 illustrates the assignment of vulnerability class for each parameter evaluated in the detailed vulnerability assessment over 78 Pagoda temples. Further detail vulnerability assessment of Nepalese Pagoda temples is presented in chapter 5.

The results of vulnerability assessment show the following important characteristics:

(a) Parameter P1 and P5 have a significant influence over the final vulnerability index, as most of the Pagoda temples are classified as C, i.e. due to lack of tie rods or ring beams, as well as weak connection between orthogonal walls. Locations of all Pagoda temples are over soft to medium soil site over plane areas (P5 taken as class C);

(b) Parameter P2 and P12 have an intermediate influence over the final vulnerability index, as most of the Pagoda temples are classified as B or C, i.e. due to the construction of these structures with average to poor quality of brick masonry and presence of well to poorly connected non–structural elements, such as cornices, pinnacle etc. respectively;

(c) Parameter P3 and P10 reveal a high influence over the final vulnerability index, as all of the Pagoda temples are classified as D, i.e. due to minimum shear strength capacity and flexible roofing structure with thrusting nature respectively;

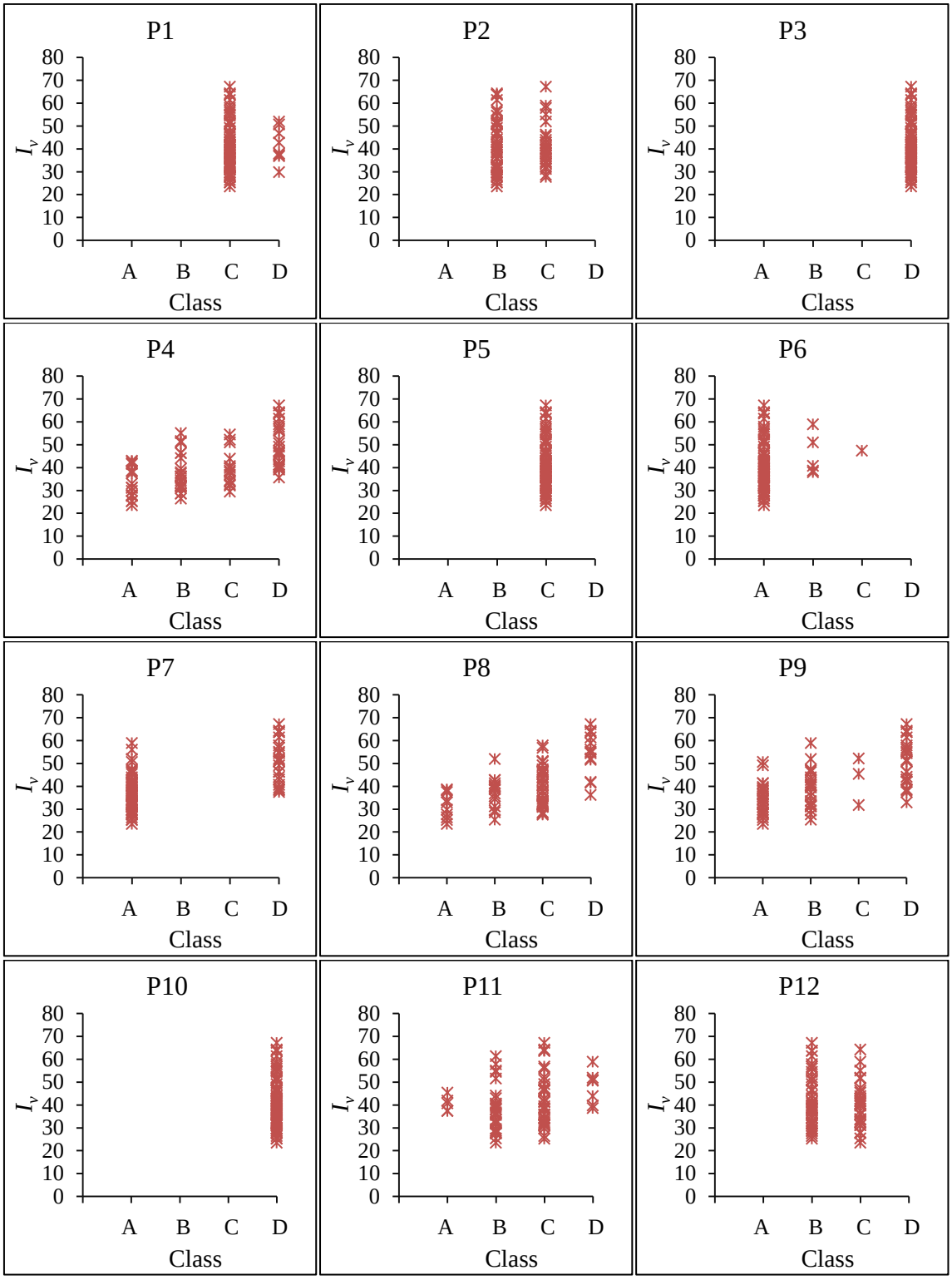

Key: P1: Type of resisting system; P2: Quality of the resisting system; P3: Conventional strength; P4: Slenderness ratio; P5: Location and soil conditions; P6: Position and interaction; P8: Irregularity in elevation; P9: Wall openings number, size and location; P10: Flooring and roofing system; P11: Fragilities and conservation state; P12: Non–structural elements

Figure 4.23: Vulnerability index and vulnerability class distribution of all parameters for the 78 Pagoda temples assessed

(d) Parameter P4 and P8 are well distributed classes A, B, C, and D. Hence, its influence in final vulnerability index is low to high, i.e. due to variation in slenderness, wall thickness and presence of turrets among the Pagoda temples;
(e) Parameter P6 has almost no influence over the final vulnerability index, as most of the Pagoda temples are highly classified as A, with some exceptional cases, i.e. due to isolated nature of these structures;
(f) Parameter P7 has low to high influence over the final vulnerability index, as most of the Pagoda temples are classified as A or D, i.e. due to size and number of door. Pagodas with 1 and 4 doors are of class A and Pagodas with 3 doors are of class D;
(g) Parameter P9 is well distributed classes A, B, and D, with few class C cases. Hence, its influence over the final vulnerability index goes from low to high, i.e. due to variation in numbers, size and location of openings;
(h) Parameter P11 has an intermediate influence over the final vulnerability index, as most of the Pagoda temples are classified as B or C corresponding to reasonable conservation states (few classified as A and D).

4.5.1.2 Masonry towers

Existing historical masonry towers with different characteristics and functions are distributed all over the world and constitute a relevant part of the architectural and cultural heritage of humanity. These important vertical structures were built either isolated or commonly included in the urban context, part of churches, castles, municipal buildings and city fortress walls. Bell and clock towers, also named civic towers, were built quite tall with the important purpose of informing people visually and with sounds by ringing bells and striking clocks about time and extraordinary events such as civil defence or fire alarm, and moreover to call the community to social meetings. Another reason that led to the construction of tall civic towers was that they were seen as a symbol, representing by the height and architecture sophistication, the richness and power of great families and communities.

For the implementation of proposed vulnerability assessment methodology, a database collection of 63 masonry tower structures was constituted through an intense literature review. Data related with all the information which influences the vulnerability assessing

parameters was collected, such as, geometric and mechanical characteristics, conservation state and construction characteristics. The database information regarding geometric characteristic reveals the total height of the such structures ranges from 16.86m (shortest) to 112m (tallest) and the width of the wall at base varying from 3m (minimum) to 15.32m (maximum). Figure 4.24 illustrates the assignment of vulnerability class for each parameter evaluated in the detailed vulnerability assessment of the 63 towers (bell towers, clock towers etc.).

The results of vulnerability assessment show the following important characteristics:

(a) Parameter P1 and P5 have a significant influence over the final vulnerability index, as most of the towers are classified as C, i.e. due to lack of tie rods or ring beams and weak connection between orthogonal walls in most of evaluated towers. Insufficient information on soil and location of all towers it was assumed to be in soft to medium soil site over plane areas (P5 taken as class C);

(b) Parameter P2, P3 and P12 has a low to intermediate influence over the final vulnerability index, as most of the towers are classified as A, B and C, i.e. due to construction of these structures with poor to good quality of masonry, variation of shear strength capacity between low and high and absence or presence of well to poorly connected non–structural elements, such as bells respectively;

(c) Parameter P4, P6, P8, P10 and P11 are well distributed classes A, B, C, and D. Hence, its influence over the final vulnerability index is low to high, i.e. due to variation in slenderness, construction of these structures in all positions, variation in roofs and floor construction system and conservation state amongst the towers, respectively;

(d) Parameter P7 has very low influence over the final vulnerability index, as most of the towers are classified as A, with some exception (i.e. presence of small openings at base causing low eccentricity between mass and rigidity centers);

(e) Parameter P9 has low influence over the final vulnerability, as most of towers are classified as A and B (i.e. lesser and small size of openings in most of the towers).

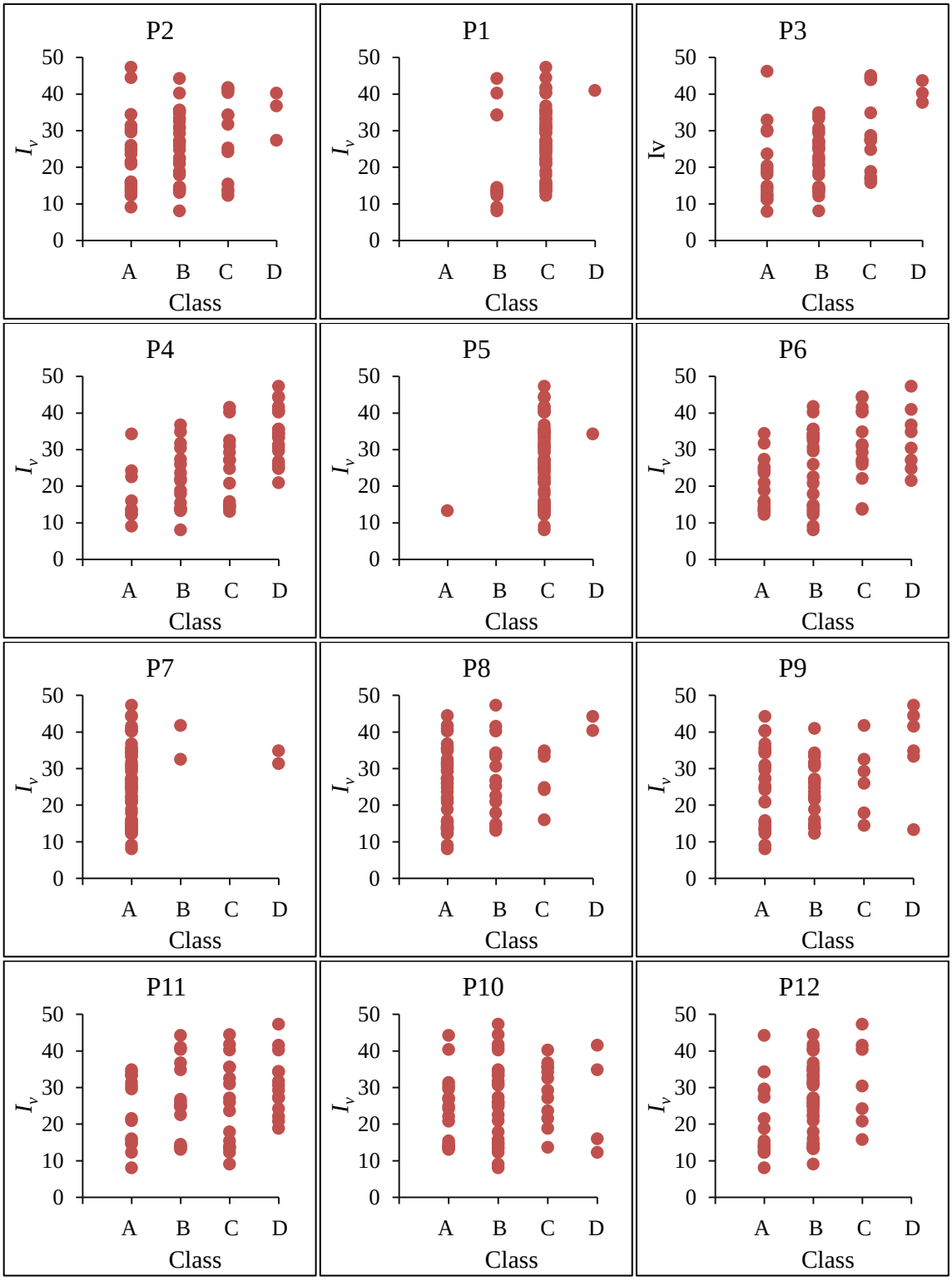

Key: P1: Type of resisting system; P2: Quality of the resisting system; P3: Conventional strength; P4: Slenderness ratio; P5: Location and soil conditions; P6: Position and interaction; P8: Irregularity in elevation; P9: Wall openings number, size and location; P10: Flooring and roofing system; P11: Fragilities and conservation state; P12: Non–structural elements

Figure 4.24: Vulnerability index and vulnerability class distribution of all parameters for the 63 masonry towers assessed

4.5.1.3 Masonry minarets

Minarets are typical form of Islamic architecture. Minarets are very slender structures, usually of cylindrical cross–section and they can stand alone or be contiguous and integral with mosque structures. Minarets were formerly used by the Muezzin to call out the adhan (ezan) to summon people to the pray [166]. In the present day, minarets are no longer used for this function due to the use of loudspeakers, but they are still built as one of the most distinctive components of the mosques. Minarets have become an integral part of Islamic faith and culture. They are deemed as the lighthouses of faith. Minarets are spread throughout the Islamic world and constitute an important heritage not only of religious value, but also great cultural interest.

For the implementation of the proposed vulnerability assessment methodology, a database collection of 32 minarets was constituted through an intense literature review. The database information regarding geometric characteristics indicates the total height of such structures ranges from 11.8m (shortest) to 74.4m (tallest). The vulnerability assessment of the 32 minarets was carried out by evaluating the information gather from detail literature reviews on individual minarets. Therefore, uncertainty in the assignment of vulnerability classes to each parameter is considered low. Figure 4.25 illustrates the assignment of vulnerability class for each parameter evaluated in the detailed vulnerability assessment of the32 minarets.

The results of vulnerability assessment show the following important characteristics:

(a) Parameter P1 has a low influence over the final vulnerability index, as most of the towers are classified as B, i.e. due to cylindrical wall section;

(b) Parameter P2, P3 has a low to intermediate influence over the final vulnerability index, as most of the minarets are classified as A and B, with few classified as C (i.e. minarets with poor to good quality of minarets construction and variation of shear strength capacity between medium to high respectively);

(c) Parameter P4, P6, P8 and P12 are well distributed classes A, B, C, and D. Hence, its influence over the final vulnerability index is low to high, i.e. due to variation in slenderness amongst the minarets, construction of these structures in all positions as defined for each class, variation in wall thickness along height and absence or presence of well to poorly connected non–structural elements, respectively;

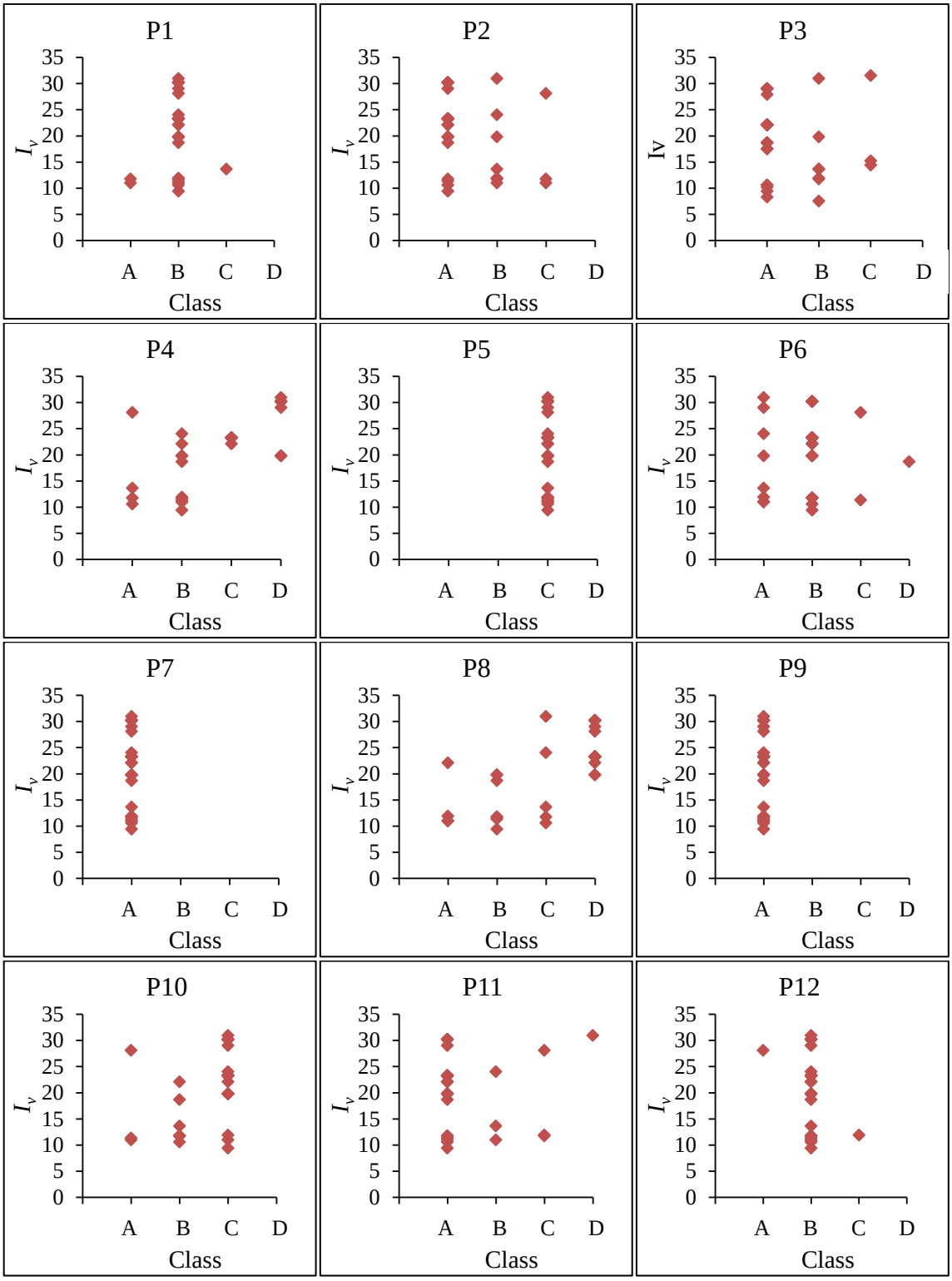

Key: P1: Type of resisting system; P2: Quality of the resisting system; P3: Conventional strength; P4: Slenderness ratio; P5: Location and soil conditions; P6: Position and interaction; P8: Irregularity in elevation; P9: Wall openings number, size and location; P10: Flooring and roofing system; P11: Fragilities and conservation state; P12: Non–structural elements

Figure 4.25: Vulnerability index and vulnerability class distribution of all parameters for the 32 masonry minarets assessed

(d) Parameter P5 has a significant influence over the final vulnerability index, as all of the minarets are low classified as C, i.e. due to insufficient information on soil property in literatures. Hence, location of all minarets is assumed to be in soft to medium soil site over plane area;

(e) Parameter P7 and P9 has no influence over the final vulnerability index, as most of the towers are highly classified as A, with some exception, i.e. due to absence or presence of small openings at base causing no or low eccentricity between mass and rigidity center and small size of openings in all of the minarets respectively;

(f) Parameter P10 has a significant influence over the final vulnerability index, as all of the towers are classified as B and C (i.e. roofs construction system are semi–rigid or flexible with thrusting nature among the minarets);

(g) Parameter P11 has a low to high influence over the final vulnerability index, as all of the minarets are classified as A, B and C, i.e. due to variation in conservation state among the minarets.

4.5.1.4 Industrial masonry chimneys

Industrial masonry chimneys began to appear around the middle of the 19th century during the industrial evolution. They were of considerable height and usually conical in shape. Their function was to remove the smoke of combustion from the furnaces required for industrial processes at that time. Very few of them remain in use, since they became obsolete when new energy generation systems made their appearance in the 20th century. At the present time, many examples of these chimneys can still be found in different parts of the world. In many cities these chimneys form a characteristic landscape and are often protected by law as part of the cultural heritage. In places where the original factory has been swallowed up by urban development, the chimney still survives as a witness to past times, often forms part of the historical heritage of the local community and may even be considered an attraction from the point of view of the cultural tourism, as part of industrial itineraries.

For the implementation of proposed vulnerability assessment methodology, a database collection of 8 industrial masonry chimney structures was constituted through an intense

literature review. Data related with all the information which influences the vulnerability assessing parameters was collected and assessed. The database information regarding geometric characteristics indicates the total height of the structures ranges from 8.2m (shortest) to 45.6m (tallest).The vulnerability assessment of 8 chimneys was carried out by evaluating the information. Figure 4.26 illustrates the assignment of vulnerability class for each parameter evaluated in the detailed vulnerability assessment of over minarets.

The results of vulnerability assessment show the following important characteristics:

(a) Parameter P1 has a low influence over the final vulnerability index, all of the towers are low classified as B (i.e. cylindrical wall section and mostly confined with metallic ring strip);

(b) Parameter P2, P6, P7, P9, P10 and P12 has an no influence over the final vulnerability index, as most of the chimneys are classified as A, i.e. due to good quality masonry construction, isolated constructions, absence or presence of small openings at base causing no or low eccentricity between mass and rigidity center, no openings above base, no influence of roof or floor as these structural component are absence in chimney and absence non–structural elements respectively;

(c) Parameter P3 and P5 has significant influence over the final vulnerability index, as most of all chimneys are classified as C, i.e. due to intermediate shear strength capacity and insufficient information on soil conditions. Hence, location of all chimneys is assumed to be in soft to medium soil site over plane area respectively;

(d) Parameter P4 is well distributed classes B, C, and D. Hence, its influence over final vulnerability index is low to high (i.e. variation in slenderness ratio amongst the chimneys);

(e) Parameter P8 and P11 has low to high influence over the final vulnerability index, as most of the chimney are classified as A or as D, i.e. due to variation in wall thickness along the height and poor or good conservation state amongst the chimneys respectively.

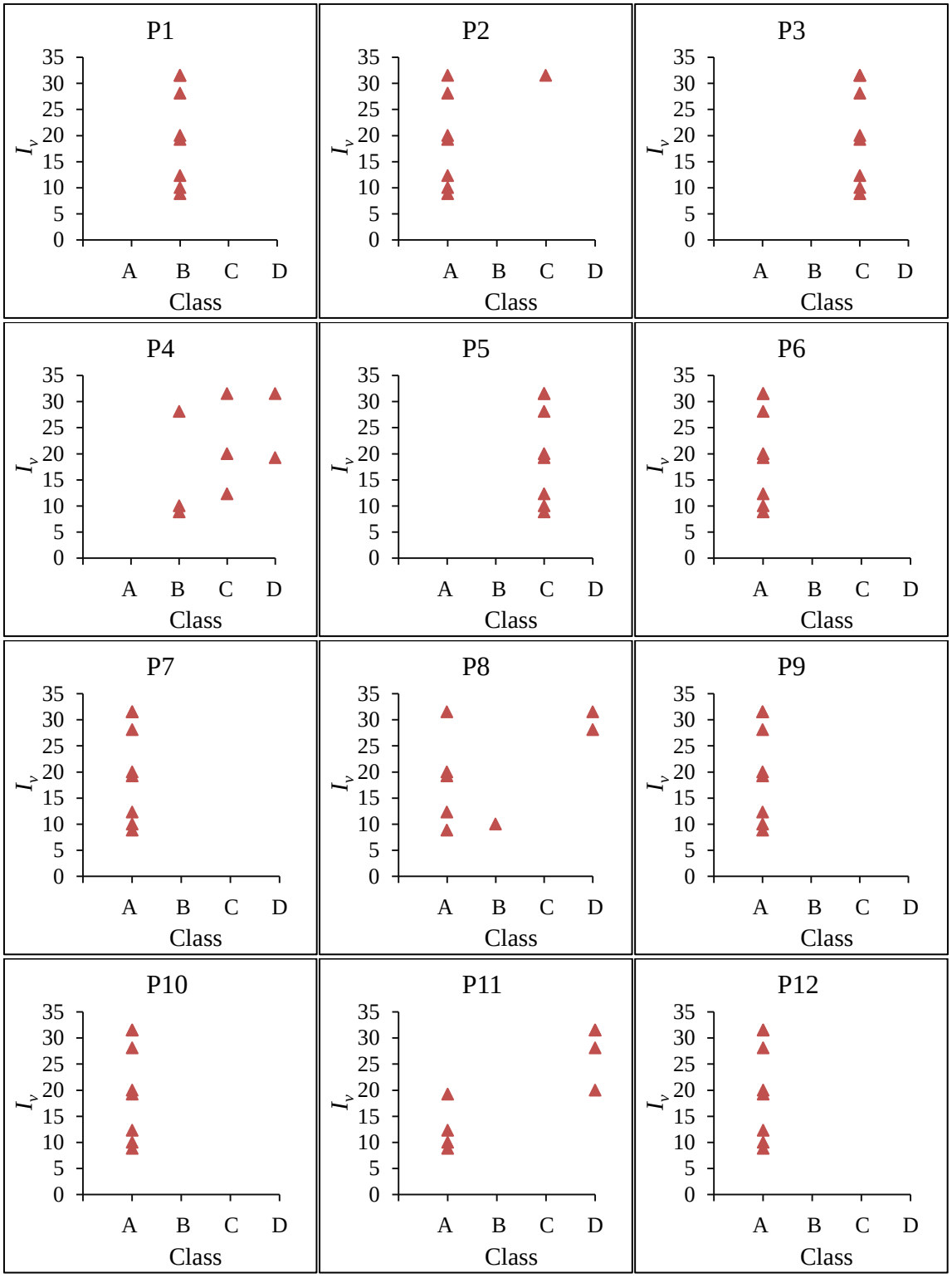

Key: P1: Type of resisting system; P2: Quality of the resisting system; P3: Conventional strength; P4: Slenderness ratio; P5: Location and soil conditions; P6: Position and interaction; P8: Irregularity in elevation; P9: Wall openings number, size and location; P10: Flooring and roofing system; P11: Fragilities and conservation state; P12: Non–structural elements

Figure 4.26: Vulnerability index and vulnerability class distribution of all parameters for the 8 industrial masonry chimneys assessed

4.5.2 Vulnerability curves for slender masonry structures

The method proposed here is based on the original GNDT II level approach [131] although with some significant modifications (as discussed in Section 4.2). However the 'backbone' parameters, shared by every vulnerability assessment according to Combescure *et al.* [167], are essentially the same. Considering this fact, the similarity in terms of the definition of the vulnerability index of the two methodologies (original and improved) enables the use of the same vulnerability functions relating vulnerability to a damage index [132]. Since this study adopted the analytical vulnerability curves of the Macroseismic Method [140], it is essential to establish the correspondence between the Macroseismic Method and the GNDT II level approach.

The former method makes reference to the EMS–98 Macroseismic Scale [142], which implicitly contains a model of vulnerability. On the basis of the definition of damage described in the EMS–98 scale [142], it is possible to derive damage probability matrices for each of the defined vulnerability classes (A to F). Through use of the linguistic definitions (Few, Many and Most) and their respective numerical interpretation, complete Damage Probability Matrices (DPM) for every vulnerability class may be obtained. Having solved the incompleteness using probability theory, the ambiguity and overlap of the linguistic definitions is then tackled using fuzzy set theory [168], in which upper and lower boundary limits for the correlation between the macroseismic intensity and mean damage grade (μ_D) of the distribution are defined and derived for each building typology and vulnerability class [142]. Mean damage grade (μ_D) allow us to know the expected distribution of the damage level (see Table 4.26), where the damage levels represent a quantitative interpretation of the consequences caused by the earthquake on the structural and non–structural elements [169].

Table 4.26: Interpretation of the mean damage grade (μ_D) [169]

μ_D	0	1	2	3	4	5
Damage level	No damage	Negligible damage	Light damage	Medium damage	Severe damage	Collapse

For the operational implementation of the methodology, an analytical expression proposed by Lagomarsino and Podestà [170] for churches and adopted by Curti [21] and Balbi *et al.* [171] for tower is adopted. This expression correlates seismic intensity with the

mean damage grade ($0 \leq \mu_D \leq 5$) of the damage distribution (discrete beta distribution) in terms of the vulnerability value, as shown in Eq. (4.4).

$$\mu_D = 2.5 \cdot \left[1 + tanh\left(\frac{I + 3.4375 \cdot V - 8.9125}{Q}\right)\right] \tag{4.4}$$

where, I is the seismic hazard described in terms of macroseismic intensity, V the vulnerability index used in the Macroseismic Method and Q a ductility factor. The vulnerability index, V, determines the position of the curve, while the ductility factor, Q, determines the slope of the vulnerability function (rate of damage increasing with rising intensity). In this study a ductility factor of 2 is adopted, a value suggested by Curti [21] and Balbi *et al.* [171] for towers.

Figure 4.27 shows the comparison of vulnerability curves plotted for possible upper, mean and lower values of vulnerability index using the proposed methodology for slender masonry structures with the vulnerability index values presented by Giovinazzi and Lagomarsino [140] for EMS–98 building topology. Although, there may be difference between vulnerability index values between slender masonry structures and building topologies, it has been adopted due to lack of sufficient vulnerability assessment information for slender masonry structures. However, the vulnerability index values by Giovinazzi and Lagomarsino [140], which closely resemble the masonry type of slender structures have been considered (i.e. unreinforced brick and stone masonry). Moreover, the mean value adopted here closely resemble with the value presented by Lagomarsino *et al.* [169] for towers. However, the mean value is adopted here is slightly lower than the value presented by Curti [21]. By comparing the two types of vulnerability curve with respect to a central mean damage value (μ_D = 2.5), the following analytical correlation was derived between the vulnerability indexes indices of the two methods:

$$V = 0.46 + 0.0056 I_v \tag{4.5}$$

Via this relationship, the vulnerability index, I_v, can be transformed into the vulnerability index, V (used in the Macroseismic Method), enabling the calculation of the mean damage grade through Eq. (4.4) and subsequently the estimation of damage and loss.

Once vulnerability has been defined, the mean damage grade, μ_D, can be calculated for different macroseismic intensities, using Eq. (4.4). Figure 4.28 to Figure 4.31 shows the vulnerability curves for the mean value of the vulnerability index as well as the upper and lower bound ranges for Nepalese Pagoda temples, towers, minarets and chimneys, respectively.

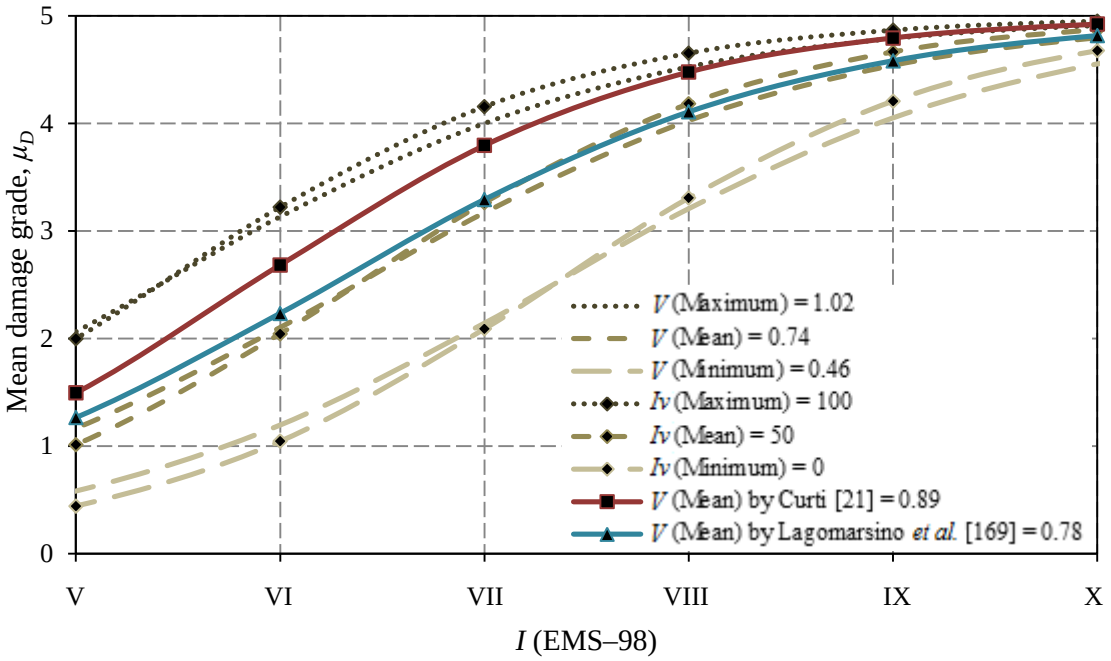

Figure 4.27: Correlation amongst vulnerability curves for maximum, mean and minimum value of the vulnerability index

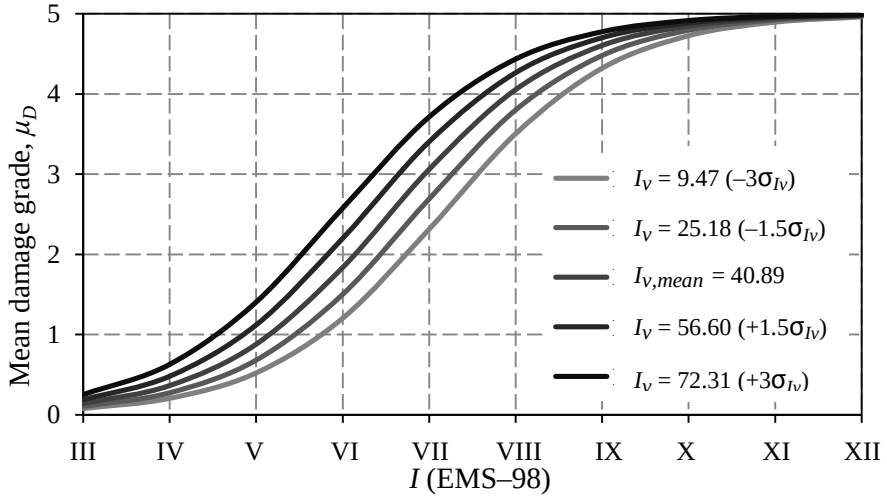

Figure 4.28: Vulnerability curves for Nepalese Pagoda temples

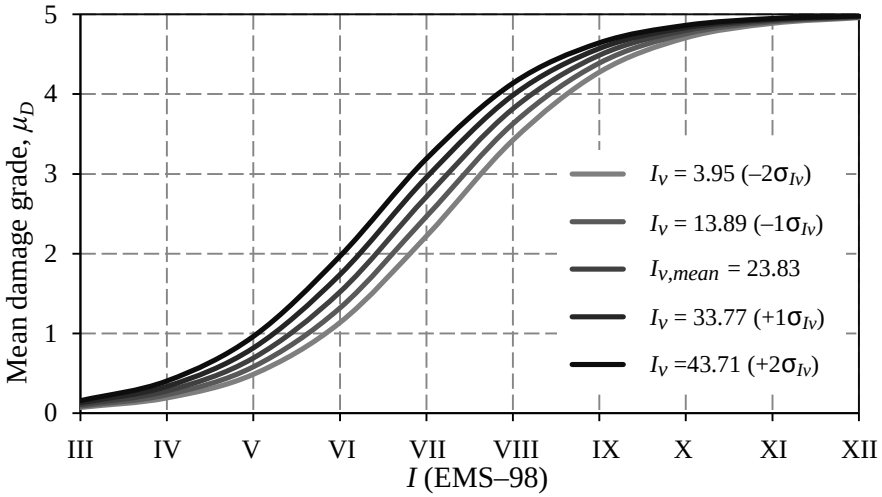

Figure 4.29: Vulnerability curves for masonry towers

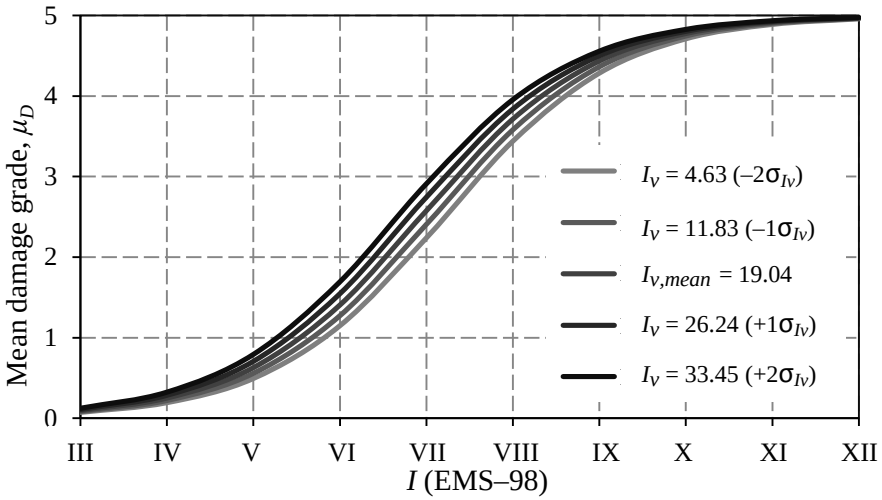

Figure 4.30: Vulnerability curves for masonry minarets

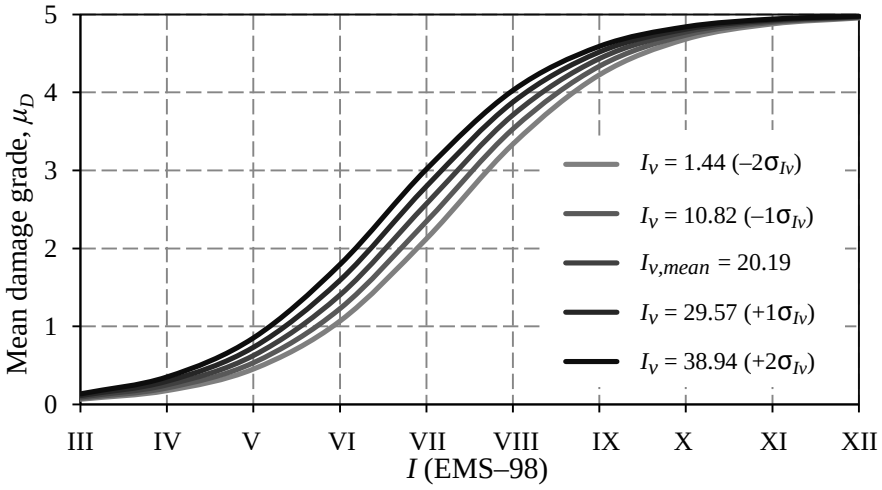

Figure 4.31: Vulnerability curves for industrial masonry chimneys

4.6 Conclusion

This chapter presented and discussed the development of a simplified seismic vulnerability assessment methodology for slender masonry structures. The vulnerability assessment method proposed here has been proven to be extremely useful and reliable for the analysis of slender masonry construction characteristics and as a consequence so are the results obtained from its use. Integration of this vulnerability assessment technique into a Macroseismic method has enabled its application for the development of damage and loss scenarios for risk mitigation and management. The proposed vulnerability assessment method can easily be adapted for specific building features and adopted for assessment of any type of slender masonry structure.

Methods of vulnerability assessment based on statistical approaches and damage observation are more suitable for large scale analysis, essentially for two reasons: they require less information and fewer resources while the currently available simplified mechanical models still require experimental testing validation. However, the uncertainties associated with the empirical vulnerability curves and the quality of vulnerability classification data are still issues that must be studied further with respect to post–seismic data collection.

CHAPTER 5

SEISMIC VULNERABILITY ASSESSMENT: A CASE STUDY

Summary *This chapter presents the application of the proposed seismic vulnerability assessment methodology on 78 Nepalese Pagoda temples as a case study. Finally, in this chapter damage and vulnerability mapping of the Nepalese Pagoda temple structures along with loss assessment and proposal of retrofitting strategy for loss mitigation is presented.*

Chapter outline

5.1 Introduction

The seismic vulnerability assessment of Nepalese Pagoda temples is essential as these monuments are recognized with high historical and heritage value. Many of these architectural and culture heritage are listed in UNESCO World heritage. Rigorous vulnerability assessment of these structures and the implementation of appropriate retrofitting solutions can help to reduce the levels of physical damage and the economic impact of future seismic events.

The main purpose of this chapter is to assess the seismic vulnerability of the Nepalese Pagoda temples. Moreover, this research has contributed to structural vulnerability identification and damage classification. Within this purpose, firstly, field survey has been carried out to evaluate the vulnerability assessing parameters of 78 Nepalese Pagoda

temples, leading to the development of a database. The seismic vulnerability assessment of the Nepalese Pagoda temples of the Kathmandu Valley was carried out using a simple methodology presented in chapter 4. With the methodology adopted, a vulnerability index, I_v, was evaluated for all 78 Pagoda temples. Secondly, the evaluated vulnerability index, I_v, in relationship with seismic intensity was used to estimate the physical damage, construct fragility curves and estimate losses. Moreover, the results of the vulnerability assessment and damage classification were integrated into a GIS tool, allowing the spatial visualation of damage scenarios, which is potentially useful for the planning of retrofitting priorities to mitigate and manage seismic risk. Seismic vulnerability was mapped resourcing to ArcGIS 10.2 [172]. Finally, the Pagoda temples were assumed to be retrofitted for improvement of seismic performance of certain parameters and was developed a seismic vulnerability comparison study between original and retrofitted conditions.

5.2 Historical seismicity in Nepal

Nepal is a Himalayan country located in one of the most severe earthquake prone areas of the world. The Bureau of Crises Prevention and Recovery of the United Nations Development Program has ranked Nepal as the eleventh most prone location in terms of earthquakes risk [173]. The Himalaya evolved as a result of the collision between the Indian and Eurasian plates around 45 to 50 million of years ago. Because of its tectonics, the Himalaya is one of the active seismic belts of the globe. Some of the devastating earthquakes in the Himalaya region are listed in Table 5.1, which evidently indicates that the entire Himalayan belt is one of the zones of significant seismic hazard.

The seismic history of Nepal shows the occurrence of a large devastating earthquake every 60 to 70 years [174]. Record of past earthquakes show that Nepal registered two major earthquakes in the last 100 years, i.e. 1934, Bihar–Nepal earthquake (magnitude 8.4), which effected over 200,000 buildings and temples that registered heavy to severe damage, nearly 81,000 of which were in Eastern Nepal completely destroyed. In Kathmandu alone, 55,000 buildings were affected, 12,397 of which were completely destroyed. Similarly, in 1988, Udayapur earthquake (magnitude 6.5), epicenter in the Southeast of Nepal caused 66,382 buildings to collapse [175]. Figure 5.1 shows the seismic

intensity (MMI) distribution map of the Kathmandu Valley during 1934 and 1988 earthquakes.

Table 5.1: Major damaging earthquakes in Himalaya region and essential human casualties [176]

Site	Date	Magnitude	Casualties
Shillong, India	June 12, 1897	8.7	1542
Bihar–Nepal border	January 1, 1934	8.4	>10,653
Quetta, Pakistan	May 30, 1935	7.6	30,000
Assam, India	August 15, 1950	8.6	1500
Udayapur, Nepal	August 21, 1988	6.5	1000
Uttar Kashi, India	October 20, 1991	6.6	>2,000
Chamoli, India	March 29, 1999	6.8	>150
Hindukush, India	November 11, 1999	6.2	0
Kashmir, Pakistan	October 8, 2005	7.6	74,698

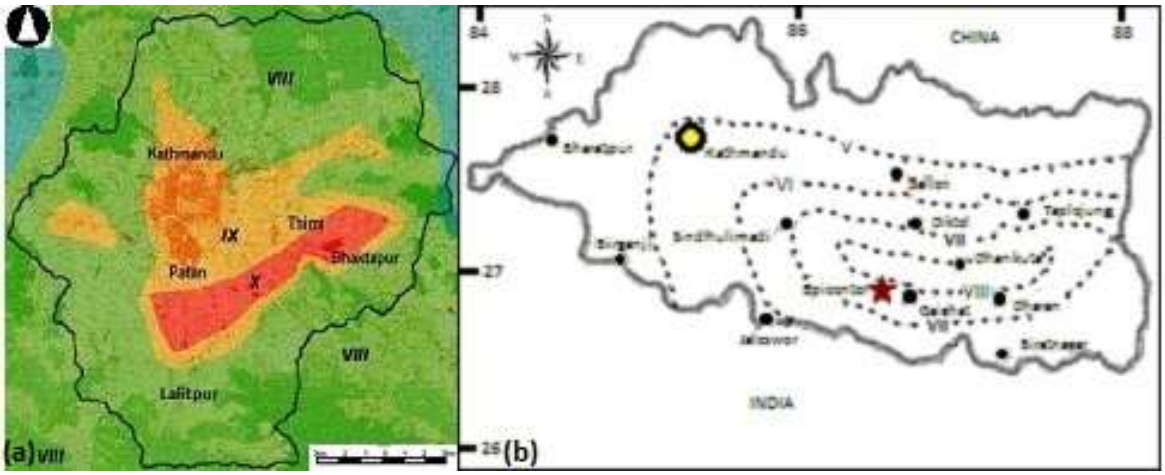

Figure 5.1: 1934 Earthquake intensity distribution map: a) 1934 Nepal–Bihar earthquake [177]; b) 1988 Udayapur earthquake [178; 179]

Figure 5.2 shows the estimated slip potential along the Himalaya, where Nepal lies. Brown shaded areas with dates next to them surround epicenters and zones of rupture of major past earthquakes in the Himalaya. Red segments along the bars show the slip potential on a scale of 1 to 10 meters, i.e. the potential slip that has accumulated since the last recorded great earthquake, or since 1800. The pink portions show possible additional slip permitted by ignorance of the preceding historic record. The simplified cross–section of the Himalaya indicates the locked sliding zone between Indian and Tibetan plates. Vertical movement, horizontal contraction, and micro earthquake seismicity are currently concentrated between them [180]. Geodetic measurements indicate that if an earthquake occurred today in the central seismic gap (western Nepal) it could slip by more than 4m, and probably by more than 6m, and possibly by as much as 10m. These ruptures

correspond roughly to M = 7.8, M = 8.0 or M = 8.3 magnitude earthquakes if the slip area extends 100km (N–S direction) by 300km (E–W direction). It is difficult to estimate how much casualties and damage will be caused if such earthquake strikes Nepal in present time.

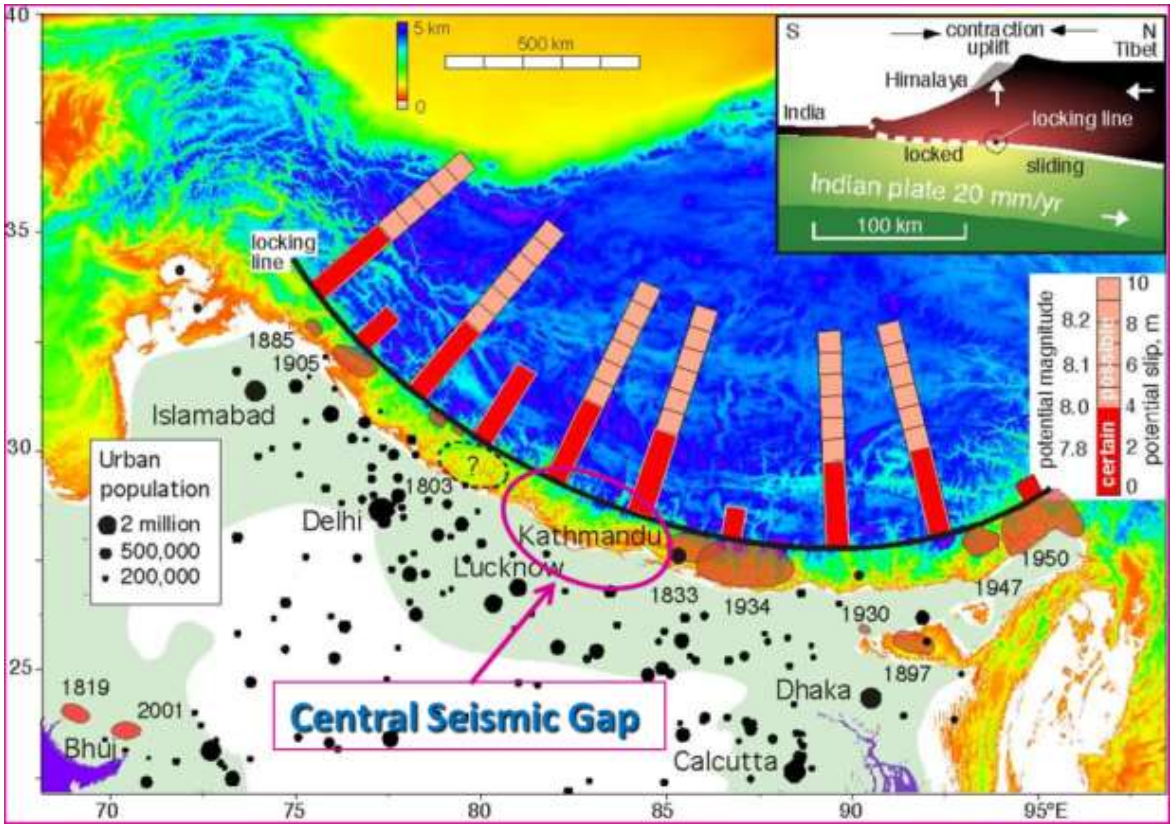

Figure 5.2: View of the Indo–Asian collision zone [180]

Moreover, JICA [181] has presented seismic intensity (MMI) distribution maps of the Kathmandu Valley for three anticipated (or scenario) earthquakes models (see Figure 5.3). These three scenario earthquake models was developed using attenuation formula, considering the past earthquakes and fault models around the Kathmandu Valley as well as incorporating the local subsurface amplification.

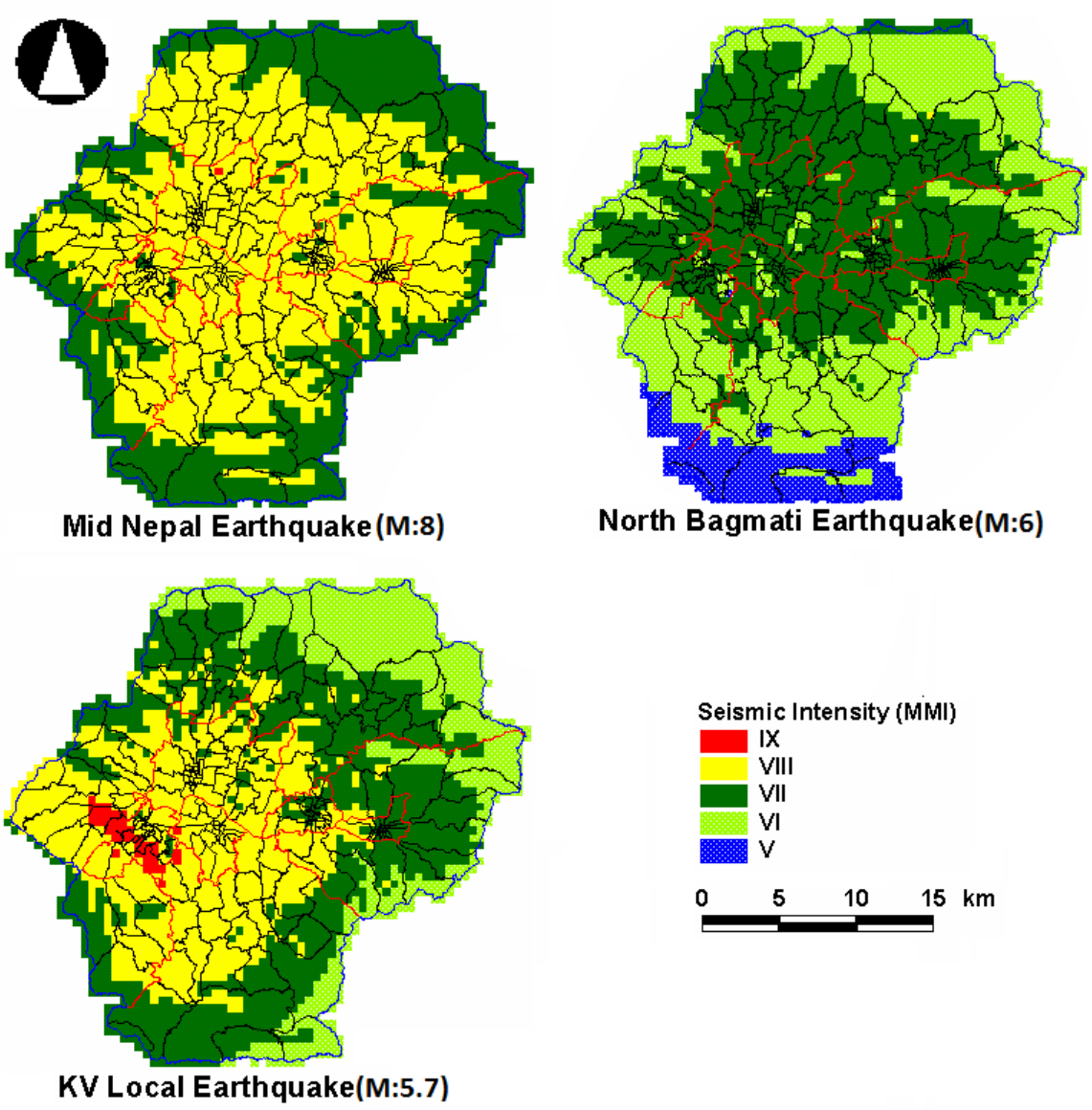

Figure 5.3: Earthquake intensity distribution map of Kathmandu for three anticipated earthquakes models [181]

5.3 Case study description

Vulnerability assessment was carried out in 78 Nepalese Pagoda temples. These Pagoda temples were located in three different cities of Kathmandu Valley, Nepal (Kathmandu, Lalitpur and Bhaktapur), as shown in map (Figure 5.4). Although, Pagoda temples were surveyed in three different cities, most of Pagoda temples were found similar to each other in many ways, such as: there construction procedure, material used for construction and the period of construction.

Figure 5.4: Map of Nepal showing the geographical location of surveyed area in three cities of Kathmandu Valley

A complete identification and inspection survey of Pagoda temples was performed within two different domains: (1) architectural typologies and drawings and (2) structural and non–structural building features and defects. Detailed inspections were performed by filling in detailed checklists developed as part of the scope of this research and used to survey each construction element (roof, façade walls, timber floors, etc.). The data gathered from the inspection of Pagoda temples, were processed, and a database management system integrated into a GIS application was developed to manage, compare and spatially analyze the information collected. The creation of a database specifically designed to gather and manage this type of information is of particular importance to the seismic vulnerability.

The overviews of the 78 Nepalese Pagoda temples surveyed are listed below.

a) Nearly 80% of Pagoda temples (with records) are built between 16^{th} to 17^{th} centuries and rests after or before them. The oldest Pagoda temple was built on 1392 and youngest on 1959;
b) Nearly 50% were renovated after 1934 earthquake;
c) Among the 78 Pagoda temples surveyed, 12% were 1 roofed, 46% of Pagoda temples were 2 roofed and 39% of Pagoda temples were 3 roofed. Two of them were 5 roofed (it is exceptional);

d) Among the 78 Pagoda temples surveyed, 71% were with 1 door and remaining 26% were with 4 doors. One was with 2 doors and one was with 3 doors (it is exceptional);
e) Among the 78 Pagoda temples surveyed, nearly 75% have wall thickness between 300 to 600mm. The thickest wall is 2143mm (it is exceptional) and thinnest wall is 250mm;
f) Among the 78 Pagoda temples surveyed, nearly 90% are symmetrical in cross–section with maximum 10.74m and minimum 1.73m wide in plan;
g) Tallest Pagoda temple is 23.717m and shortest Pagoda temple is 4.2m. Among the 78 Pagoda temples surveyed, nearly 60% of Pagoda temples height fall between 4 to 8 m and rest are taller than 8m.

5.4 Vulnerability assessment of the Nepalese Pagoda temples

5.4.1 Seismic vulnerability assessment

The 78 Pagoda temples of the Kathmandu Valley were assessed, with each temple assigned a vulnerability index, I_v, value. The mean I_v value lays between 40 and 41, corresponding to a building typology of earth and old brick and vulnerability classes A to B by adjusting the construction description described by Giovinazzi and Lagarmarsino [140], making reference to EMS–98 scale [142]. Table 5.2 shows the correspondence between various vulnerability classes and the calculated mean vulnerability, $I_{v,mean}$.

Table 5.2: Mean vulnerability index (I_v), Vulnerability class and topology

$I_{v,mean}$ (Mean vulnerability index)	EMS–98 Vulnerability class	Typology
40.89	A and B (most probable)	Earth and old brick

Figure 5.5 shows the histogram and the best–fit normal distribution curves that resulted from the detailed assessment. While detailed evaluation of overall Pagoda temples resulted in a mean vulnerability index value of $I_v = 40.89$. Around 46% of the Pagoda temples have a vulnerability index value over 40 and 31% over 45, which is equivalent to vulnerability class B according to EMS–98. The maximum and minimum I_v values obtained for the whole Pagoda temple stock assessed are 72.31 and 9.47, respectively.

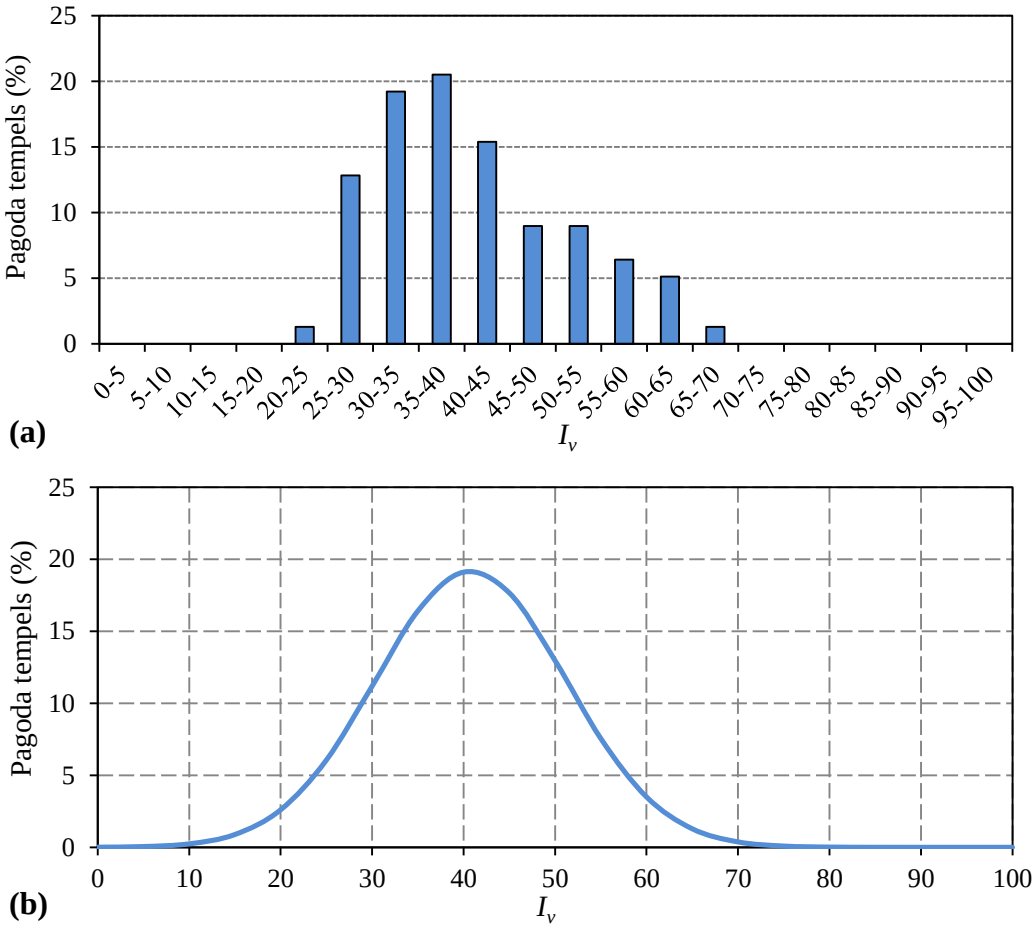

Figure 5.5: Vulnerability index distributions: a) Histogram; b) Best fit normal distributions

Figure 5.6 shows the variation of vulnerability index with respect to slenderness ratio which is evaluated as effective height to minimum radius of gyration and height to breadth ratio and also with respect to height of Pagoda temple. Result shows that vulnerability of the Nepalese Pagoda temples increases with the increase in slenderness ratio. Approximately, it can be interpreted that Pagoda temples with high slenderness ratio are more vulnerable than the Pagoda temples with low slenderness ratio. However, there are many other parameters which influence the final vulnerability index of Pagoda temple structure. Similarly, results also show that the vulnerability of the Pagoda temples is not a function of height, which means that the increase or decrease in the height of Pagoda temples should not be interpreted as the increase or decrease in vulnerability of the Pagoda temple structures.

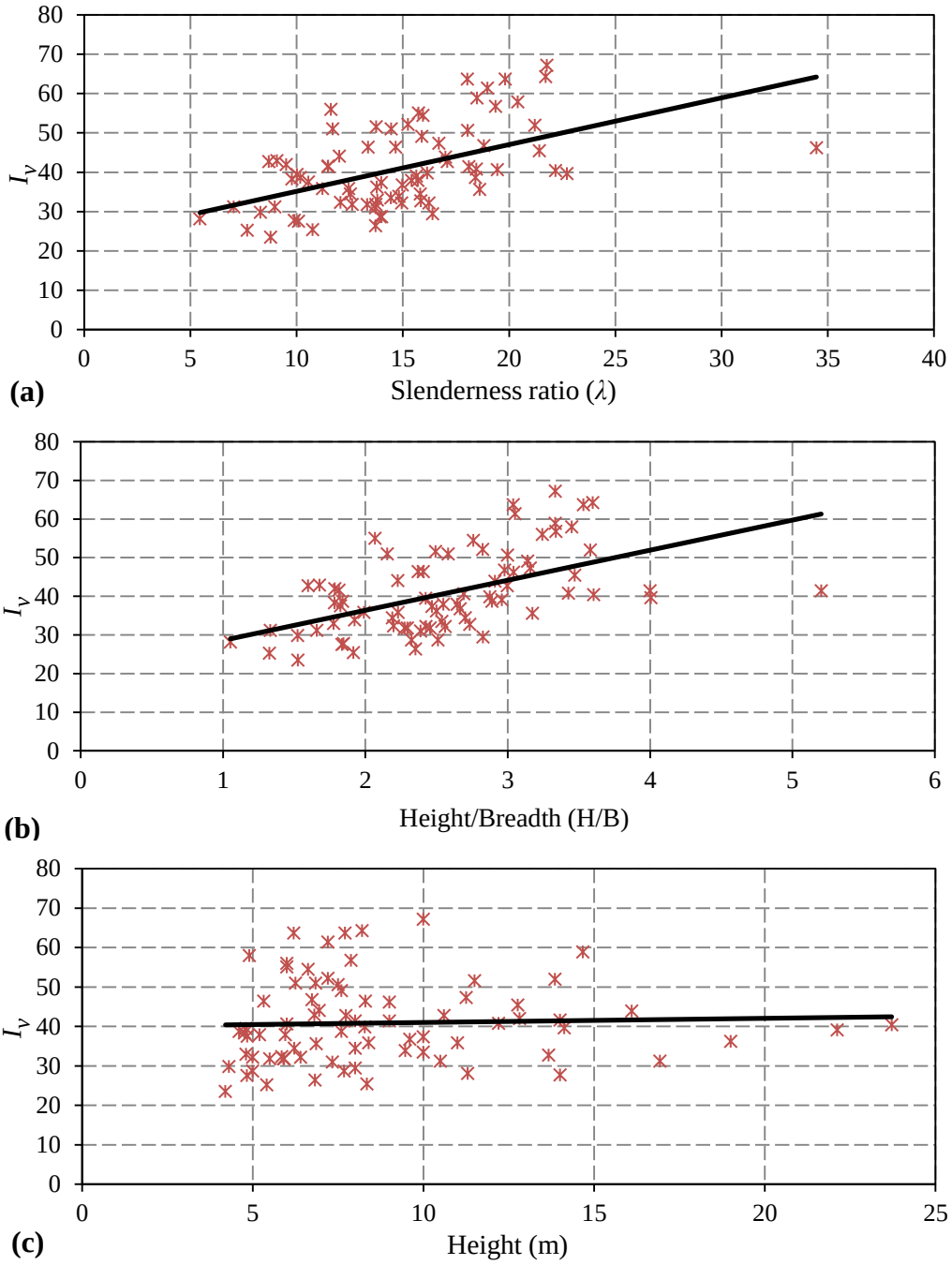

Figure 5.6: Vulnerability index distributions w.r.t.: a) Slenderness ratio; b) Height/Breadth ratio; c) Height

Figure 5.7 shows the spatial distribution of Pagoda temples. The construction of seismic vulnerability scenarios using a spatial analysis tool can provide georeferenced information and integrate the entire probabilistic algorithm into the generation of different intensity defined risk scenarios [182]. Hence, such seismic vulnerability maps enable the identification of more vulnerable Pagoda temples and their location, which can be very useful for the planning of protection strategies.

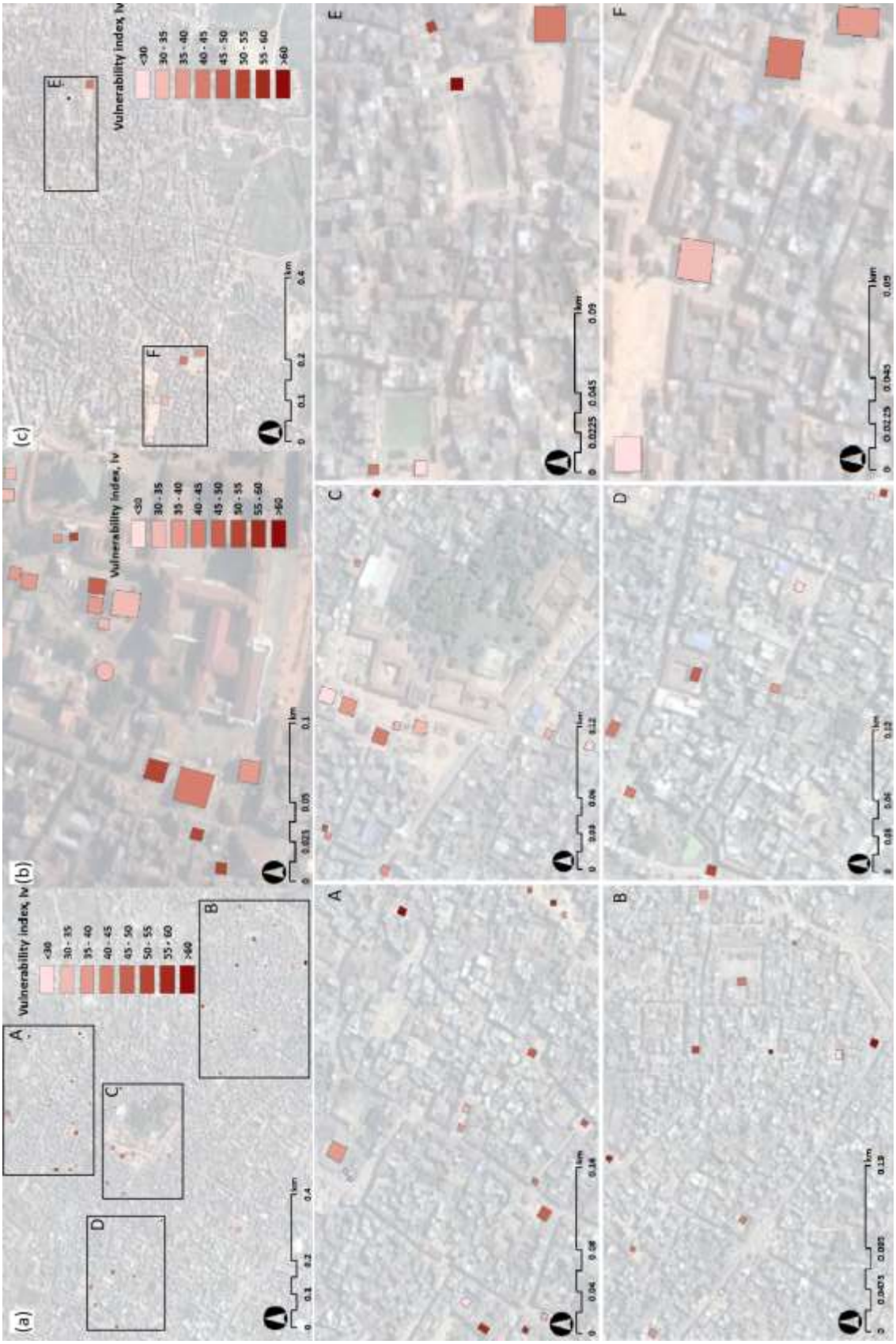

Figure 5.7: Vulnerability distribution map for Nepalese Pagoda temples of three different cities at Kathmandu Valley: a) Lalitpur; b) Kathmandu; c) Bhaktapur

5.4.2 Physical damage distribution and scenario

From mean damage grade values, μ_D, different damage distribution histograms for events of varying seismic intensity and their respective vulnerability index values can be defined, using a probabilistic approach. The idea is to complete the EMS–98 model introducing a proper discrete probability distribution of damage grade. The most commonly applied methods are based on the binomial probability mass function and the beta probability density function and moreover, the damage distribution of masonry buildings appears to quite well [183]. The probability mass function (PMF) of binomial distribution is expressed in Eq. (5.1).

$$PMF = p_k = \frac{5!}{k!\,(5-k)!} \times \left(\frac{\mu_D}{5}\right)^k \times \left(1 - \frac{\mu_D}{5}\right)^{5-k};\ 0 \le p \le 1 \tag{5.1}$$

The mean damage grade, μ_D, given by the Macroseismic Method represents the mean damage value that is used to define a discrete damage distribution and is expressed by Eq. (5.2). It ranges from 0 to 5 and is the barycentric value of the discrete damage distribution.

$$\mu_D = \sum_{k=0}^{5} p_k \times D_k \tag{5.2}$$

where, p_k is the probability of attaining a damage grade D_k, with $k \in [0, 5]$.

In this work the damage distribution adopted was fitted to a beta distribution function. Research carried out by Giovinazzi [168] has shown that the beta distribution is the most versatile, as by controlling the shape of the distribution, it enables the fitting of both very narrow and broad damage distributions. This continuous beta probability density function (PDF) is expressed as Eq. (5.3).

$$PDF: p_\beta(x) = \frac{\Gamma(t)}{\Gamma(r)\Gamma(t-r)}(x-a)^{r-1}(b-x)^{t-r-1}; a \le x \le b; a = 0; b = 5 \tag{5.3}$$

where, a, b, t and r are the parameters of the distribution and Γ is the gamma function.

As a function of the same parameters the mean value μ_x of the continuous variable x, which ranges between a and b and its variance σ_x^2 are related to t and r as expressed in Eq. (5.4) and Eq. (5.5).

$$t = \frac{\mu_x(a + b - \mu_x) - ab}{\sigma_x^2} - 1 \tag{5.4}$$

$$r = t\left(\frac{\mu_x - a}{b - a}\right) \tag{5.5}$$

Parameters t and r control the shape of the distribution. In this study, the unique value for parameter t is adopted as proposed by Giovinazzi [168] for unreinforced old brick masonry building topology, where $t = 5$. In order to use the beta distribution, it is necessary to reference damage grade, D_k, defined in Table 5.3.

Table 5.3: Interpretation of damage grade, D_k [168]

D_k	0	1	2	3	4	5
Damage level	No damage	Slight	Moderate	Heavy	Very heavy	Destruction

Assuming, $a = 0$, and $b = 5$, it is possible to calculate the probability associated to each damage grade, D_k, with $k \in [0, 5]$, using following equations.

$$P(D_0) = p(0) = \int_0^{0.5} \frac{\Gamma(t)}{\Gamma(r)\Gamma(t-r)} (x-a)^{r-1}(b-x)^{t-r-1}\, dx$$

$$P(D_k) = p(k) = \int_{k-0.5}^{k+0.5} \frac{\Gamma(t)}{\Gamma(r)\Gamma(t-r)} (x-a)^{r-1}(b-x)^{t-r-1}\, dx \tag{5.6}$$

$$P(D_5) = p(5) = \int_{4.5}^{5} \frac{\Gamma(t)}{\Gamma(r)\Gamma(t-r)} (x-a)^{r-1}(b-x)^{t-r-1}\, dx$$

The mean damage grade, μ_D, is obtained as a function of the vulnerability index (I_v) and intensity (I), as expressed in Eq. (4.4), while the variance of the distributions is defined using the previously assumed value of 5 for parameter t. Figure 5.8 presents examples of

damage distributions obtained through the use of the beta probability distribution for events of different seismic intensity and the mean value of the Pagoda temple vulnerability index ($I_{v,mean} = 40.89$).

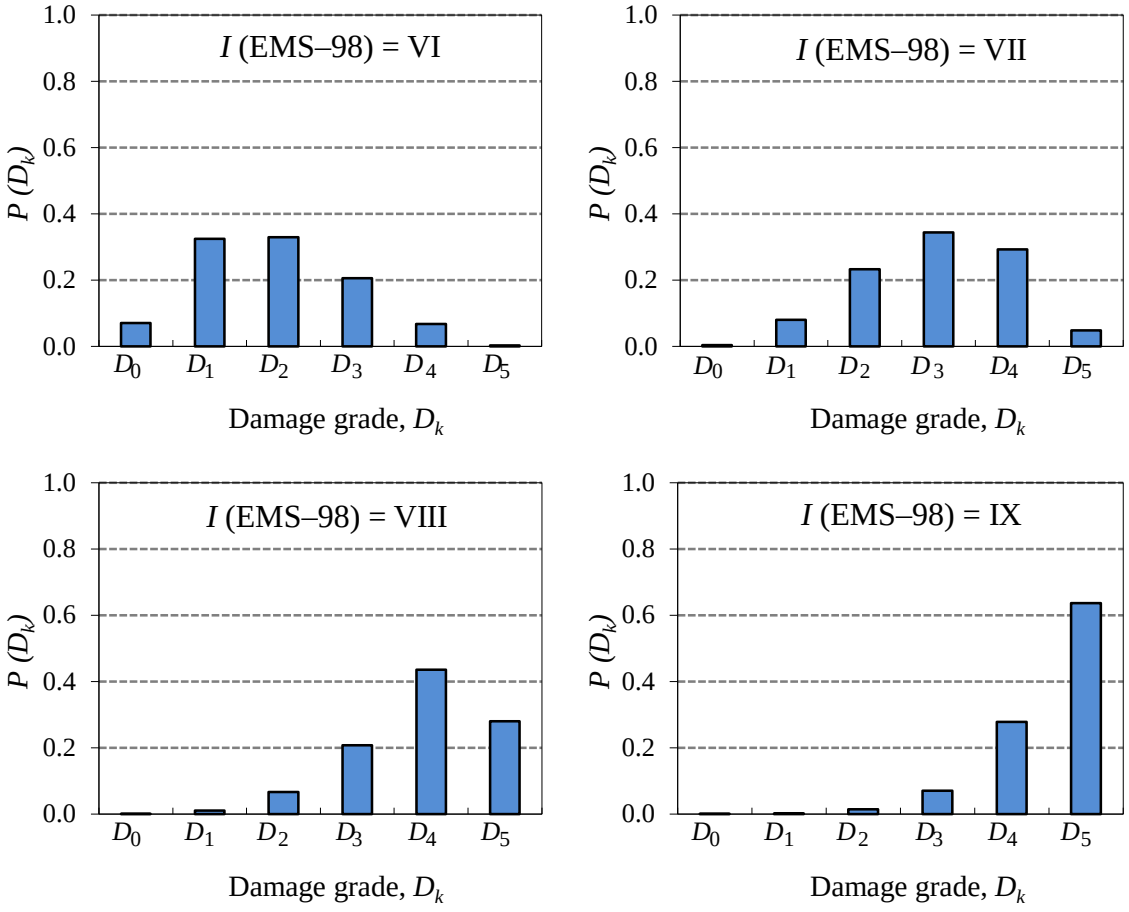

Figure 5.8: Discrete damage distribution histograms for $I_{v,mean} = 40.89$ with different intensities

Another method of representing damage using damage distribution histograms involves the use of fragility curves. The fragility curve defining the probability of reaching or exceeding each damage grade, D_k, with $k \in [0, 5]$ are obtained directly from the beta cumulative density function, as expressed in Eq. (5.7).

$$P(D > D_k) = 1 - P(D_k) \tag{5.7}$$

Just like the vulnerability curves, fragility curves define the relationship between earthquake intensity and damage in terms of the conditional cumulative probability of

reaching a certain damage state. Fragility curves are influenced by the parameters of the beta distribution function and allow the estimation of damage as a continuous probability function. Figure 5.9 shows fragility curves corresponding to the damage distribution histograms of the mean vulnerability index value $I_{v,mean} = 40.89$ as well as for $I_{v,mean} + 1.5\sigma_{I_v} = 56.60$.

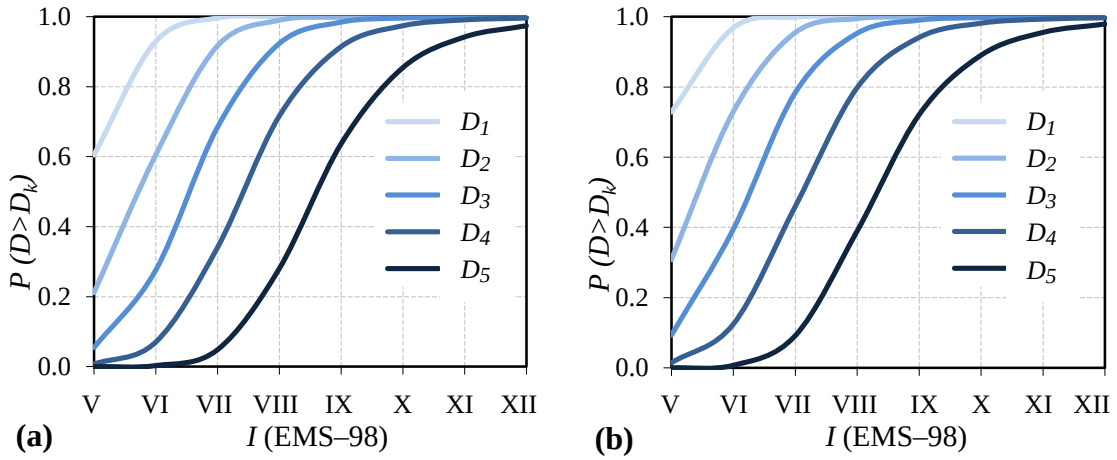

Figure 5.9: Fragility curves for different values of I_v: a) $I_{v,mean} = 40.89$; b) $I_{v,mean} + 1.5\sigma_{I_v} = 56.60$

Figure 5.10 and Figure 5.11 present the damage scenarios using GIS, combining Pagoda temples vulnerability and seismic hazard data for earthquake intensities of VI and IX respectively. These two seismic scenarios correspond to the strongest historically earthquake ever experienced in the Kathmandu valley (in 1988 and 1934 respectively). Damage estimation ranges from 1.47 to 2.45 for the earthquake scenario using *I* (EMS–98) = VI and from 4.46 to 4.75 for *I* (EMS–98) = IX.

Figure 5.12 and Figure 5.13 present the damage scenarios mean damage grade assessment, combining Pagoda temples vulnerability and seismic hazard data for earthquake intensities of VII and VIII. These two seismic scenarios correspond to the possible strongest anticipated earthquake in the Kathmandu valley [181]. Damage estimation ranges from 2.65 to 3.62 for the earthquake scenario using *I* (EMS–98) = VII and from 3.77 to 4.38 for *I* (EMS–98) = VIII.

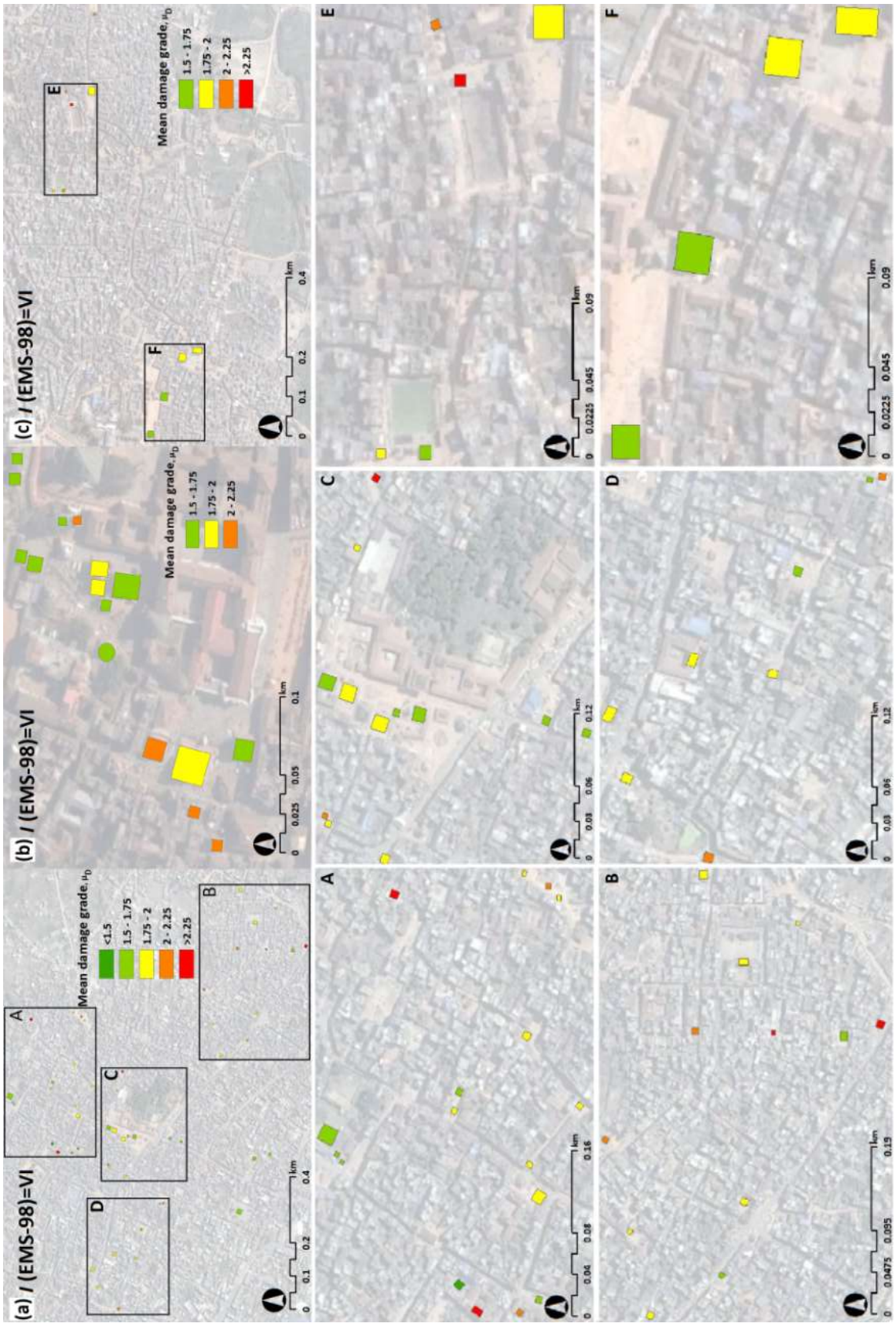

Figure 5.10: Spatial damage distribution corresponding *I* (EMS–98) = VI for Nepalese Pagoda temples of three different cities in the Kathmandu Valley: a) Lalitpur; b) Kathmandu; c) Bhaktapur

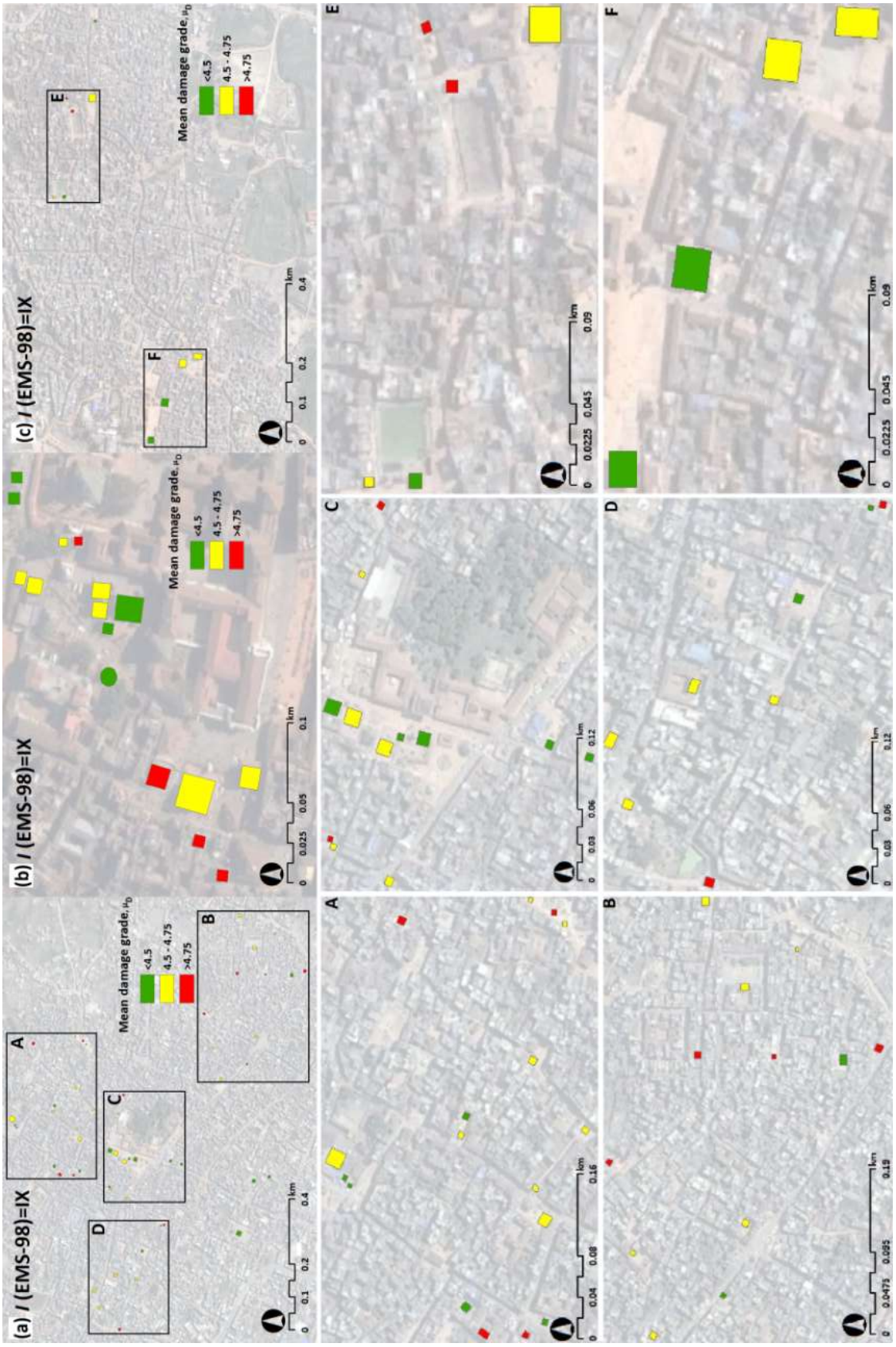

Figure 5.11: Spatial damage distribution corresponding *I* (EMS–98) = IX for Nepalese Pagoda temples of three different cities in the Kathmandu Valley: a) Lalitpur; b) Kathmandu; c) Bhaktapur

5.5 Seismic loss assessment of the Nepalese Pagoda temples

5.5.1 Collapsed and unusable Pagoda temples

Nepal felt a major earthquake in 1934, photographic evidence shows that a vast number of monuments were infected, but due to the lack of research in this field, there is no loss estimation model for Nepalese Pagoda temple. Hence, the loss estimation model adopted in this research is based on damage grades that relate the probability of exceeding a certain damage level with the probability of collapse and functional loss. Among the existing approaches based on observed damage data, the one adopted in this work has been proposed by the Italian National Seismic Survey, based on the work of Bramerini *et al.* [184]. This approach involves the analysis of data associated with the probability of unusable buildings to minor and moderate earthquakes that produce lower levels of structural and non–structural damage and higher mean damage values that are associated to the probability of collapse [185]. In Italy, data processing undertaken by Bramerini *et al.* [184] has enabled the establishment of these weighted factors and respective expressions for their use in the estimation of losses. Eq. (5.8) and Eq. (5.9) were used for the analysis of collapsed and unusable Pagoda temples respectively.

$$P_{collapse} = P(D_5) \tag{5.8}$$

$$P_{unusable} = P(D_3) \times W_{uPt,3} + P(D_4) \times W_{uPt,4} \tag{5.9}$$

where, $P(D_k)$ is the probability of the occurrence of a certain level of damage (D_1 to D_5) and $W_{uPt,3}$; $W_{uPt,4}$ are weights indicating the percentage of buildings associated with the damage level D_k , that are considered unusable or have suffered collapse respectively. For the analysis of Nepalese Pagoda temples the following weights were applied: $W_{uPt,3} = 0.4$; $W_{uPt,4} = 0.6$.

Figures 5.12 and 5.13 presents the probability of collapse and unusable Pagoda temples for the mean value of the vulnerability index, $I_{v,mean} = 40.89$ and for other characteristic values of the vulnerability index ($I_{v,mean} - 3\sigma_{I_v}$; $I_{v,mean} - 1.5\sigma_{I_v}$; $I_{v,mean} + 1.5\sigma_{I_v}$; $I_{v,mean} + 3\sigma_{I_v}$), respectively. It is important to note that the number of unusable Pagoda temples decrease with the intensity, as the number of Pagoda temples that suffered collapse

increased. The overall results for moderate to strong–intensity seismic events, considering macroseismic intensities of VI to X on the EMS–98 scale, and for the mean value of the estimated vulnerability obtained for the 78 Pagoda temples evaluated in the cities of Kathmandu Valley are listed in Table 5.4.

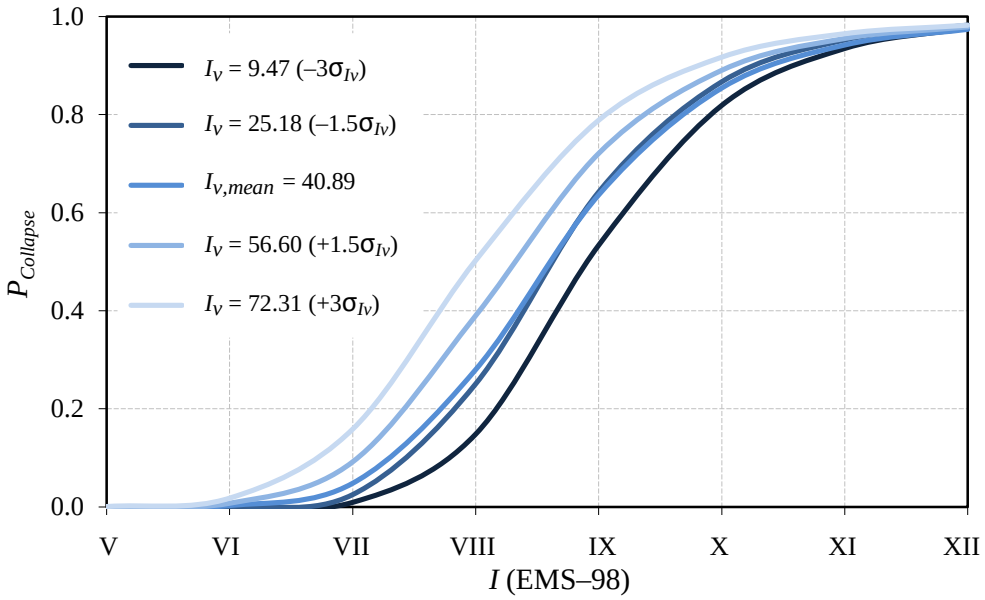

Figure 5.12: Probability of collapsed Pagoda temples for different vulnerability index values

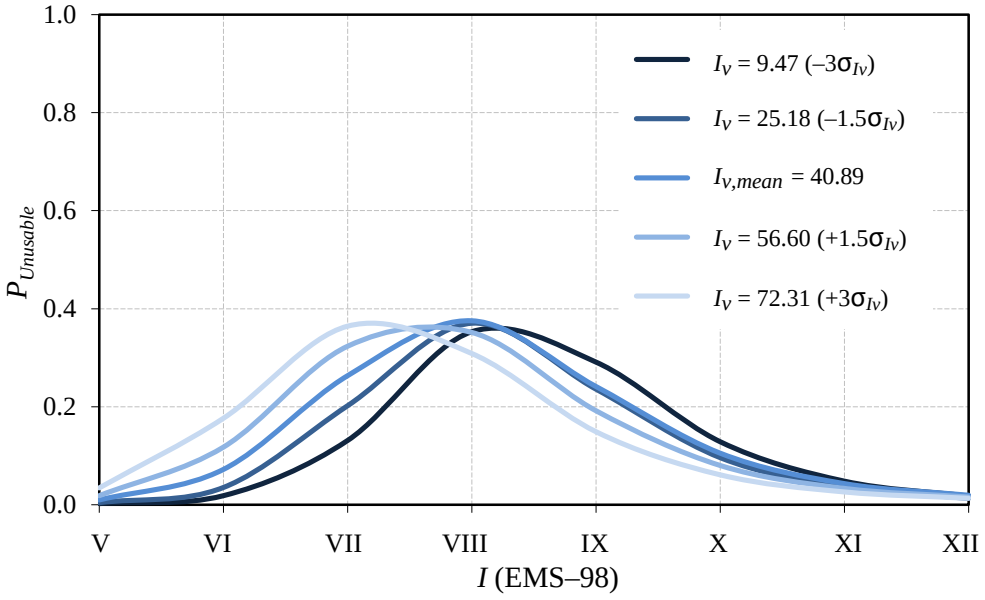

Figure 5.13: Probability of unusable Pagoda temples for different vulnerability index values

Table 5.4: Estimation of the number of collapsed and unusable Pagoda temples

Pagoda temples (78)	Intensity, I (EMS–98)				
	VI	VII	VIII	IX	X
Collapsed Pagoda temples	0 (0%)	4 (5%)	22 (28%)	50 (64%)	67 (85%)
Unusable Pagoda temples	6(7%)	21 (26%)	29 (38%)	19 (24%)	8 (11%)

5.5.2 Estimation of repair costs

The estimated damage grade can be interpreted either economically or as an economic damage index that represents the ratio between the repair costs and the replacement costs (i.e. building value) [132]. The correlation between damage grades and the repair/rebuilding costs can be obtained by the processing and analysis of post–earthquake damage data [186]. The correlation adopted in this work has been established by Dolce *et al.* [186]. The statistical values obtained by these authors are derived from analysis of the data collected, using the GNDT–SSN–1994 [131] procedure, after the 1997 Umbria–Marche and 1998 Pollino earthquakes and are based on the estimated cost of typical repair actions for more than 50,000 buildings [165].

The repair cost probabilities for a certain seismic event characterized by an intensity I, $P[R|I]$, can be obtained from the product of the conditional probability of the repair cost for each damage level, $P[R|D_k]$, with the conditional probability of the damage condition for each level of building vulnerability and seismic intensity, $P[D_k|I_v, I]$, given by Eq. (5.10).

$$P[R|I] = \sum_{D_k=1}^{5} \sum_{I_v=0}^{100} P[R|D_k] \times P[D_k|I_v, I] \tag{5.10}$$

To estimate the repair costs associated with the different vulnerability values used in the loss evaluation ($I_{v,mean} - 3\sigma_{I_v}$; $I_{v,mean}$; $I_{v,mean} + 3\sigma_{I_v}$), an average repair cost value per unit area of 7000 \$/m^2 was considered for the Nepalese Pagoda temple according to KVPT [119].

Figure 5.14 shows the estimated global costs of repair for the entire study of 78 Pagoda temples. Based on observation of Figure 5.14, it should be stressed that for intensities within the range of V to VIII, the difference between the minimum and maximum repair costs estimated for the vulnerability scenarios under consideration is quite significant. This

difference is much smaller for higher earthquake intensities due to the high damage levels caused by severe seismic events.

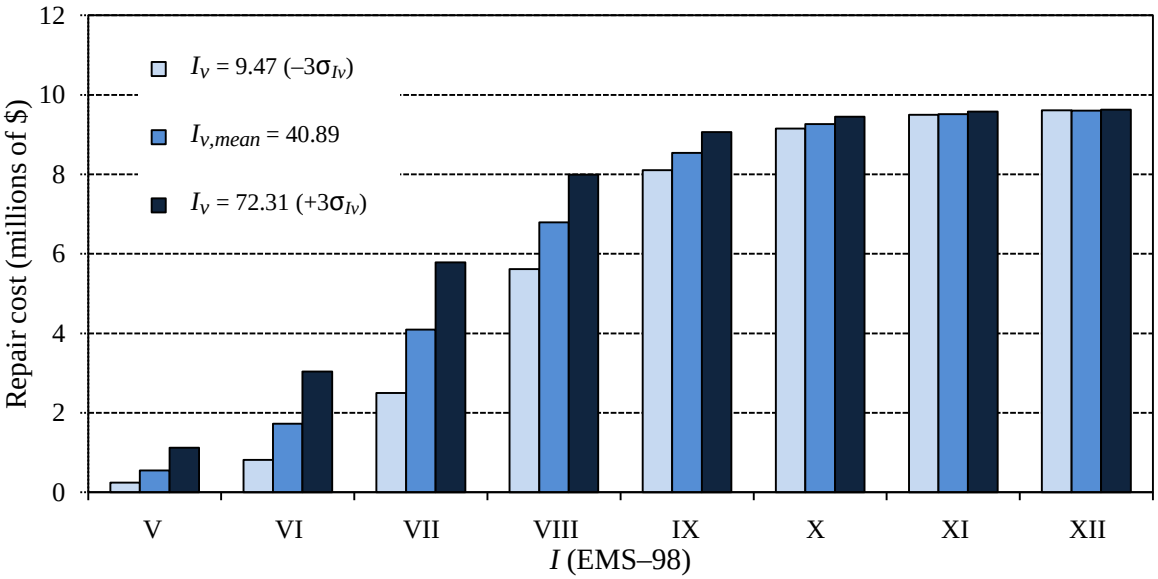

Figure 5.14: Estimation of repair costs

5.6 Seismic vulnerability and loss comparison: Original state and retrofitted

5.6.1 Proposed repair and strengthening interventions

Proper restoration of cultural heritage must focus on preserving the original features of the structure. If repair or strengthening actions are needed, they should cause the minimum possible alteration. Compatibility, durability and reversibility are the fundamental features recommended in the literature to be taken into account when strengthening cultural valued heritage buildings. Presently, there is a broad of techniques and materials available for the protection of historical constructions. Among them, two main techniques are distinguished, the rehabilitation or restoration and the retrofitting. The rehabilitation or restoration works aim to use materials of similar characteristics of original construction and to mainly apply the same construction techniques, in order to locally correct the damage of certain structural elements, e.g. sealing of cracks and reposition of mortar and masonry units. In general terms, the objective of these works is to preserve the construction in good conditions, mainly to withstand the vertical loading generated by self–weight. On the other hand, the structural retrofitting resourcing to modern techniques and in addition of

advanced materials in order to mainly improve the seismic performance of the buildings, by increasing its ultimate lateral load capacity (strength), ductility and energy dissipation.

Dismantling and reassembling or substituting is the current trend of restoration procedure followed in Nepalese Pagoda temples. This consists on the complete dismantling of an element or a structure to repair, extract or substitute part of the components, and then rebuilding it accurately according the original organization and shape. The purpose is to recover the functionality of a structure while maintaining its historical and cultural value.

In order to improve the structural behaviour of the Nepalese Pagoda temples, a series of repair and strengthening techniques are proposed to be executed both at a local and global level. Some remarks regarding the basic design choices and the selection of the most appropriate materials and techniques for the restoration of the Nepalese Pagoda temples are presented in this section.

Following are some proposed retrofitting actions for seismic vulnerability reduction of the Nepalese Pagoda temples:

a) The observations of masonry buildings when subjected to earthquakes have shown that the structural behaviour is strongly dependent on how the walls are interconnected and anchored to floors and roofs. Hence, tie beam (timber or RC) and metallic tie rods on several sections along the height of the temples prove to be efficient intervention strategy for improving the connectivity between walls. Furthermore, the wooden structures (roofs and floors) can be anchored by metal elements nailed on the beams and restrained to the wall;

b) Deep repointing is a widely applied technique in all types of masonry. This operation involves the partial replacement of the mortar joints with better quality mortar, in order to improve the masonry mechanical characteristics, and it should be applied in the case of localized deterioration of the mortar joint. This method can increase the masonry resistance for vertical and horizontal loads, but the best results are obtained especially in terms of deformation, which are also greatly reduced due to the confinement effect of the joints;

c) The application of the reinforced repointing technique diffused on various portions of the walls to counteract the creep damage, and concentrated on some pilaster strips to strengthen the corners. Adequate durability of the reinforcement

(especially when using metals), as well as adequate mechanical connection, require the placement of the bars at sufficient depth within the bed joint;

d) Injection of fluid mortar or other adequate repair materials through cracks or holes previously drilled. The purpose is to fill cracks, existing cavities and internal voids. Injection improves the continuity of masonry and contributes to enhance the average mechanical properties of masonry. Injection should only be carried out using injected materials with proven compatibility with the original masonry fabric;

e) Crack stitching is another repair work that can be done in Nepalese Pagoda temples. In general, crack stitching is locally joining two independent wall sections, which can rock or overturn about their base. However, the effectiveness of the crack stitching in terms of restoring structural continuity or uniform load distribution of horizontal loads on a wall is related to the diffusion of the intervention, since force transfer is limited to the points where the stitches are introduced;

f) Metallic plates and diagonals can be used in roofs and floors to reduce their flexibility and ensure effective horizontal diaphragm behaviour (mobilizing a global response of the walls equitably);

g) Seismic improvement of Nepalese Pagoda temples can be carried out by strengthening the traditional timber peg joinery between different timber members with bolt and steel plate. These interventions obviously aid in low intensity earthquakes, but what happens in larger quakes still is to be study;

h) It is also important to improve the connectivity of non–structural elements (e.g. pinnacle, cornices, tympanum etc.) with the structural members. Since, its improper connection can increase the level of damage during earthquake.

5.6.2 Results of proposed retrofitting actions over vulnerability assessment and loss estimation

The Pagoda temples are assumed to be retrofitted with the proposed retrofitting techniques referred section 5.6.1, in order to carry out the comparison study between original and retrofitted conditions. Although, effectiveness of retrofitting depends on various inherent factors, such as: quality, quantity, techniques etc. In this comparison, the level of seismic vulnerability reduction is assessed in terms of vulnerability index (I_v),

damage grades (D_k), damages probability ($P(D_k)$) and repair costs for different seismic intensities (I).

The improvement in seismic behaviour of Nepalese Pagoda temples is assumed in this study by upgrading the vulnerability class of six vulnerability parameters. The six vulnerability parameters are: P1 (Type of resisting system), P2 (Quality of the resisting system), P3 (Conventional strength), P10 (Flooring and roofing system), P11 (Fragilities and conservation state) and P12 (Non–structural elements) are selected for upgrading and it was assumed that they are upgraded by one vulnerability class (i.e. B to A, C to B and D to C) reflecting retrofitting measure discussed before. The seismic performance of the structural system defined by these selected parameters can be easily improved by applying the retrofitting strategy explained in section 5.6.1, where as it is not easy or possible in case of the remaining six other vulnerability parameters (i.e. P4 (Slenderness ratio), P5 (Location and soil conditions), P6 (Position and interaction), P7 (Irregularity in plan), P8 (Irregularity in elevation) and P9 (Number, size and location of wall openings)).

Figure 5.15 shows the comparison of histogram and the best–fit normal distribution curves that resulted from the detailed assessment of original and retrofitted Pagoda temples. After upgrading the six parameters by one vulnerability class of overall Pagoda temples, it resulted in a mean vulnerability index value of $I_v = 25.92$, which corresponds to a 39% reduction. Originally, around 46% of the Pagoda temples have a vulnerability index value of over 40, and 31% over 45 (equivalent to vulnerability class B according to EMS–98) which will be reduced to 11% and 5% respectively, after retrofitting.

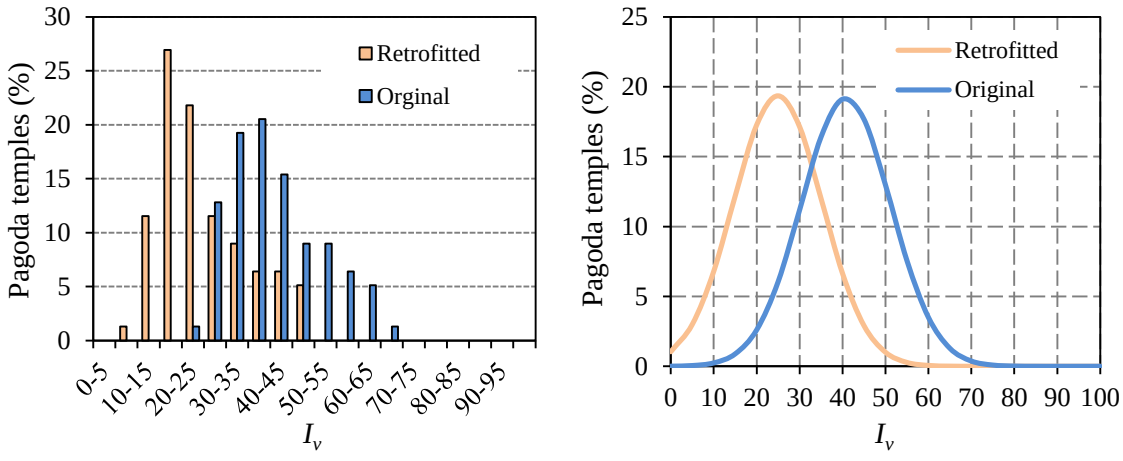

Figure 5.15: Comparison of histogram and the best–fit normal distribution curves

Figure 5.16 shows the comparison of damage distributions obtained through the use of the beta probability function for events of different seismic intensity and the mean values of the Pagoda temples vulnerability index ($I_{v,mean}$ (Original) = 40.89 and $I_{v,mean}$ (Retrofitted) = 24.92). Results show that, if the Nepalese Pagoda temples are retrofitted as proposed than there will be an important reduction of the damage probability of higher damage grades ($D_k = 4$ and $D_k = 5$).

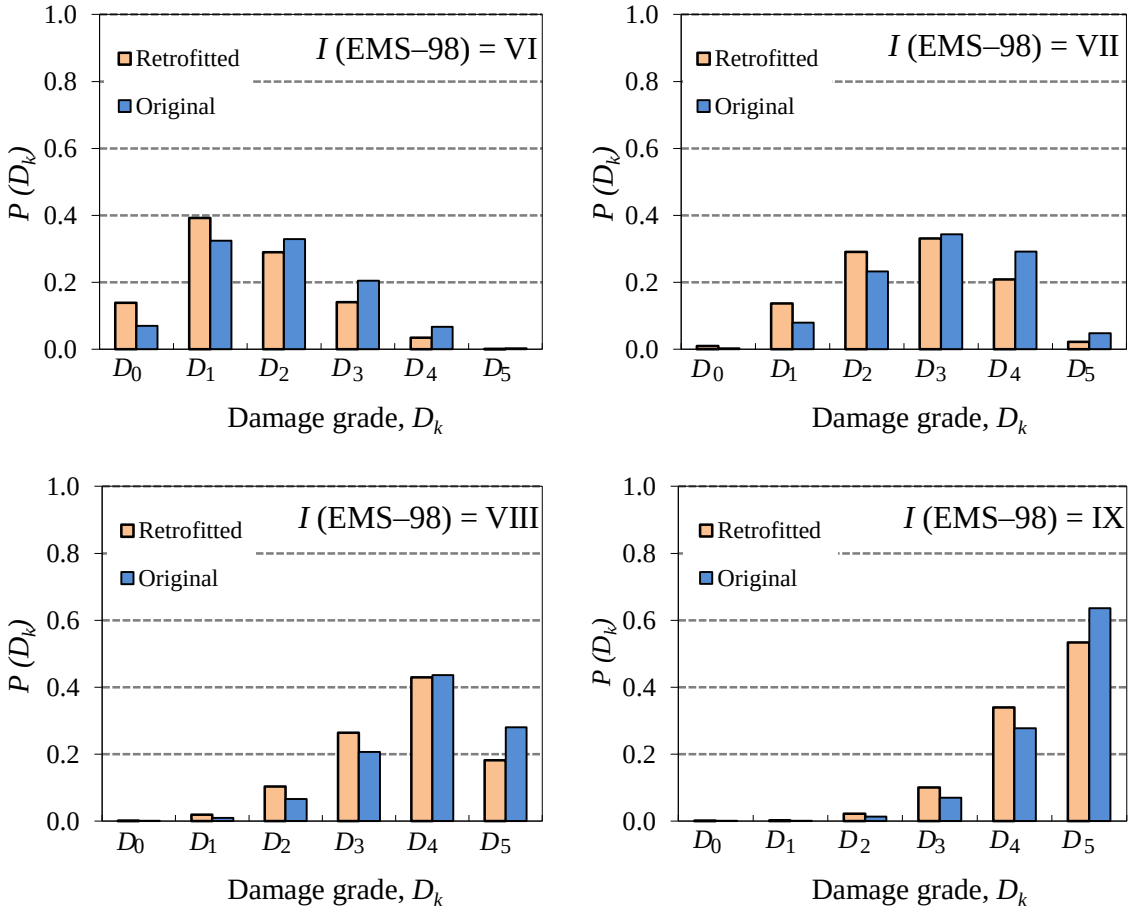

Figure 5.16: Comparison of discrete damage distribution histograms for $I_{v,mean}$ (Original) = 40.89 and $I_{v,mean}$ (Retrofitted) = 24.92 with different intensities

Figure 5.17 shows the comparison of the fragility curves corresponding to the damage distribution histograms of the mean vulnerability index values ($I_{v,mean}$ (Original) = 40.89 and $I_{v,mean}$ (Retrofitted) = 24.92). Fragility curves show that, if the Pagoda temples are retrofitted as proposed than there will be significant reduction in probability of exceeding each damage grade in comparison to original state.

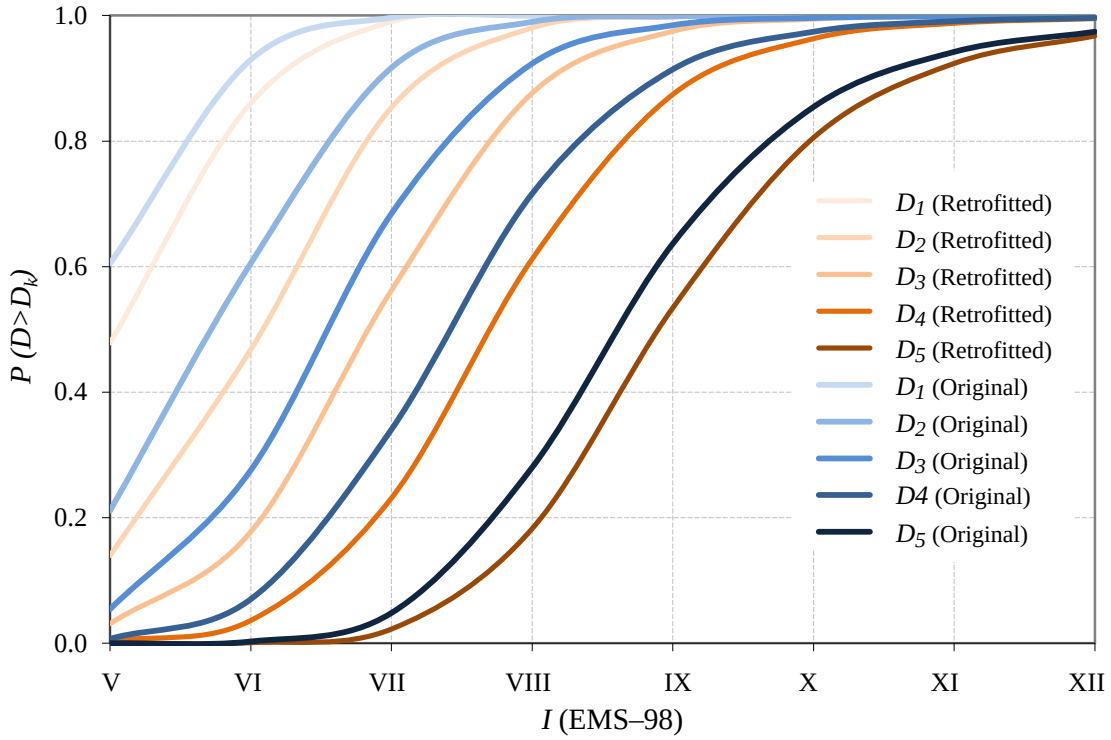

Figure 5.17: Comparison of Fragility curves for $I_{v,mean}$ (Original) = 40.89 and $I_{v,mean}$ (Retrofitted) = 24.92

Figure 5.18 and Figure 5.19 shows the comparison of probability of Pagoda temples collapse and unusable Pagoda temples for the mean values of the vulnerability index, $I_{v,mean}$ (Original) = 40.89 and $I_{v,mean}$ (Retrofitted) = 24.92, respectively. The results regarding percentage reduction in the probability of retrofitted Pagoda temples to collapse and unusable in comparison to original condition for the mean values of vulnerability index ($I_{v,mean}$ (Original) = 40.89 and $I_{v,mean}$ (Retrofitted) = 24.92) are listed in Table 5.5. It is important to note that the percentage of unusable Pagoda temples increases with intensity (for intensities IX and X) as compared to original unusable Pagoda temples, as the percentage of Pagoda temples that suffer collapse decrease.

Table 5.5: Estimation of the reduction of collapsed and unusable Pagoda temples after retrofitting actions

Total Pagoda temples (78)	Intensity, *I* (EMS–98)				
	VI	VII	VIII	IX	X
Reduction of collapsed Pagoda temples	0%	3%	10%	11%	4%
Reduction of unusable Pagoda temples	3%	6%	1%	5%	3%

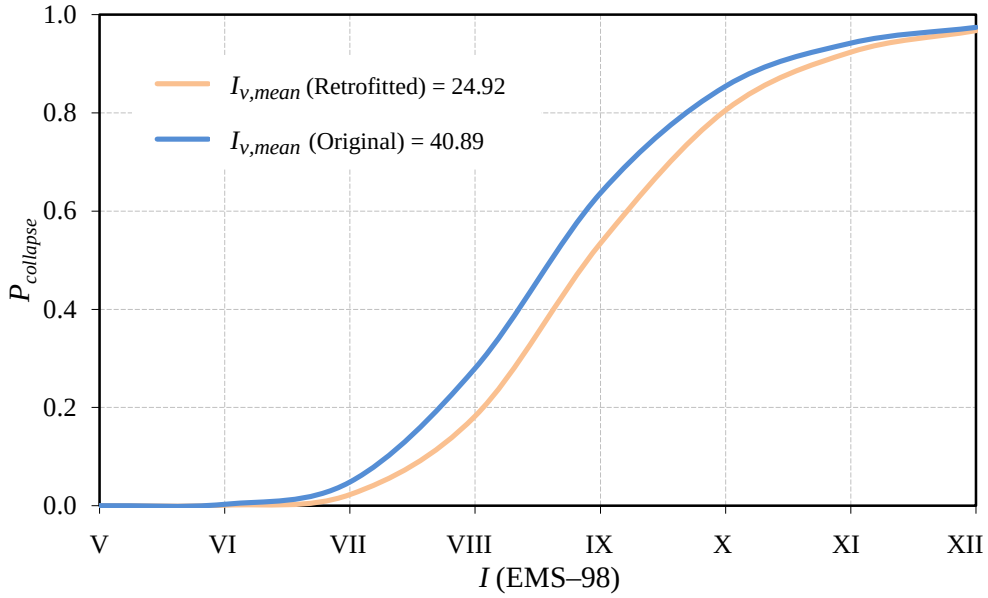

Figure 5.18: Comparison of probability of collapse Pagoda temples for $I_{v,mean}$ (Original) = 40.89 and $I_{v,mean}$ (Retrofitted) = 24.92

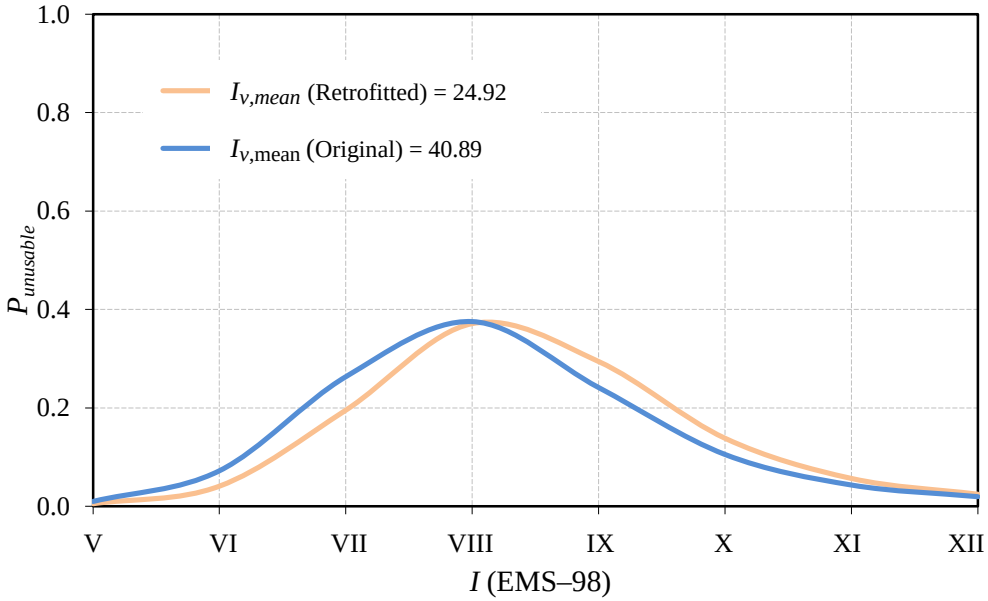

Figure 5.19: Comparison of probability of unusable Pagoda temples for $I_{v,mean}$ (Original) = 40.89 and $I_{v,mean}$ (Retrofitted) = 24.92

Figure 5.20 shows the comparison of the estimated global costs of repair for the mean values of the vulnerability index, $I_{v,mean}$ (Original) = 40.89 and $I_{v,mean}$ (Retrofitted) = 24.92, within the intensities range of V to VIII. The results show that if the Nepalese Pagoda temples are retrofitted as proposed than there will be decrease in repair costs of

minimum (0.2 million dollars) to maximum (0.8 million dollars), within the intensities range of V to VIII, as compared to original repair costs. For *I* (EMS–98) = VII, maximum difference in repair cost of 0.8 million dollars is estimated amongst the other earthquake intensities. Here, the repair cost of 4 million dollars is reduced to 3.2 million dollars. Nevertheless, significant reduction in repair cost highly depends upon the effectiveness of retrofitting. For example, if the vulnerability class of six parameters described above were upgraded by two classes instead of one class, which means more effective retrofitting, than the reduction in repair cost would be more significant, i.e. minimum of 0.2 million dollars to maximum of 1.2 million dollars, within the intensities range of V to VIII. In this case, for *I* (EMS–98) = VII, maximum difference of 1.2 million dollars is estimated. Moreover, not much significant reduction in repair cost is seen for earthquake intensities greater than VIII due to the high damage levels caused by severe seismic events.

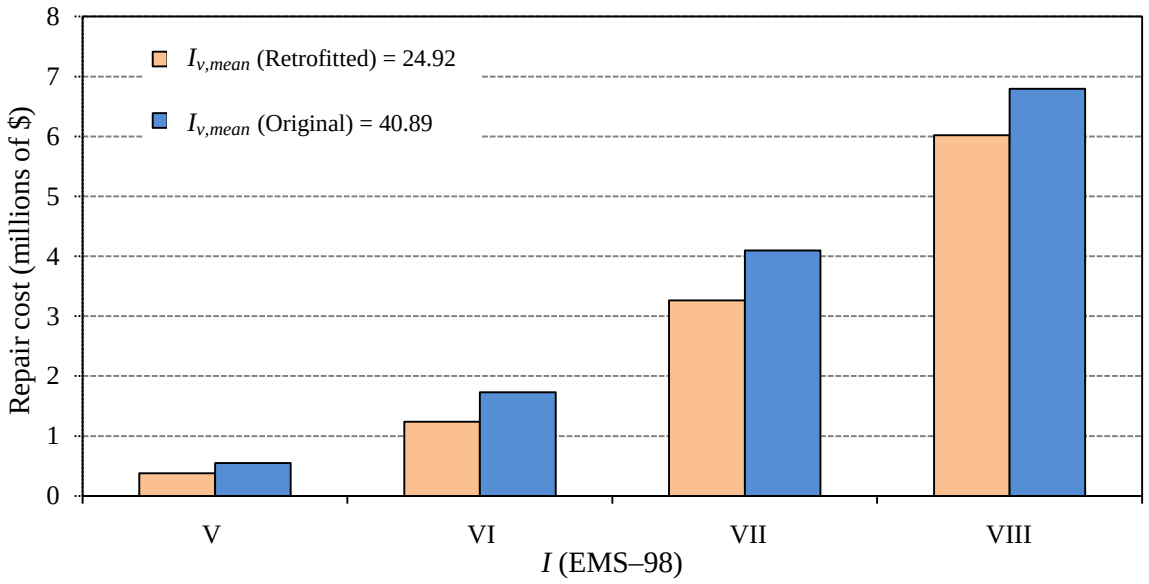

Figure 5.20: Comparison of repair cost for $I_{v,mean}$ (Original) = 40.89 and $I_{v,mean}$ (Retrofitted) = 24.92

5.7 Conclusions

The seismic vulnerability assessment methodology adapted in this case study is specially developed for slender masonry structures, like Nepalese Pagoda temples. However, the uncertainties associated with the empirical vulnerability curves and the quality of vulnerability classification data are still issues that must be studied further with respect to post–seismic data collection to obtain even more reliable results. Correlation of

this vulnerability assessment methodology with the Macroseismic method has enabled the development of damage and loss scenarios for seismic risk reduction and management. Analysis of the deterministic scenarios of damage and loss created in this study allow for the verification of these scenarios' relationship with the identified structural fragilities and construction features of Nepalese Pagoda temples.

The application of a GIS tool in this study has enabled the storage of Pagoda temples features and survey information, assessment of seismic vulnerability and damage scenario construction at a large scale. These features, which provide the possibility of spatial result presentation, make GIS an effective tool in the support of mitigation strategies and management of seismic risk.

The cities of Kathmandu Valley are located in a high seismic hazard region; hence, the level of damage associated with moderate to high seismic events is considerable. The level of damage estimated for these Pagoda temples is an indicator of their low resistance to seismic actions, and the moderate to high values of damage and loss obtained for intensities VI and IX are a consequence of these Pagoda temples' high vulnerability. Therefore, interventions focusing on the improvement of seismic performance and conservation of cultural heritage, assisted by materials' characterization and mechanical modelling, are required for seismic risk reduction. Moreover, the comparative study presented in the last section of this chapter has shown the impact and importance of retrofitting actions in seismic risk reduction and cost effectiveness. More precisely considering the same earthquake intensities, the comparative study shows a reduction in repair cost for 78 Nepalese Pagoda temples studied by 0.8 to 1.2 million dollars after retrofitting.

In conclusion, a rigorous vulnerability assessment and the implementation of appropriated retrofitting solutions can significantly reduce physical damage and economic losses from future seismic events. In this sense, studies based on macroseismic approaches play an important role in the seismic vulnerability assessment of a cultural heritage in seismic prone regions. This research enables the development of a framework for a comprehensive database and guidance tool for local authorities responsible for rehabilitation and restoration of Nepalese Pagoda temples.

CHAPTER 6

SYNOPSIS AND FUTURE RESEARCH

Summary *This final chapter presents a summary and conclusions of the most relevant comments highlighted in the previous chapters as well as some work for future research is discussed.*

Chapter outline

6.1 Summary

Existing historical slender masonry structures with different characteristics and functions are distributed all over the world and constitute a relevant part of the architectural and cultural heritage of humanity. The cultural importance of these structures poses the problem for their safeguarding and preservation. Unfortunately, several historical constructions suffered partial or total collapse in the course of time due to earthquakes, fatigue, deterioration, soil movements, etc. These losses are simply not economically quantifiable, neither lives nor cultural heritage can be reinstated by post–earthquake reconstruction plans. Their protection is a topic of great concern among the scientific community. This concern mainly arises from the observed damages after every strong earthquake and the need and interest to preserve them. Although the recent progress in technology, seismology and earthquake engineering, the preservation of these brittle and massive monuments still represent a major challenge. Since the seismic hazard is unavoidable and is not in our hands to reduce or modify it, therefore efforts are to be made for reducing the structural vulnerability by the implementation of seismic strengthening strategies. Before carrying out a multi–disciplinary seismic strengthening strategy approach it requires an intensive seismic vulnerability assessment. At present, a number of studies are available in the technical literature dealing with numerical and experimental analyses of slender masonry structures. However, there is no sufficient research work

carried out on developing the relevant seismic vulnerability assessment tools for such structures at a wider scale.

In the present research work, a simplified methodology for vulnerability assessment of slender masonry structures is proposed. This methodology estimates the seismic vulnerability index for the structure. The evaluated vulnerability index can then be used to estimate structural damage in respect to a specified intensity of a seismic event. Firstly, the research was carried out with intensive literature review. The objective of this literature review was to identify major parameter influencing the vulnerability of slender masonry structures. The knowledge of dynamic properties, together with local site seismicity and stratigraphy, is the starting point for an accurate estimation of the seismic safety of such structures. Hence, the parameter influencing the dynamic properties, precisely fundamental frequency of the structures was to be identified. Comparative analysis between experimental fundamental frequency and predictive fundamental frequency was carried out to develop empirical formulas capable of predicting reliable fundamental frequency for slender masonry structures.

Secondly, Sensitivity analysis was carried out over Nepalese Pagoda temples, which was specially considered for case study among different types of slender masonry structures. Three different Nepalese Pagoda temples were selected for parametric analysis. These three Pagoda temples were analytically modelled and one was calibrated using ambient vibration test results and following the same procedure for the remaining. In order to study the change of the fundamental frequency of the three selected temple structures, due to variation in the stiffness simulating in a simple manner, damage or degradation of vulnerable members, a number of parametric analyses were carried out. Stiffness variation is carried out to simulate damage or degradation of timber or masonry elements. Damage or degradation of members was simulated, by reducing the Young's modulus of elasticity (E value) of different members. Linear elastic parametric analyses were carried out to study the decrease in global stiffness of the temple structures. These results were revealed in terms of change in fundamental frequency of temple structures.

Finally, a simplified methodology for seismic vulnerability assessment of slender masonry structures is proposed. This method is based on vulnerability index formulation proposed on the GNDT II level approach, for the vulnerability assessment of residential masonry buildings. In this approach, the overall vulnerability is calculated as the weighted

sum of 12 parameters used in the formulation of the seismic vulnerability index. The definition of each parameter class and weight is proposed taking into account values proposed in the literature for similar methodology, the opinion of experts and parametric analyses results.

Furthermore, this research work devoted to assess the seismic vulnerability of the Nepalese Pagoda temples as a case study. Within this purpose, firstly, field survey has been carried out to evaluate the vulnerability assessing parameters of 78 Nepalese Pagoda temples, leading to the development of a database. The seismic vulnerability assessment of the Nepalese Pagoda temples of the Kathmandu Valley was carried out using the proposed methodology. With the methodology adopted, a vulnerability index, I_v, was evaluated for all 78 Pagoda temples. Secondly, the evaluated vulnerability index, I_v, in relationship with seismic intensity was used to estimate the physical damage, construct fragility curves and estimate losses. Moreover, the results of the vulnerability assessment and damage classification were integrated into a GIS tool, allowing the spatial visualation of damage scenarios, which is potentially useful for the planning of retrofitting priorities to mitigate and manage seismic risk. Finally, the Pagoda temples were assumed to be retrofitted for improvement of seismic performance of certain parameters and was developed a seismic vulnerability comparison between the original and retrofitted conditions.

6.2 Conclusions and future research

In this thesis the proposal of a seismic vulnerability assessment method has been addressed with the main objective of their implementation in the framework of a seismic vulnerability assessment, in order to draw damage and consequence scenarios for risk reduction and risk management purposes.

The research carried out in these years permitted to identify the most important aspects that determine the vulnerability of slender masonry structures under earthquake ground motion. A deep understanding of these aspects was the basis towards the development of a vulnerability assessment methodology, which corresponds to the main objective of this thesis. It is concluded in the initial stage of this research that fundamental frequency, one of the important dynamic properties which defines seismic behaviour of slender masonry structures, is significantly influenced by its geometric characteristics. Moreover four

empirical formulas are proposed for efficient and reliable evaluation of the fundamental frequency of such structures.

The results of parametric analysis carried out on the three Nepalese Pagoda temples chosen as representative show that the masonry wall structure (which represents 70–80% of total mass of temple) as the most vulnerable structural component to be safeguarded from damages and conserved. More precisely, damage or degradation to one–third of the height of the base storey masonry wall and masonry wall corners is fundamental in the reduction of stiffness of the temple structures. The results reveal no effect of the timber strut and floor damage in the overall stiffness of the temple structures. In summary, it is concluded that more local modeling is needed to understand the local behaviour of timber components and structural vulnerability and should be carried out in future research work.

The seismic analyses were developed on the Nepalese Pagoda temples by assuming the materials of structural components as a homogeneous, isotropic and linearly elastic model due to the material model´s limitation and to simplify the simulations. However, most of the Nepalese Pagoda temples have been built with complex materials, therefore further intensive research is recommended on the mechanical experimental campaigns. In all the cases the Nepalese Pagoda temples were assumed as fixed disregarding the actual state of the foundation and soil. Even when the soil–structure interaction has been a topic of intensive research in this decade, so less could be found in literature about these types of ancient masonry structures, being an interesting topic for further research.

The seismic vulnerability assessment method proposed here has been proven to be extremely useful and reliable for the analysis of slender masonry construction characteristics and as a consequence so are the results obtained from its use. Integration of this vulnerability assessment technique into a Macroseismic method has enabled its application for the development of damage and loss scenarios for risk mitigation and management. The proposed vulnerability assessment method can easily be adapted for specific building features and adopted for assessment of any type of slender masonry structure. Methods of vulnerability assessment based on statistical approaches and damage observation are far more suitable for large scale analysis, essentially for two reasons: they require less information and fewer resources while the currently available simplified mechanical models still require experimental testing validation. However, the uncertainties associated with the empirical vulnerability curves and the quality of vulnerability

classification data are still issues that must be studied further with respect to post–seismic data collection.

The level of damage estimated for these Pagoda temples is an indicator of their low resistance to seismic action, and the moderate to high values of damage and loss obtained for intensities VI to IX are a consequence of these Pagoda temples' high vulnerability. Therefore, interventions focusing on the improvement of seismic performance and conservation of cultural heritage, assisted by materials' characterization and mechanical modeling, are required for seismic risk reduction. Moreover, the comparative study presented in chapter 5 has shown the impact and importance of retrofitting in seismic risk reduction. However, future research is recommended to carry out a performance based design philosophy to find a simple device which is able to successfully reduce the seismic risk of these structures as well as maintain the cultural and technological value.

In correspondence with this methodology, the application of GIS tools and database management system in the future enables the storage of building features and survey information, assessment of seismic vulnerability and damage and risk scenario prediction, as well as allowing the upgrading and improvement of data. This integrated tool can be helpful for the development of strengthening strategies, cost–benefit analyses, civil protection and emergency planning.

In conclusion, a rigorous vulnerability assessment and the implementation of appropriated retrofitting solutions can significantly reduce physical damage and economic losses from future seismic events. In this sense, studies based on macroseismic approaches may play an important role in the seismic vulnerability assessment of cultural heritage in seismic–prone regions. It is believed that this research could enable the development of a framework for a comprehensive database and guidance tool for local authorities responsible for rehabilitation and restoration of Nepalese Pagoda temples.

REFERENCES

[1] Sepe V, Speranza E, Viskovic A, A method for large–scale vulnerability assessment of historic towers. *J. Struct. Ctrl. Health Monit.* 2008; **15**:389–415.

[2] Casolo S, Milani G, Uva G, Alessandri C, Comparative seismic vulnerability analysis on ten masonry towers in the coastal Po Valley in Italy. *J. Eng. Struct.* 2012; **49**:465–90.

[3] Salvatore W, Bennti S, Maggiora MD, On the collapse of masonry tower subjected to Earthquake loadings. *Earthquake Resistant Engineering Structures IV* 2003, ISSN: 1743–3509, doi: 10.2495/ER030141.

[4] Modena C, Valluzzi MR, Folli RT, Binda L, Design choices and intervention techniques for repairing and strengthening of the Monza cathedral bell–tower. *J. Constr. Build. Mater.* 2002; **16**:385–95.

[5] Binda L, Gatti G, Mangano G, Poggi C, Landriani GS, The Collapse of the Civic Tower of Pavia: a Survey of the Materials and Structure. *Masonry International* 1992; 11–20.

[6] Casolo S, Pena F, Dynamics of slender masonry towers considering hysteretic behaviour and damage. In: *Proceedings of the ECCOMAS Thematic Conference on Computational Methods in Structural Dynamics and Earthquake Engineering*, June 13–16, Rethymno, Crete, Greece, 2007.

[7] Pineda P, Robador MD, Gil–Martí1 MA, Seismic Damage Propagation Prediction in Ancient Masonry Structures: an Application in the Non–Linear Range Via Numerical Models. *The Open Construction and Building Technology Journal* 2011; **5 (Suppl 1–M4)**:71–9.

[8] Abruzzese D, Miccoli L, Vari A, Ferraioli M, Mandara A, Froncillo S, Dynamic investigation of medieval masonry towers: Seismic resistance and strengthening techniques. In: *Proceedings of the international conference on protection of historical buildings (PROHITEC)*, Rome, 2009.

[9] D'Ambrisi A, Mariani V, Mezzi M, Seismic assessment of a historical masonry tower with nonlinear static and dynamic analysis tuned on ambient vibration tests. *J. Eng. Struct.* 2012; **36**:210–19.

[10] Lermitte SJ, Fournely E, Lamadon T, Juraszek N, Learning from the post–earthquake mission following the L'Aquila earthquake. *Bull. Soc. Geol. France.* 2011; **182(4)**:381–8.

[11] Ferraioli M, Mandara A, Abruzzese D, Miccoli L, Dynamic identification and seismic safety of masonry bell towers. In: *Proceedings of the 14th conference of Associazione Nazionale Italiana di Ingegneria Sismica (ANIDIS)*, September 18–22, Bari, Italy, 2011.

[12] Rainieri C, Fabbrocin G, Predictive correlations for the estimation of the elastic period of masonry towers. In: *Proceedings of the Experimental Vibration Analysis for Civil Engineering Structures EVACES*, October 3–5, Varenna, Italy, 2011, pp. 513–20.

[13] Bartoli G, Betti M, Giordano S, In situ static and dynamic investigations on the ''Torre Grossa'' masonry tower. *J. Eng. Struct.* 2013; **52**:718–33.

[14] Pekgökgöz RK, Gürel MA, Mammadov Z, Çili F, Dynamic Analysis of Vertically Post–Tensioned Masonry Minarets. *J. Earthq. Eng.* 2013, **17**:560–89.

[15] Lopes V, Guedes JM, Paupério E, Arêde A, Costa A, Ambient vibration testing and seismic analysis of a masonry chimney, Palgrave Macmillan 1742–8262. *J. Build. Appr.* 2009; **5 (2)**:101–21.

[16] Russo G, Bergamo O, Damiani L, Lugato D, Experimental analysis of the ``Saint Andrea" Masonry Bell Tower in Venice. A new method for the determination of Tower Global Young's Modulus E". *J. Eng. Struct.* 2010; **32**:353–60.

[17] Corradi M, Borri A, Vignoli A, Strengthening techniques tested on masonry structures struck by the Umbrian–Marche earthquake of 1997–1998. *J. Const. Build. Mater.* 2002; **16(4)**:229–39.

[18] Buffarini G, Clemente P, Cimellaro GP, De Stefano A, Experimental dynamic analysis of Palazzo Margherita in L'Aquila after the April 6th, 2009. In: *Proceedings of the Earthquake. Experimental Vibration Analysis for Civil Engineering Structures*, EVACES, October 3–5, Varenna, Italy, 2011, pp. 247–54.

[19] Curti E, Lagomarsino S, Podestà S, Dynamic models for the seismic analysis of ancient bell towers. In: *Proceedings of the 5th Structural analysis of historical constructions (SAHC*), 6–8 November, New Delhi, India, 2006, ISBN 972–8692–27–7.

[20] Milani G, Russo S, PizzolatoM, Tralli A, Seismic Behaviour of the San Pietro di Coppito Church Bell Tower in L'Aquila, Italy. *The Open Civil Engineering Journal*, 2012; **6(Suppl 1–M3)**:131–47.

[21] Curti E, Vulnerabiltà sismica delle Torri Campanarie: modelli meccanici e macrosismici. *PhD Thesis*, Dipartimento di Ingegneria delle Costruzioni, Università degli Studi di genova, dell'Ambiente e del Territorio, 2007. (In Italian)

[22] Dogangun A, Acar R, Sezen H, Livaoglu R, Investigation of dynamic response of minaret structures. *Bull. Earthq.Eng.* 2008; **6**:505–17, doi: 10.1007/s10518–008–9066–5.

[23] Lamei S, Destruction of Sacral and Profane Buildings in Historic Cairo, CHWB cultural heritage without border. *Seminar Earthquake protection in historical buildings*, Kotar, September 2005.

[24] Curti E, Parodi S, Podesta S, Simplified models for seismic vulnerability analysis of bell towers. In: *Proceedings of the 6th International Conference on Structural Analysis of Historical Constructions* (SAHC), July 2–4, Bath, UK, 2008.

[25] Firat YG, A study of the structure response of minarets in 1999 Anatolian earthquakes. *MSc Thesis*, Purdue University, 2001.

[26] Oliveira CS, Cakti E, Stengel D and Branco M, Minaret behaviour under earthquake loading: The case of historical Istanbul. *J. Earthq. Eng. Struct. Dyn*. 2012; **41**:19–39.

[27] Anzani A, Garavaglia E, Binda L, Long–term damage of Historic Masonry: a probabilistic model. *J. Constr. Build. Mater*. 2009; **23**:713–24.

[28] Bennati S, Nardini L, Salvatore W, Dynamic behaviour of a Medieval Masonry Bell Tower. II: measurement and modeling of the tower motion. *J. Struct. Eng*. 2005; **131**:1656–64.

[29] Binda L, Zanzi L, Lualdi M, Condoleo P, The use of georadar to assess damage to a Masonry bell tower in Cremona, Italy. *J. NDT & E Int.* 2005; **38**:171–79.

[30] Bonato P, Ceravolo R, De Stefano A, Molinari F, Cross–time frequency techniques for the identification of Masonry buildings. *J. Mech. Syst. Signal Process.* 2000; **14**:91–109.

[31] Carpinteri A, Lacidogna G, Damage evaluation of Three Masonry towers by acoustic emission. *J. Eng. Struct.* 2007; **29**:1569–79.

[32] Gentile C, Saisi A, Ambient vibration testing of Historic Masonry towers for structural identification and damage assessment. *J. Constr. Build. Mater.* 2007; **21**:1311–21.

[33] Giannini R, Pagnoni T, Pinto PE, Vanzi I, Risk analysis of a medieval tower before and after strengthening. *J. Struct. Safety* 1996; **18**:81–100.

[34] Lucchesi M, Pintucchi B, A numerical model for non–linear dynamic analysis of Slender Masonry structures. *Eur. J. Mech. A/Solids* 2007; **26**:88–105.

[35] Reale E, Paguni C, Floridia S, Static and dynamic analysis of S. Peter tower in Modica, Ragusa, Sicily. Lourenço PB & Roca P (eds.) *Historical Constructions 2001: Possibilities of Numerical and Experimental Techniques*, pp. 887–96. University of Minho, Guimarães, Portugal, 2001. http://www.civil.uminho.pt/masonry/.

[36] Riva P, Perotti F, Guidoboni E, Boschi E, Seismic analysis of the Asinelli tower and earthquakes in Bologna. *J. Soil Dyn. Earthq. Eng.* 1998; **17**:525–50.

[37] Valluzzi MR, On the vulnerability of Historical Masonry structures: analysis and mitigation. *J. Mater. Struct.* 2007; **4**:723–43.

[38] Ivorra S, Pallares FJ, Dynamic investigation on a masonry bell tower. *J. Eng. Struct.* 2006; **28**:660–67.

[39] Julio ENBS, DA Silva Rebelo CA, Dias–DA–Costa D, Structural assessment of the tower of the University of Coimbra by modal identification. *J. Eng. Struct.* 2008; **30**:3648–77.

[40] Lepidi M, Gattulli V, Foti D, Swinging –bell resonance ant their cancellation identified by dynamic analysis in a modern bell tower. *J. Eng. Struct.* 2009; **31(7)**:1486–1500.

[41] El–Attar AG, Saleh AM, Zaghw AH, Conservation of a slender historical Mamluk–style minaret by passive control technique. *J. Struct. Ctrl Health monit.* 2005; **12**:157–77.

[42] Pesci A, Casula G, Bonchi E, Laser scanning the Garisenda and Asinelli towers in Bologna (Italy): detail deformation patterned of two ancient leaning buildings. *J. Cult. Herit.* 2010; **12**:117–27.

[43] Valluzzi MR, Porto F, Modenza C, Structural investigation and strengthening of the civic tower in Vicenza. In: *Proceedings of the structural faults and repairs*, London, UK, 2003.

[44] Carpinteri A, Lacidogna G, Structural monitoring and diagnostic by the acoustic emission technique: Scaling of dissipated energy in compression. In: *Proceedings of the 9th int. congress on sound and vibration*, 2002, Paper no. 166.

[45] Carpinteri A, Lacidogna G, Structural monitoring and integrity assessment of medieval towers. *J. Struct. Eng. (ASCE)* 2006; 1681–90.

[46] De Stefano A, Clemente P, S.H.M. on historical heritage: Robust methods to face large uncertaines. *SAMCO Final Report*. 2006. pp. 1–18.

[47] Carpinteri A, Invernizzi S, Lacidogna G, In situ damage assessment and nonlinear modeling of a historical masonry tower. *J. Eng. Struct.* 2005; **27**:387–95.

[48] Bayraktar A, Türker T, Sevım B, Altunisik, AC, Yildirim F, Modal Parameter Identification of Hagia Sophia Bell–Tower via Ambient Vibration Test. *J. Nondestructive Evaluation* 2009; **28**:37–47.

[49] Bernardeschi K, Padovani C, Pasquinelli G, Numerical modeling of the structural behaviour of Buti's bell tower. *J. Cult. Herit.* 2004; **5**:371–78.

[50] De Sortis A, Antonacci E, Vestroni F, Dynamic identification of a masonry building using forced vibration tests. *J. Eng. Struct.*2005; **27**:155–65.

[51] Abruzzese D, Miccoli L, Yuan J, Mechanical behaviour of leaning masonry Huzhu Pagoda. *J. Cult. Herit.* 2009; **10**:480–86.

[52] Peña F, Lourenço PB, Mendes N, Oliveira DV, Numerical models for the seismic assessment of an old masonry tower. *J. Eng. Struct.* 2010; **32**:1466–78.

[53] Crispino M, D'Apuzzo M, Measurement and prediction of traffic–induced vibrations in a heritage building. *J. Sound and Vibration* 2001; **246(2)**:319–35.

[54] Jaras A, Kačianauskas R, Markauskas D, Stupak E, FE modeling of wall structures of Vilnius Arch–Cathedral Belfry. In: *Proceedings of the 8th Conference on Shell Structures: Theory and Applications.* October 12–14, Jurata, Poland, 2005. Taylor and Francis, pp. 563–67.

[55] Carpinteri A, Invernizzi S, Lacidogna G, Numerical assessment of three medieval masonry towers subjected to different loading conditions. *Masonry International* 2006; **19**:65–75.

[56] Heyman J, Leaning towers, *Meccanica* 1992; **27**: 153–9.

[57] Casolo S, A three dimensional model for vulnerability analyses of slender masonry Medieval towers. *J. Earthq. Eng.* 1998; **2(4)**:487–512.

[58] Casolo S, Significant ground motion parameters for evaluation of the seismic performance of slender masonry tower. *J. Earthq. Eng.* 2001; **5(2)**:187–204.

[59] Anzani A, Binda L, Carpinteri A, Invernizzi S, Lacidogna G, A multilevel approach for the damage assessment of Historic masonry towers. *J. Cult. Herit.* 2010; **11**:459–70.

[60] Lourenço PB, Assessment, diagnosis and strengthening of Outeiro Church, Portugal. *J. Constr. Build. Mater*. 2005; **19**:634–45.

[61] Binda L, Saisi A, Tiraboschi C, Investigation Procedures for the Diagnosis of Historic Masonries. *J. Const. Build. Mater.* 2000; **14**:199–34.

[62] Ceroni F, Pecce M, Manfredi G, Seismic Assessment of the Bell Tower of Santa Maria Del Carmine: Problems and Solutions. *J. Earthq. Eng*. 2010; **14**:30–56.

[63] Stavroulaki ME, Bartoli G, Betti M, Stavrolakis GE, Strengthening of masonry using metal reinforcement: A parametric numerical investigation. In: *Proceedings of the Protection of Historical Buildings* PROHITECH 09, Mazzolani FM (ed), 2009, ISBN 978–0–415–55803–7.

[64] Figueiras JA, Povoas RHCF, Modeling of prestress in non–linear analysis of concrete structures. *J. Comp. Struct.* 1994; **53**:173–87.

[65] Leftheris B, Tzanaki E, Stavroulaki ME, Dynamic criterion for reinforcement of old buildings. In: *Proceedings of the STREMA 93, Structural Studies, Repairs and Maintenance of Historical buildings III'*, Brebbia CA & Frewer RJB (eds), UK, 1993.

[66] Leftheris B, Stavroulaki ME, Sapounaki AC, Stavroulakis GE, *Computational methods for heritage structures*. WIT Press, Southampton, U.K, 2006.

[67] Bongiovanni G, Clemente P, Buffarini G, Analysis of the seismic response of a damaged masonry bell tower. In: *Proceedings of the 12th World Conference on Earthquake Engineering*, January 30–February 4, Auckland, New Zealand, 2000.

[68] Camata G, Cifelli L, Spacone E, Conte J, Torrese P, Safety analysis of the bell tower of S. Maria Maggiore cathedra in Guardiagrele (Italy). In: *Proceedings of the*

14th World Conference on Earthquake Engineering, October 12–17, Beijing, China, 2008.

[69] Carone AS, Foti D, Giannoccaro NI, Nobile R, Non–destructive characterization and dynamic identification of an historical bell tower. In: *Proceedings of the 4th International Conference on Integrity, Reliability and Failure*, June 23–27, Funchal/Madeira, 2013, Paper no. 3988.

[70] Ramos LF, Marques L, Lourenco PB, De Roeck G, Costa A, Roque J, Monitoring historical masonry structures with operational modal analysis: Two case studies. *J. Mech. Syst. Signal Process.* 2010; **24**:1291–1305.

[71] Tomaszewska A, Influence of statistical errors on damage detection based on structural flexibility and mode shape curvature. *J. Comp. Struct.* 2010; **88**:154–64.

[72] Guerreiro L, Azevedo J, Análise e reforço da torres do relógio da Horta, Faial. In: *Proceedings of the 5th Encontro national de sismologia e engenharia sismica*, October 24–27, 2001, pp. 639–50. (In Portugese)

[73] Pelella T, Mannara G, Cosenza E, Iervolino I, Lecce L, Structural dynamic investigations on the bell tower from the S. Lucia's church–Serras. Quirico (Ancona). In: *Proceedings of the 7th International Seminar on Seismic Isolation, Passive Energy Dissipation and Active Control of Vibrations of Structures*, October 2–5, Assisi, Italy, 2001.

[74] Ceriotti M, Luca Mottola L, Picco GP, Murphy AL, Guna S, Corrà M, Pozz M, Zonta D, Zanon P, Monitoring Heritage Buildings with Wireless Sensor Networks: The Torre Aquila Deployment. In: *Proceedings of the 8th ACM/IEEE International Conference on Information Processing in Sensor Networks*, April 13–16, San Francisco, CA, 2009 .

[75] Foti D, Chorro SI, Sabbà MF, Dynamic Investigation of an Ancient Masonry Bell Tower with Operational Modal Analysis: A Non–Destructive Experimental Technique to Obtain the Dynamic Characteristics of a Structure. *The Open Construction and Building Technology Journal* 2012; **6**:384–91.

[76] Ivorra S, Pallares FJ, Adam JM, Tomas R, An evaluation of the incidence of soil subsidence on the dynamic behaviour of a Gothic bell tower. *J. Eng. Struct.* 2010; **32**:2318–25.

[77] Gentile C, Sais A, Operational modal testing of historic structures at different levels of excitation. *J. Constr. Build. Mater*. 2013; **48**:1273–85.

[78] Ivorra S, Cervera JR, Analysis of the dynamic actions when bells are swinging on the bell tower of Bonreposi Mirambell Church (Valencia, Spain). In: *Proceedings of the Historical Constructions*, Lourenço PB & Roca P (eds), Guimarães, Portugal, 2001.

[79] Casciati S, Al–Saleh R, Dynamic behaviour of a masonry civic belfry under operational conditions. *J. Acta. Mech.* 2010; **215**:211–24, doi: 10.1007/s00707–010–0343–4.

[80] Balduzzi B, Mazza D, Papis D, Rossi C, Rossi PP, Experimental and numerical analysis for the strengthening intervention of the bell tower of St. Sistós Church in Bergamo. In: *Proceedings of the 5th International Conference on Structural Analysis of Historical Constructions (SAHC)*, 6–8 November, New Delhi, India, 2006, ISBN 972–8692–27–7.

[81] Peeters B, Sforza G, Sbaraglia L, Germano F, Efficient operational modal testing and analysis for design verification and restoration baseline assessment: Italian case studies. In: *Proceedings of the Experimental Vibration Analysis for Civil Engineering Structures (EVACES),* October 3–5, Varenna, Italy, 2011.

[82] Kohan PH, Nallim LG, Gea SB, Dynamic characterization of beam type structures: Analytical, numerical and experimental applications. *J. Applied Acoustics* 2011; **72**:975–81.

[83] Jaras A, Kliukas R, Kačianauskas R, The dynamic loading of Vilnius archcathedral belfry –Investigation and analysis. In: *Proceedings of the 10th international conference on Modern Building materials*, Structures and Techniques, May 19–21, Vilnius, Lithuania, 2010, pp. 635–40.

[84] Costa A, *Ambient vibration measurement of bell tower*. Porto. University of Aveiro, Portugal, 2011.

[85] Diaferio M, Foti D, Giannoccaro NI, Vitti M, On the use of modal analysis and ground penetrating radar test for the physical parameter identification of an historical bell tower. In: *Proceedings of the Vienna Congress on Recent Advances in Earthquake Engineering and structural Dynamics* (VEESD), August 28–30, Vienna, Austria, 2013, Paper no. 560.

[86] Pieraccini M, Fratini M, Dei D, Atzeni C, Structural testing of Historical Heritage Site Towers by microwave remote sensing. *J. Cult. Herit. 2009;* **10**:174–82.

[87] Zaki MA, Hassan AF, Mourad SA, Osman AM, Evaluation of the structural integrity of historical stone minarets. In: *Proceedings of the 14th World Conference on Earthquake Engineering*, October 12–17, Beijing, China, 2008.

[88] Pau A, Vestroni F, Dynamic Characterization of Ancient Masonry Structures. *Advances in Vibration Analysis Research*, 2011, pp. 213–30.

[89] Turk AM, Cosgun C, Seismic Behaviour and Retrofit of Historic Masonry Minaret. *GRADEVINAR 64* 2012; **1**:39–45.

[90] Krstevska L, Tashkov L, Gramatikov KK, Landolfo R, Mammana O, Portioli F, Mazzolani F, Large–Scale Experimental Investigation on Mustafa Pasha Mosque. *J. Earthq. Eng. 2010;* **14**:842–73.

[91] Aoki T, Sabia D, *Theoretical and Experimental Analysis of Brick Chimneys, Tokoname, Japan*. Computational Mechanics, WCCM VI in conjunction with APCOM'04, September 5–10, 2004, Beijing, China, 2004, Tsinghua University Press & Springer–Verlag.

[92] Costa A, *Relatório de inspeção de uma chaminé sita em Vila franca de Xira, relatório técnico.* Projecto e Flscallzação Lda, malo, 2010. (In Portuguese)

[93] Yamamoto T, Maeda T, Earthquake safety assessment of a tall brick chimney in Tokoname based on the micro–tremor measurement. In: *Proceedings of the 14th World Conference on Earthquake Engineering*, October 12–17, Beijing, China, 2008.

[94] Grande R, Açores SM, *Relatório dos ensaios dinmicos de vibraçao ambiental e avaliaçao de segurança estrutural face à acçao sismica*. University of Porto, 2009. (In Portuguese)

[95] Eusani F, Benedettini F, Modal and Structural Identification of a Masonry Chimney. In: *Proceedings of the 19th Congress of Italian Association for Theoretical and Applied Mechanics*, September 14–17, Ancona, Italy, 2009.

[96] Costa A, Guedes J, Silva B, Lopes V, *Inspecção diagnóstico e caracterização material– chaminé em Matosinhos*. Relatório técnico, Março, 2011. (In Portuguese)

[97] Jaishi B, Ren WX, Zong ZH, Maskey PN, Dynamic and seismic performance of old multi–tiered temples in Nepal. *J. Eng. Struct.* 2003; **25**:1827–39.

[98] Shakya M, Varum H, Vicente R, Costa A, Seismic sensitivity analysis of the common structural components of Nepalese Pagoda temples. *Bull. Earthq. Eng.* 2013, doi: 10.1007/s10518–013–9569–6.

[99] Faccio P, Podestà S, Saetta A, *Campanile della Chiesa di Sant'Antonin, Esempio 5*, in Linee Guida per la valutazione e riduzione del rischio sismico del patrimonio culturale allineate alle nuove Norme tecniche per le costruzioni (D.M. 14/01/2008). Circolare 26/2010. Venezia, 2011. (In Italian)

[100] NSCE–02, *Norma de Construcciòn Sismorresistente. Parte General y Edificaciòn* (Spanish Standard). Ministerio de Fomento, Spain, 2002. (In Spanish)

[101] Clough RW, Penzien J, *Dynamics of Structures.* 2nd Ed., McGraw–Hill Book Company, New York, 1993.

[102] Parajuli YK, Bhaktapur Development Project (BDP): *Experiences in preservation and restoration in medieval town (1974–1985)*. Frankfurt: Deutsche Gesellschaft fuer Technisches Zuzammenarbeit (GTZ), 1986.

[103] Ranjitkar RK, Heritage homeowner's preservation manual. Kathmandu Valley World Heritage site, Nepal: advice for maintenance of historic houses in the Kathmandu Valley. *Integrated Community Development and Cultural Heritage Site Preservation in Asia and the Pacific through Local Effort Programme (LEAP)*, UNESCO Bangkok, UNESCO Kathmandu, 2006.

[104] Tiwari SR, *Temples of the Nepal Valley*. Himal Books, Kathmandu, Nepal, 2009, ISBN: 9789937814430.

[105] Nienhuys S, Options for reconstruction and retrofitting of historic Pagoda Temples. *Reconstruction of Temples in Kathmandu*, HUYS ADVIES, September 2003. http://www.nienhuys.info/mediapool/49/493498/data/Retrofitting_KVPT_HA_2003.pdf

[106] Kathmandu valley preservation trust (KVPT), Patan, Nepal/Bhaktapur municipality (BKT), Bhaktapur, Nepal, *The collection of information and drawings of Nepalese Pagoda temples*, 2011. http://www.kvptnepal.org, http://www.bkt–municipality.gov.np

[107] Thapa JB, Test and simulation of brick masonry wall of historic buildings. *Msc thesis*. Institute of Engineering, Pulchowk campus, Tribhuvan University, Nepal, 2011.

[108] Indirli M, Kouris LAS, Formisano A, Borg RP, Mazzolani FM, Seismic damage assessment of unreinforced masonry structures after the Abruzzo 2009 earthquake: the case study of the historical centers of L'Aquila and Castelvecchio Subequo. *Int. J. of Architectural Herit.* 2013; **7**:536–78.

[109] Ranjitkar RK, Seismic Strengthening of the Nepalese Pagoda: Progress report, Earthquake–Safe: Lessons to Be Learned from Traditional Construction. In: *Proceedings of the International Conference on the Seismic Performance of Traditional Buildings*: November 16–18, Istanbul, Turkey, 2000. Istanbul: ICOMOS International Wood Committee, http://www.icomos.org/iiwc/seismic/Ranjitkan.pdf

[110] Faggiano B, Marzo A, Formisano A, Mazzolani FM, Innovative steel connections for the retrofit of timber floors in ancient buildings: A numerical investigation. *J. Compt. & Struct.* 2009; **87**:1–13.

[111] Bonapace B, Sestini V, *Traditional materials and construction technologies used in the Kathmandu valley*. Paragraphic for the United Nations Educational, Scientific and Cultural, 7 Place de Fontenoy, 75352 Paris 07 SP, France.

[112] Neves F, Costa A, Vicente R, Oliveira CS, Varum H, Seismic vulnerability assessment and characterization of the buildings on Faial Island, Azores. *Bull. Earthq. Eng.* 2012; **10**:27–44, doi: 10.1007/s10518–011–9276–0.

[113] Pradhan R, Seismicity and Traditional Buildings of Kathmandu Valley, Nepal, Earthquake–Safe: Lessons to Be Learned from Traditional Construction. In: *Proceedings of the International Conference on the Seismic Performance of Traditional Buildings*: November 16–18, Istanbul, Turkey, 2000. Istanbul: ICOMOS International Wood Committee. http://www.icomos.org/iiwc/seismic/Pradhan.pdf

[114] Theophile E, Ranjitkar RK, Timber conservation problems of the Nepalese Pagoda temple. In: *Proceedings of the 8th int. Symposyum of ICOMOS International Wood Committee*, Norway, 1992, pp. 85–124.

[115] Faggiano B, Grippa MR, Marzo A, Mazzolani FM, Experimental study for non–destructive mechanical evaluation of ancient chestnut timber. *J. Civil Struct. Health Monit.* 2011; **1**:103–12.

[116] Tomazevic M, Sheppard P, Zarnic R, Assessment of earthquake resistance of old urban and rural nuclei. *Institute for Testing and Research in Materials and Structures*, 12, 61000 Ljubljana, Yugoslavia, 1985.

[117] Parajuli HR, Kiyono J, Taniguch H, Toki K, Furukawa A, Maskey PN, Parametric Study and Dynamic Analysis of a Historical Masonry Building of Kathmandu. *Disaster Mitigation of Cultural Heritage and Historic Cities* 2010; Vol. 4.

[118] Jaishi B, Seismic capacity evaluation of multi–tiered temples of Nepal. *Msc thesis*, Pulchowk campus, Tribhuvan University, Nepal, December, 2001.

[119] KVPT, *Retrofitting, Restoration, and Reconstruction of Nepalese Pagoda temples.* Kathmandu valley preservation trust, Patan Darbar Square, Nepal, 2014. http://www.kvptnepal.org

[120] Shakya M, Modal analysis using ambient vibration measurement and damage identification of three–tiered *Radha Krishna* Temple. *ME thesis*, Purbanchal University, Nepal, 2010.

[121] Shakya M, Varum H, Vicente R, Costa A,Structural Vulnerability of Nepalese Pagoda Temples. In: *Proceedings of the 15th World Conference on Earthquake Engineering*, September 24–28, Lisbon, Portugal, 2012, Paper no. 2919.

[122] SAP 2000 Ultimate 15.0.0., *Structural analysis program.* Computer and Structures. Inc. 1976–2011, Berkeley, CA, 2011.

[123] ARTeMIS, *Extractor Pro software*. Issued by Structural Vibration Solutions Aps. NOVI Science Park, Niels Jernes Vej 10, DK 9220 Aalborg East, Denmark, 2011.

[124] Júlio ENBS, Silva Rebelo CA, Dias–da–Costa DASG, Structural assessment of the tower of the University of Coimbra by modal identification. *J. Eng. Struct.* 2008; **30**:3468–77.

[125] Krstevska L, Tashkov L, Naumovski N, Florio G, Formisano A, Fornaro A, Landolfo R, In–situ experimental testing of four historical buildings damaged during the 2009 L'Aquila earthquake. In: *Proceedings of the COST Action C26 Final Conference "Urban Habitat Constructions under Catastrophic Events"*, September 16–18, Naples, 2010, CRC Press, Taylor & Francis Group, London, ISBN: 978–0–415–60685–1, pp. 427–32.

[126] Aras F, Krstevska L, Altay G, Tashkov L, Experimental and numerical modal analyses of a historical masonry palace. *J. Eng. Struct.* 2011; **25**:81–91.

[127] Chen JF, Morozov EV, Shankar K, A combined elastoplastic damage model for progressive failure analysis of composite materials and structures. *J. Composite Struct.* 2012; **94**:3478–89.

[128] Orduña A, Preciado A, Galván JF, Araiza JC, Vulnerability assessment of churches at Colima by 3D limit analysis models. In: *Proceedings of the 6th International Conference on Structural Analysis of Historical Constructions (SAHC)*, July 2–4, Bath, UK, 2008.

[129] Sandi H, Vulnerability and risk analysis for individual structures and system, Report of the European Association of Structural Engineering. In: *Proceedings of the 8th Congress of the ECEE*, Lisbon, Portugal, 1986.

[130] Speranza E, Viskovic A, Sepe V, Integrated methods for the assessment of the structural vulnerability of historic towers. In: *Proceedings of the 5th International Conference on Structural Analysis of Historical Constructions (SAHC)*, 6–8 November, New Delhi, India, 2006, pp. 651–58.

[131] GNDT–SSN–1994, *Gruppo Nazionale per la Difesa dai Terremoti, Scheda di esposizione e vulnerabilità e di rilevamento danni di primo livello e secondo livello (muratura e cemento armato*). Gruppo Nazionale per la Difesa dai Terremoti: Roma, Italy, 1994. (In Italian)

[132] Benedetti D, Petrini V, Sulla vulnerabilitá sismica di edifici in muratura i proposte di un metodo di valutazione. *L'industria delle Construzioni* 1984; **149**:66–74.

[133] GNDT–1990, *Seismic risk of public buildings, National Council of Investigation.* Gruppo Nazionale per la Difesa dai Terremoti, Italy, 1990. (In Italian)

[134] Corsanego A, Petrini V, Seismic vulnerability of buildings. In: *Proceedings of the SEISMED 3.* Trieste, Italy, 1990.

[135] Speranza E, An integrated method for the assessment of the seismic vulnerability of historic buildings. *Phd thesis*, Department of Architecture and Civil Engineering, University of Bath, U.K., 2003.

[136] Whitman RV, Reed JW, Hong ST, Earthquake damage probability matrices. In: *Proceedings of the 5th world conference on earthquake engineering*, Rome, 1974, Paper no. 2531.

[137] ATC–21, *Rapid visual screening of building for potential seismic hazards: a handbook*. Applied Technology Council, FEMA 145, Redwood City, California, 1988.

[138] ATC–13, *Earthquake damage evaluation data for California*. Applied Technology Council, California, 1985.

[139] HAZUS MH, *Earthquake loss estimation methodology–technical and user manuals*. Federal Emergency Management Agency, Washington, D.C., 1999.

[140] Giovinazzi S, Lagomarsino S, A macroseismic model for the vulnerability assessment of buildings. In: *Proceedings of the 13th world conference on earthquake engineering*, August 1–6, Vancouver, Canada, 2004, Paper no. 896.

[141] Dolce M, Kappos A, Zuccaro G, Coburn AW, Report of the EAEE working group 3: vulnerability and risk analysis, Technical Report. In: *Proceedings of the 10th European Conference on Earthquake Engineering*, Vienna, No. 4, 1994, pp. 3049–77.

[142] Grünthal G, *European Macroseismic Scale EMS–98*. Notes of the European Center of Geodynamics and Seismology, Volume 15, Luxembourg, 1998.

[143] Midas FEA, *Nonlinear and detail FE Analysis System for civil structures*. Midas Information Technology Co., 2013.

[144] Calderini C, Lagomarsino S, A micromechanical inelastic model for historical masonry. *J. Earthq. Eng*. 2006; **10(4)**:453–79.

[145] Gambarotta L, Lagomarsino S, Damage models for the seismic response of brick masonry shear walls, Part I and II. *J. Earthquake Eng. & Struct. Mech.*1997; **26**:441–62.

[146] Preciado A, Seismic Vulnerability Reduction of Historical Masonry Towers by External Prestressing Devices. *PhD thesis*, Department of Architecture, Civil Engineering and Environmental Sciences University of Braunschweig–Institute of Technology, Germany, September 2011.

[147] Vecchio FJ, Collins MP, The Modified Compression Field Theory for Reinforced Concrete Elements Subjected to Shear. *ACI J.* 1986; **83(22)**:219–31.

[148] Chen W, Han DJ, *Plasticity for Structural Engineers*. New York: Springer–Verlag, 1988.

[149] Lourenço P, Computational strategies for masonry structures. *PhD Thesis*, Delft University. Netherlands, 1996.

[150] Pieraccini M, Parrini F, Dei D, Fratini M, Atzeni C, Spinelli P, Dynamic characterization of a bell tower by interferometric sensor, *NDT&E International* 2007; **40**:390–496.

[151] Vicente RS, Strategies and methodologies for urban rehabilitation interventions. The vulnerability assessment and risk evaluation of the old city centre of Coimbra. *PhD Thesis*, University of Aveiro, 2008. (In Portuguese)

[152] González JRA, *Introducción al estudio de la vulnerabilidade sísmica de los edifícios históricos de Granada*. 2003. (In Spanish)

[153] Indian Standard, *Criterion for earthquake resistant design of structures*. IS: 1893–1984.

[154] Binda L, Poggi C, Roberti GM, Folli RT, *On site investigation and monitoring of the Torrazzo of Cremona, Polytechnique de Milan*. University of Reggio Calabria, 2000.

[155] CEN, *Eurocode 8: design of structures for earthquake resistance–Part 1: general rules*. seismic actions and rules for buildings, Standardization, European Committee for Brussels, 2008.

[156] Pineda P, Robador MD, Perez–Rodriguez JL, Characterization and repair measures of the medieval building materials of a Hispanic–Islamic construction. *J. Const. & Bldg. Mater.* 2013; **41**:612–33.

[157] Arêde A, Costa A, Moreira D, Neves N, Seismic analysis and strengthening of Pico Island Churches. *Bull. Earthq. Eng.* 2012; **10**:181–209, doi: 10.1007/s10518–011–9325–8.

[158] Cosenza E, Iervolino I, Case Study: Seismic Retrofitting of a Medieval Bell Tower with FRP. *J. Composites for Const. ASCE*, DOI: 10.1061/ (ASCE) 1090–0268 (2007) 11:3 (319)

[159] Zonta D, Pozzi M, Zanon P, Anese GA, Busetto A, Real–time probabilistic health monitoring of the Portogruaro Civic Tower. *Structural Analysis of Historic Construction* – D'Ayala & Fodde (eds), 2008, Taylor & Francis Group, London, ISBN 978–0–415–46872–5.

[160] Kliukas R, Kacianauskas R, Jaras A, A monument of historical heritage– Vilnius arch cathedral belfry: The dynamic investigation. *J. Civil Eng. & Mgmt.* 2008; **14(2)**: 139–146

[161] Bayraktar A, Şahin A, Özcan A, Yildirim F, Numerical damage assessment of Haghia Sophia bell tower by nonlinear FE modeling. *J. Applied Mathematical Modeling* 2010; **34**:92–121.

[162] Okuyucu D, Aydin AC, An Evaluation On Erzurum Double Minaret Madrasah By Structural Engineerıng Perspective, KSU. *J. Eng. Sciences* 2010; **13(1)**:24–44

[163] Kouris SS, Weber MKK, *Numerical Analysis of Masonry Bell–Towers under Dynamic Loading Journal of Civil Engineering and Architecture*. ISSN 1934–7359, USA, August 2011, Volume 5, No. 8 (Serial No. 45), pp. 715–22.

[164] Soyluk A, İlerisoy ZY, Dynamic analysis of Dolmabahce masonry clock tower. *GRAĐEVINAR* 65 2013; **4**:345–52, UDK 725.94.001.5:699.84(496.1)

[165] Vicente R, Parodi S, Lagomarsino S, Varum H, Mendes S, Seismic vulnerability and risk assessment: case study of the historic city centre of Coimbra, Portugal. *Bull. Earthq. Eng* 2011; **9**:1067–96, doi: 10.1007/s10518–010–9233–3.

[166] Dogangun A, Tuluk OI, Livaoglu R, Acar R, Traditional Turkish minarets on the basis of architectural and engineering concepts. In: *Proceedings of the 1st International Conference on Restoration of Heritage Masonry Structures*, Cairo, Egypt, April 24–27, 2006, P34, pp. 1–10.

[167] Combescure D, Guéguen P, Lebrun B, Vulnérabilité sismique du bâti existant: approche d'ensemble. *Cahier technique AFPS* **25**:121, 2005. (In Italian)

[168] Giovinazzi S, The vulnerability assessment and damage scenario in seismic risk analysis. *PhD Thesis*, International doctorate, University of Florence, Technical University of Carolo–Wilhelmina, 2005.

[169] Lagomarsino S, Podestà S, Resemini S, Observation and mechanical models for the vulnerability assessment of monument buildings. In: *Proceedings of the 13th world conference on earthquake engineering*, August 1– 6, 2004, Vancouver, Canada, Paper no. 942.

[170] Lagomarsino S, Podestà S, Seismic Vulnerability of Ancient Churches: II. Statistical Analysis of Surveyed Data and Methods for Risk Analysis. *J. Earth. Spectra* 2004; **20(2)**:395–412

[171] Balbi A, Lagomarsino S, Parodi S, Vulnerabilità sismica e rilevanza dei centri strorici e delle emergenze architettoniche: un'applicazione alla provincia di Imperia. In: *Proceedings of the La messa in sicurezza del terriotorio da eventi calamitosi di tipo naturale: Esperienze e nuove prosptettive*, Lerici, Italy, Sepetmber 12 2005, Minciardi R, Ugolini P (eds), Alinea, Ialy, 2007. (In Italian)

[172] ESRI, *Geographic information systems (GIS)*. 380 New York Street, Redlands, CA 92373–8100, USA, 2013.

[173] UNDP/BCPR, Reducing Disaster Risk: *A Challenge for Development A Global Report*. New York: United Nations Development Programme/Bureau for Crisis Prevention and Recovery, 2004.

[174] Chaulagain H, Rodrigues R, Jara J, Spacone E, Varum H, Seismic response of current RC buildings in Nepal: A comparative analysis of different design/construction. *J. Eng. Struct.* 2013; **49**:284–94.

[175] Ministry of Home Affairs (MoHA) and Nepal Disaster Preparedness Network–Nepal (DPNet), Nepal Disaster Report*: The Hazardscape and Vulnerability*. ISBN: 9937–2–1301–1, 2009.

[176] Chamlagain D, Earthquake scenario and recent efforts toward earthquake risk reduction in Nepal. *J. South Asia Disaster studies 2009*, Vol. 2.

[177] Roy SC, Dunn J, Auden JA, Ghosh AMN, *The Bihar–Nepal Earthquake of 1934*. Memoirs of the Geological Survey of India, v.73, 1939.

[178] Bhattarai GK, Chamlagain D, Rajaure S, Seismic hazard assessment for eastern Nepal using 1934 and 1988 earthquakes. *J. Nepal Geological Society* 2011; **42**:85–93.

[179] Dixit AM, Geological effects and intensity distribution of the Udayapur (Nepal) Earthuquake of August 20, 1988. *J. Nepal Geological Society*1991; **7**:1–17.

[180] Bilham R, Gaur VK, Molnar P, Himalayan Seismic Hazard, *Science* 2001; **293 (5534)**:1442–44.

[181] JICA, *The study on earthquake disaster mitigation in the Kathmandu Valley Kingdom of Nepal*. Japan International Cooperation Agency (JICA) and Ministry of Home Affairs, His Majesty's Government of Nepal, vol. 1, 2002.

[182] Ferreira T, Vicente R, Mendes da Silva JAR, Varum H, Aníbal Costa A, Seismic vulnerability assessment of historical urban centres: case study of the old city centre in Seixal. Portugal. *Bull. Earthq. Eng.* 2013, doi: 10.1007/s10518–013–9447–2.

[183] Spence R, Bommer J, Del Re D, Bird J, Aydinoglu N, Tabuchi S, Comparison Loss Estimation with Observed Damage: A study of the 1999 Kocaceli Earthquake in Turkey. *Bull. Earthq. Eng.* 2003; **1**:83–113.

[184] Bramerini F, Di Pasquale G, Orsini A, Pugliese A, Romeo R, Sabetta F, *Rischio sismico del territorio italiano.* Proposta per una metodologia e risultati preliminari. Servizio Sismico Nazionale, Rapporto Tecnico, SSN/RT/95/01, Roma, 1995.

[185] Coburn AW, Spence R, PomodisA, Factors determining human casualty levels in earthquakes: mortality prediction in building collapse, In: *Proceedings of the 10th World Conference of Earthquake Engineering*, Madrid, 1992, pp. 5989–94.

[186] Dolce M, Kappos A, Masi A, Penelis G, Vona M, Vulnerability assessment and earthquake damage scenarios of the building stock of Potenza (Southern Italy) using Italian and Greek methodologies. *J. Eng. Struct.* 2006; **28(3)**:357–71.9